Nanofiltration and Tight Ultrafiltration Membranes for Drinking Water Treatment – System Design and Operation

by

Joerg Winter

Dipl.-Ing., Dresden University of Technology, 2010

A THESIS SUBMITTED IN PARTIAL FULFILLMENT OF

THE REQUIREMENTS FOR THE DEGREE OF

Doctor of Philosophy

in

THE FACULTY OF GRADUATE AND POSTDOCTORAL STUDIES

(Civil Engineering)

THE UNIVERSITY OF BRITISH COLUMBIA

(Vancouver)

August 2017

Abstract

Nanofiltration (NF) and tight Ultrafiltration (UF) membranes represent a technology that is well suited for high quality drinking water production from source waters with high concentrations of natural organic matter (NOM) or other contaminants. However, the application of these membranes is limited, mainly because of the challenges related to fouling, concentration polarization (CP), system complexity and cost. The aim of the present study was to address these issues and to enable a more widespread application of this technology.

Opportunities for simplifying NF and tight UF systems by, for instance, operation in dead-end mode, were explored. Experiments were conducted to evaluate the contribution of CP and fouling to the increase in resistance to permeate flow when filtering raw waters containing NOM. Continuous and periodic hydraulic measures to control CP and fouling were assessed. When filtering model raw waters containing humic substances, the increase in resistance to permeate flow was dominated by CP. When humic substances are effectively rejected and are present at high concentrations, CP becomes extensive, leading to a significant increase in the resistance to permeate flow by the formation of a cake/gel layer at the membrane surface. In the presence of calcium and particulate matter, the increase in resistance to permeate flow was dominated by fouling rather than CP. Filtration tests using periodic hydraulic measures to control fouling indicated that it was difficult to hydraulically remove the accumulated material once a foulant layer had been formed. Therefore, cross-flow operation, which reduces CP and prevents the formation of a foulant layer, is recommended.

To optimize cross-flow operation, a framework was developed to compare the performance of NF membranes of different configurations (i.e. spiral wound and hollow fiber configurations)

and geometries in terms of the permeate flux that can be sustained, and to optimize the operating set point of NF membranes with respect to system configuration, cross-flow velocity and operating flux with respect to cost. The results suggest that, despite higher manufacturing costs for hollow fiber NF, hollow fiber NF can be cost competitive to spiral wound NF. Because of operational advantages, the application of hollow fiber configurations is recommended.

Lay Summary

Nanofiltration and tight ultrafiltration membranes are very selective filters which are superior to alternative technologies in producing high quality drinking water from source waters with high concentrations of contaminants. However, challenges of this technology are related to phenomena called fouling and concentration polarization which increase energy demand. Fouling and concentration polarization make it more difficult for water to flow through the membranes after retained material accumulates. Approaches to prevent fouling and concentration polarization result in expensive and complex designs. Fouling and concentration polarization caused by substances that are commonly present in source waters were studied and possibilities to simplify the design of nanofiltration and tight ultrafiltration membranes systems were evaluated. A significant contribution was made by the development of a framework which is expected to lower the costs and enable a more widespread application of this technology.

Preface

This statement confirms that the author is the primary person responsible for the research contained in this thesis. All experimental design and procedures were conceived of by the author with input from the supervisory committee, namely Dr. Pierre R. Bérubé, Dr. Benoit Barbeau and Dr. Madjid Mohseni. The specific names of those who assisted in conducting experiments are recognized in the Acknowledgements section of this thesis.

Several manuscripts in journals and in conference proceedings have been published or are under consideration for publication pertaining the results of this thesis. The following is a list of these manuscripts:

Journals:

- Winter J., Barbeau, B., Bérubé P.R., 2017. NF and tight UF Membranes for Natural Organic Matter Removal – Contribution of Concentration Polarization and Fouling to Filtration Resistance, Membranes 7, 34.
- Winter J., Barbeau, B., Bérubé P.R., 2017. Mitigation of Fouling and CP in Nanofiltration and tight Ultrafiltration Range Membranes. (completed)
- Winter J., Sepideh Jankhah, Barbeau, B., Bérubé P.R, 2017. Nanofiltration for Surface Water Treatment – Hydrodynamics and System Configuration. (completed)
- Winter J., Barbeau, B., Bérubé P.R, 2017. Cost Estimation and Optimization of Hollow Fiber and Spiral Wound Nanofiltration for Surface Water Treatment. (80% completed)

Conference Proceedings

- Winter J., Bérubé P.R., Barbeau B, 2017. Nanofiltration for Drinking Water Treatment – Hydrodynamics and System Configuration. IWA Membrane Technology Conference, Singapore. (accepted)
- Winter J., Bérubé P.R., Barbeau B, 2017. NF and tight UF range Membranes for High Quality Drinking Water Treatment. AWWA/AMTA Membrane Technology Conference, Long Beach, CA.
- Winter J., Bérubé P.R., Barbeau B., 2016. NF-tight UF for NOM Removal – System Design and Operating Conditions. AWWA Water Quality Technology Conference, Indianapolis, IN.
- Winter J., Bérubé P.R. (2015) NF-UF Range Membranes for Surface Water Treatment: Fouling and Concentration Polarization due to NOM of various Composition. AWWA/AMTA Membrane Technology Conference, Orlando, FL.

Table of Contents

List of Tables

List of Figures

Glossary

$A_{Cross\text{-}Section,Module}$	Cross-Sectional Area of a Membrane Module's Flow Channel [m^2]
$A_{Membrane,Module}$	Membrane Surface Area Per Module [m^2]
AOM	Algal Organic Matter
AOC	Assimilable Organic Carbon
AOP	Advanced Oxidation Process
BAC	Biological Activated Carbon
BDOC	Biodegradable Organic Carbon
CA	Cellulose Acetate
CP	Concentration Polarization
δ	Density of Water [kgm^{-3}]
d_h	Hydraulic Diameter [m]
DL	Design Life [a]
DOC	Dissolved Organic Carbon [mgL^{-1}]
EC	Total Energy Cost [$]
EC_a	Annual Energy Cost [$]
EfOM	Effluent Organic Matter
f	Friction Factor [/]
FA	Fulvic Acids
GAC	Granular Activated Carbon
HA	Humic Acids
HAAs	Haloacitic Acids

HF	Hollow Fiber
HPLC	High Performance Liquid Chromatography
J	Permeate Flux [$Lm^{-2}h^{-1}$]
J_0	Initial Permeate Flux [$Lm^{-2}h^{-1}$]
J'_0	Initial Permeate Flux (fitted parameter) [$Lm^{-2}h^{-1}$], [mh^{-1}]
J_{SS}	Permeate Flux at Steady State [$Lm^{-2}h^{-1}$]
$J_{SS,Avg}$	Average Permeate Flux at Steady State [$Lm^{-2}h^{-1}$]
k_C	Fouling Coefficient for Cake Filtration [m^{-2}]
k_{CB}	Fouling Coefficient for Complete Blocking [s^{-1}]
k_{IB}	Fouling Coefficient for Intermediate Blocking [m^{-1}]
k_{SB}	Fouling Coefficient for Standard Blocking [m^{-1}]
L_{Module}	Membrane Module Length [m]
L_P	Membrane Permeability [$Lm^{-2}Pa^{-1}$]
LC-OCD	Liquid Chromatography with Organic Carbon Detection
MC	Total Membrane Cost [$]
MC_j	Membrane Cost per Replacement [$]
MF	Microfiltration
ML	Membrane Lifetime [a]
MWCO	Molecular Weight Cut Off
μ	Dynamic Viscosity [Pa s]
NF	Nanofiltration
η	Pump Efficiency [/]

$P_{Permeation}$	Power required for Permeation [W]
$P_{Cross\text{-}Flow}$	Power Required for Cross-Flow Operation [W]
PA	Polyamide
PAC	Powdered Activated Carbon
PE	Polyethylene
PES	Polyethylsulfone
PP	Polypropylene
PVDF	Polyvinylidene Difluoride
$Q_{Permeate}$	Permeate Flow [m^3s^{-1}]
RO	Reverse Osmosis
SEC	Size Exclusion Chromatography
SW	Spiral Wound
THMs	Trihalomethanes
τ_{Avg}	Average Shear Stress
TMP	Trans-Membrane Pressure [Pa], [psi]
TMP_{Avg}	Average Trans-Membrane Pressure [Pa]
TOC	Total Organic Carbon
UF	Ultrafiltration
UVA_{254}	UV Absorbance at 254 nm [m^{-1}]
V	Volume Filtered [Lm^{-2}], [m]
$v_{cross\text{-}flow}$	Cross-Flow Velocity [ms^{-1}]

Acknowledgements

First, I would like to thank my supervisor, Prof. Pierre Bérubé, for providing me with guidance, encouragement, and project resources. Thank you, Pierre, for the valuable discussions and for all what I have learned through you during my years at UBC. I would also like to thank you for the great opportunities you gave me aside from my PhD research project, including teaching involvements and the participation and a wide range of research projects. Thank you for all the trust and continuous support throughout the years.

I wish to thank Prof. Benoit Barbeau for all the insightful comments and the contribution to my research and the publications resulting from this work. Benoit, it have always enjoyed discussing my research and about water treatment in general with you. Thank you for always being positive and enthusiastic.

I would also like to thank my committee members Prof. Madjid Mohseni and Prof. Benoit Barbeau for all the guidance, suggestions during the realization of this project, and for reviewing this document.

I wish to thank Dr. Sepideh Jankhah for her collaboration on measuring the shear stress in membrane test cells and Dr. Noboru Yonemitsu for being available to discuss my questions related to fluid mechanics.

Many thanks to the support staff at UBC for their help in the lab and their technical support for realizing the experiments. Thank you, Paula Parkinson, Tim Ma, Bill Leung, Scott Jackson, and John Wong.

I appreciate the discussions and great times I had with my friends and colleagues. I would like to thank Syed Zaki Abdullah, Sepideh Jankhah, Christina Starke, Patricia Oka, Shona

Robinson, Mike Beswick, Francois St-Pierre, Rony Das, Martin Schulz, Heather Wray, and all the people whose names I may forget at the moment.

I also would like to thank all the Faculty at UBC who provided me with opportunities to get involved in teaching their courses as a graduate teaching assistant and sessional lecturer. Thank you, Prof. Pierre Bérubé, Prof. Susan Nesbit, Prof. Bernard Laval, Prof. Gregory Lawrence and Dr. Noboru Yonemitsu.

With respect to teaching, I especially want to thank Prof. Susan Nesbit for providing me with all the opportunities for involvements in teaching and course development. Thank you, Susan, for all the mentorship, trust, and support throughout the years, as well as our valuable discussions about engineering and sustainability education.

I express all my gratitude to my family. Thank you for your unconditional support. Finally, I would especially like to thank Claire. Thank you for being understanding and supportive during my ups-and-downs of this thesis. I am deeply grateful for having you in my life and am excited to see what our next adventures will be.

I wish to thank Res'Eau WaterNet and IC Impacts for providing funding for this research.

To my parents Erika and Gottfried

To my fiancé Claire

To my sisters Gundula and Konstanze

Chapter 1: Introduction

1.1 Scope

Over the past 20 years, membrane filtration has been increasingly implemented in water purification processes (Gao et al., 2011). This increase has mainly been driven by the decreasing costs of membrane systems and increasingly stringent drinking water quality regulations. In drinking water treatment applications, ultrafiltration membranes (UF) can effectively remove particulate contaminants such as protozoa and bacteria from raw water sources. However, effective removal of natural organic matter (NOM) and viruses is generally limited in UF systems (i.e. virus removal < 4 log) (ElHadidy et al., 2013; Song et al., 2011). This is because the pore sizes of commercially available UF membranes typically range from 0.02 μm to 0.045 μm, which corresponds to a molecular weight cut off (MWCOs) of greater than 100,000 Dalton. In contrast, nanofiltration (NF) membranes and tight UF membranes, hereafter referred as NF and tight UF membranes, which have MWCOs of less than 10,000 Daltons, can effectively remove all pathogens including viruses (i.e. greater than 4 log), NOM and many emerging synthetic organic contaminants (Lee et al., 2004; Lee et al., 2005a; Odegaard et al., 2010; Patterson et al., 2012; Sadmani et al., 2014; Bartels et al., 2008; Gorenflo and Frimmel, 2002). The removal of NOM from source waters is of importance in drinking water treatment because of its contribution to colour, taste and odour issues, increase chlorine demand as well as its contribution to disinfection by-product formation and microbial regrowth in distribution systems (Chin and Bérubé, 2005; Croue et al., 1999; Hozalski et al., 1999; Rittmann and Stilwell, 2002; Sarathy and Mohseni, 2009; Wang and Hsieh, 2001). Because NF and tight UF membranes can achieve sufficient primary disinfection (i.e. > 4 log removal of all pathogens) and extensive removal of NOM, they can provide effective and comprehensive drinking water treatment in a single step. A

simple single step approach is of particular interest for small/remote communities because of the limited financial and technical resources generally available to implement and operate complex water treatment systems.

While NF membranes are very effective at removing NOM, NOM can also substantially increase the resistance to permeate flow by concentration polarization (CP) and fouling (Lee et al., 2004; Schäfer et al., 1998; Yoon et al., 2005). Because fouling and CP increase the energy demand and/or decrease the volume of water produced, a major objective for the design and operation of NF systems is the mitigation of CP and fouling. Also, the application of NF and tight UF membranes in drinking water treatment applications is still limited, because of the high energy demand and the complexity of NF and tight UF systems. Spiral wound configurations are commonly used for NF and tight UF (Burbano et al., 2007), which generally require extensive pre-treatment and a high inlet pressure. In addition, fouling control measures, such as backwashing or surface scouring cannot be applied to spiral wound configurations. However, recent developments in NF and tight UF membrane geometries, such as hollow fiber NF/tight UF systems, promise to address these limitations, enabling the application of backwash and surface scouring using air bubbles (Bequet et al., 2002; Frank et al., 2001; Futselaar et al., 2003; Spruck et al., 2013; Verissimo et al., 2005; Verberk and van Dijk, 2006; Payant et al., 2017). It has been reported that, when using NF and tight UF spiral wound or hollow fiber membranes with similar rejection characteristics, a substantially higher permeability can be maintained using hollow fiber geometries (Frank et al., 2001). Other studies have, however, reported that spiral wound configurations are more effective in mitigating fouling and CP than hollow fiber configurations (Geraldes et al., 2002; adopted from Thorsen and Flogstat, 2006). This is likely because the feed

spacers in spiral wound configurations generate zones of high shear stresses at the membrane surface, which can reduce the extent of CP and fouling (Koutsou et al., 2007).

In the present study, opportunities for simplifying NF and tight UF systems by, for instance, operation in dead-end mode, were explored. Experiments were conducted to gain insight into CP and fouling to develop recommendations for the design and operation of NF and tight UF systems to enable greater adoption of this advanced treatment technology. The contribution of CP and fouling was investigated for various NOM constituents and membrane molecular weight cut offs (MWCOs). Because Fouling by NOM can be further enhanced in the presence of calcium and turbidity (Lee et al., 2005b; Contreras et al., 2009; Mahlangu et al., 2015; Li and Elimelech, 2006), their impact was considered in the present study. The present study also assessed the effect of cross-flow operation and permeate flux interruption as hydraulic control measures, on the extent of CP and fouling and/or CP and fouling control. To assess the impact of the system configuration (spiral wound or hollow fiber) on CP and fouling control as well as on the energy demand of NF and tight UF membrane systems, a framework was developed to compare the performance of NF membranes of different configurations (i.e. spiral wound and hollow fiber configurations) and geometries in terms of the permeate flux that can be sustained, and to optimize the operating set point of NF membranes with respect to system configuration, cross-flow velocity and operating flux. Further, an approach for the cost optimization was developed that allows for a comprehensive optimization with respect to operating flux and cross-flow velocity.

1.2 Organization of the Dissertation

The structure of this this thesis is presented below. It is comprised of seven chapters:

Chapter 1: Introduction

An introduction to the thesis is given in Chapter 1, summarizing the scope of the research.

Chapter 2: Background and Literature Review

A comprehensive summary and discussion of the relevant literature is given in Chapter 2, discussing natural organic matter (NOM) and NOM removal in drinking water treatment, and explaining the challenges related to concentration polarization (CP) and fouling in NF and tight UF membrane applications, and how these might affect the design and operation of NF and tight UF membrane systems.

Chapter 3: Objectives of the Study

A brief summary of the current knowledge gaps and the corresponding objectives that were formulated to address these knowledge gaps.

Chapter 4: Materials and Methods:

A general description of all the materials and methods used in the present study is provided in Chapter 4.

Chapter 5: The Contribution of Concentration Polarization and Fouling to the Increase in Resistance

Chapter 5 provides an assessment of the contribution of CP and Fouling to the increase in resistance to permeate flow for various NOM constituents and membrane MWCOs and an identification of critical operational conditions and development of recommendations for the operation of NF and tight UF membranes.

Chapter 6: Mitigation of Fouling and Concentration Polarization

Chapter 6 contains a comprehensive analysis of hydraulic control measures, namely cross-flow and permeate flux interruptions (i.e. relaxation), applied to mitigate CP and fouling in NF and tight UF membranes applied for NOM removal.

Chapter 7: Hydrodynamics, System Configuration and Geometry

Chapter 7 contains a comprehensive analysis of the hydrodynamic conditions in spacer filled and empty flow channel configurations, representing spiral wound and hollow fiber membrane configurations. The hydrodynamic conditions analyzed are related to filtration data. A framework is presented to compare the performance of NF membranes of different configurations (i.e. spiral wound and hollow fiber configurations) and geometries in terms of the permeate flux that can be sustained, and to optimize the operating set point of NF membranes with respect to system configuration, cross-flow velocity and operating flux.

Chapter 8: Cost Comparison and Optimization for Hollow Fiber and Spiral Wound Configurations

Chapter 8 discusses a cost analysis based on the framework and relationships presented in Chapter 7. An approach for the cost optimization is proposed that allows for a comprehensive optimization with respect to operating flux and cross-flow velocity, which is expected to allow for lowering costs of NF membrane systems applied for drinking water treatment.

Chapter 9: Overall Discussion and Engineering Implications

The outcomes of the present study presented in the separate chapters are discussed in the overall context of the present dissertation and with the focus on engineering implications.

Chapter 10: Conclusions and Recommendations

Overall conclusions from each chapter of this thesis are presented and future research recommendations are suggested.

Chapter 2: Background and Literature Review

2.1 Organic Matter in Drinking Water Treatment

Organic matter in raw drinking water sources consists mainly of natural organic matter (NOM). NOM is a complex mixture of organics that are predominantly derived from the decay of plant and animal material (Leenher and Croue, 2003), and is present in surface water and groundwater.

NOM is typically classified based on several characteristics. It is divided in particulate organic matter and dissolved organic matter. In water treatment, the latter is defined as the fraction of the organic matter, which passes a membrane filter with a pore size of 0.45 μm. Chemically, NOM is typically classified into two major categories: humic and non-humic substances (Croue et al., 1999; Zumstein and Buffle, 1989). The non-humic fraction consists of biochemically well-defined compounds such as amino acids, proteins, sugars, polysaccharides and peptides (Zumstein and Buffle, 1989; Croue et al., 1999). Non-humic substances are more polar or hydrophilic, while humic substances are less polar or hydrophobic. Humic substances are subdivided into two subcategories: Humic acids (HA) and fulvic acids (FA) differ in their solubility. Humic acids are predominantly darker in colour. Although chemically similar to humic acids, fulvic acids have a greater oxygen content, are slightly more hydrophilic, less aromatic, more acidic and more effective in complexing metal ions than humic acids (Her et al., 2008). In aquatic systems, humic substances are mainly resistant to microbial degradation and the main portion of humic substances can be considered as refractory organic matter (Quentel and Filella, 2008; Zumstein and Buffle, 1989). Organic matter in raw drinking water sources can also originate from the effluent of secondary wastewater treatment plants. Effluent organic matter (EfOM) consists of NOM from drinking water, soluble microbial substances released by

microorganism within the biological wastewater treatment process, persistent organic matter, endocrine disturbing chemicals and pharmaceuticals and personal care products. Soluble microbial substances are similar to dissolved extracellular polymeric substances released by water organism such as cyanobacteria or algae. In contrast, persistent organic matter, endocrine disturbing chemicals and pharmaceuticals and personal care products are classified as synthetic organic matter (Shon et al., 2006).

With respect to its origin, NOM can be differentiated into aquagenic (autochthonous) and pedogenic (allochthonous) or microbial derived and terrestrial NOM, respectively (Amy and Her, 2004; Biber et al., 1996). Terrestrial (allochthonous) NOM contains more humic material than aquagenic NOM, which is of mainly microbial origin. The latter is often produced by algae and thus referred to algal organic matter (AOM) (Amy and Her, 2004). Whereas pedogenic NOM mainly consists of humic substances, aquagenic NOM mainly consists of non-humic substances. Fulvic acids originate from soil and can also be produced in lakes by microbial activity. Hence, they can be pedogenic as well as aquagenic.

Although there are no known direct negative health effects associated with NOM in drinking water (Hozalski et al., 1999), water quality may be significantly impacted by NOM. NOM impacts water quality with respects to its appearance by adding colour, taste and odour. Indirectly, some fractions of organic matter are easily biodegradable, decreasing the biological stability of the water. Furthermore, NOM can act as a precursor for Disinfection by-products. Disinfection by-products are of concern for human health because of their potential risk for cancer and reproductive and developmental health effects (Singer, 1994; USEPA, 2002; WHO,

2008). Commonly, Disinfection by-products are differentiated into chlorinated and non-chlorinated Disinfection by-products. The latter result from oxidation of water compounds with oxidants other than chlorine. During ozonation, organic by-products are formed from the oxidation of natural organic matter (von Gunten, 2003). Disinfection by-products produced during ozonation can be divided in three groups: (i) non-brominated organic compounds, (ii) brominated organic compounds and (iii) halogenates (Hammes et al., 2006). Aldehydes, ketones and low molecular weight organic acids have been reported as the main substances resulting from the oxidation of NOM by ozone (Singer, 1994, von Gunten, 2003a; Huang et al., 2004; Karnik et al., 2005; Hammes et al., 2006). Chlorine, commonly used as a disinfectant in drinking water treatment, can react with NOM forming a number of disinfection by-products that are referred to as chlorinated Disinfection by-products (Wang and Hsieh, 2001; Chin and Bérubé, 2005; Sarathy and Mohseni, 2009). Trihalomethanes (THMs) and Haloacitic acids (HAAs) are the Disinfection by-products that can be found at the highest concentrations after chlorination of drinking water (Singer, 2004; WHO, 2008). Maximum levels for THMs and HAAs are specified in several drinking water regulations and guidelines (Singer, 2004; Health Canada, 2006; USEPA, 2002; WHO, 2008). Another group of Disinfection by-products of concern are nitrogen containing disinfection by-products (N-DBPs), such as haloactonitriles, halonitromethanes and nitroamines (e.g. NDMA). Although not yet regulated and normally present in at lower concentrations, N-DBPs are more carcinogenic and mutagenic compared to the regulated Disinfection by-products (i.e. THMs and HAAs) (Dotson and Westerhoff, 2009; Lee et al., 2007; Westerhoff and Mash, 2002).

Biodegradable organic carbon (BDOC) or assimilable organic carbon (AOC) are fractions of dissolved organic matter that are easily biodegradable and thus readily available for microorganism as substrate. Hence, they are of concern due to their ability to promote the formation of biofilms as well as microbial regrowth in distribution systems, commonly referred to as biological stability (Haas et al., 1983, van der Kooij, 1992). A higher biological stability is related to a lower potential for a change of microbial quality of the water over time (i.e. within water distribution). Some treatments such as ozonation, advanced oxidation processes (AOPs) and chlorination may increase the content of BDOC, and AOC and with that lower the biological stability of water (Karnik et al., 2005; Hammes et al., 2006; Sarathy and Mohseni, 2009).

Synthetic organic matter is of concern because of potential toxic or endocrine effects on environment and human health. These compounds are also referred to as organic micropollutants, as they not only are typically present at very low concentrations (i.e. in the nanogram range), but also may have effects on the environment and health at very low levels. More recently, increasing attention has been paid to these constituents in wastewater effluents due to the increasing importance of wastewater reclamation and concerns about their effects in wastewater impacted waters (Chen et al., 2009; Joss et al., 2005; Joss et al., 2008; Hollender et al., 2009).

Beside its effects on water quality, NOM can affect the performance of several treatment processes such as by consuming oxidants or competing with other compounds to be removed. The latter may, for example, lead to a decrease of the removal of other target substances like microplollutants (e.g. endocrine disturbing substances) during activated carbon filtration. As

NOM can more readily adsorb on activated carbon than other compounds to be removed (e.g. micropolutants), it may occupy a main part of its adsorption capacity. Gerenflo (2003) reported that humic substances may form soluble complexes with heavy metals and inhibit their sedimentation. During ozonation, NOM causes instantaneous ozone demand (Cho et al., 2003). This may decrease ozone available for other treatment goals such as disinfection or oxidation of other compounds. In membrane filtration applications NOM is known as a major foulant, decreaseing the volume of water produced and/or the increasing the energy demand.

Overall, NOM plays an important role in water treatment due to its impact on process unit performance, cost of treatment and water quality. In many source waters, NOM concentration are rising. Along with the process of global warming, the content of NOM in surface water increases directly through higher temperatures, increasing biological activity and degradation of plant and animal material, or indirectly by an increase in the duration and/or intensity of rain events. Along with the latter phenomena, more NOM from terrestrial origin (i.e. allochthonous) may reach lakes or streams to greater extent (Hejzlar et al., 2003). Also, higher temperatures and more rain may increase eutrophication (Domnisoru, 2007). Higher run off from urban areas and agriculture increases not only the content of organic substances, but also nutrients in surface water bodies further enhancing eutrophication. A consequence of eutrophication is algal blooms, which contribute to the organic matter content of the raw water. Higher temperatures do not only raise growth rates of microorganism and algae, but in longer periods of summer stratification it is more likely, as a result anoxic conditions develop below the thermocline and phosphate, which is considered to be the most limiting nutrient for eutrophication, may be released from the sediment (Domnisoru, 2007)

2.2 Characterization of Organic Matter

Dissolved organic carbon (DOC) or total organic carbon (TOC) concentrations and UV absorbance at 254 nm (UVA_{254}) can be used to quantify the NOM content. The parameter DOC quantifies all organic matter that passes a 0.45 μm filter. UVA is proportional to the content of UV absorbing organic material (i.e. chromophoric NOM). Specific UVA absorbance (SUVA) describes the ratio of UVA_{254} and TOC or DOC. Changes in SUVA indicate changes in the structure of NOM. In source waters, SUVA can be used as a rough indicator for predominant content of aquagenic or pedogenic NOM with higher values indicating a higher fraction of NOM of pedogenic origin (Zumstein and Buffle, 1987). It correlates well with aromatic and hydrophobic content. High hydrophobic content is generally associated with good treatability by, for instance, coagulation flocculation (Juhna and Melin, 2006) or a higher potential for adsorptive fouling in membrane systems (Schäfer et al., 2005; Mulder 1996; Jermann et al. 2007). For biological treatment processes, lower SUVA values generally indicate a higher biodegradability, as biodegradable aliphatic compounds adsorb less UV light. According to Juhna and Melin (2006), a SUVA of less than 2 $L/mg_C/m$ indicates that the water contains biodegradable fractions which are removable with biological filtration. However, the NOM characterization approaches discussed above represent bulk parameters that provide limited information on the NOM properties.

A method commonly used to obtain a more detailed characterization of NOM is size exclusion chromatography. Size exclusion chromatography (SEC) techniques are commonly used for the determination of NOM molecular weight distribution. The use of multiple detectors (e.g. UV detector, organic carbon detector, organic nitrogen detector, fluorescence detector) coupled with

SEC does not only allow to determine molecular weight distribution, but can also provide additional insight into NOM characteristics (Shon et al., 2006; Huber et al., 2011). During SEC, samples pass a stationary phase, packed in a column, which contains a porous material. Smaller compounds can access more of the internal pore volume of the stationary phase, whereas larger ones are excluded. Hence the retention time is larger for smaller compounds. According to the theory of SEC, retention time decreases linearly with the logarithm of the hydrodynamic diameter or molecular mass. Hence, retention time can be used to estimate the molecular weight of different compounds. However, it is important to note that non-ideal interactions between the column stationary phase and solute, such as charge interactions, steric effects and hydrophobic interactions can result in a separation not exclusively based on size (Pelekani et al., 1999; Perminova et al., 2003; Bradley et al., 2005; Specht and Frimmel, 2000; Lankes et al., 2009). The output from SEC provides a "fingerprint" that is specific to a given source water. Based on the retention time and the signal of different detectors (i.e. the organic carbon detector and the UVA detector), five distinctive fractions can typically be observed and related to impacts on water treatment processes and water quality (Huber et al., 2011). The highest molecular weight fraction is typically referred to as the biopolymer fraction that contains biopolymeric and colloidal material, which mainly include polysaccharides and proteins. Biopolymers typically have a molecular weight larger than 10,000 Da (Jarusutthirak et al., 2002; Huber et al., 2011). The next smaller fraction are humics or humic substances with a molecular weight of around 1,000 Da (Chin et al., 1994; Her et al., 2002). Building blocks mainly result from the degradation of humic substances and exhibit a molecular weight of 300 to 500 Da. The low molecular weight organics contain low molecular weight acids and low molecular weight humic substances, which elute at the same time. The smallest fraction and thus considered to eluting latest, is defined as

low molecular weight neutrals. Low molecular weight humics, low molecular weight acids and low molecular weight neutrals typically have a molecular weight of less than 350 Da. Additional characterizations of these five fractions are provided elsewhere (Huber et al., 2011).

Other NOM characterization techniques that are not discussed in more detail in the present thesis are (Croue et al., 1999; Chen, 2016):

- Nuclear Magnetic Resonance Spectroscopy (NMR) to determine aromaticity and degree of humification in NOM,
- Fourier Transformation Infrared Spectroscopy (FTIR) to identify proteinaceous components and abundance of carbohydrates and hydrocarbons in NOM,
- Mass Spectrometry (GC-MS, LC-MS) to identify molecular building blocks of NOM,
- Fluorescence Spectroscopy and Excitation-Emission Matrix (FEEM) to indentify humic like and potein like compounds, and
- Polar fractionation using XAD-8 and XAD-4 resins to evaluate the hydrophobic and hydrophilic properties of NOM.

2.3 Organic Matter Removal in Drinking Water Treatment

2.3.1 Coagulation

Coagulation is widely applied to agglomerate small colloids to larger particles that can subsequently be removed by sedimentation or filtration. However, coagulation is also commonly considered as a good option of NOM removal (Matilainen et al., 2010). Mechanisms for NOM removal include charge neutralization, entrapmet, adsorption, and complexation with metal ions into insoluble aggregates (Matilainen et al., 2010). It has been reported that high molecular

weight fractions and hydrophobic intermediate molecular weight fractions are preferentially removed by coagulation (Haberkamp et al., 2007; Sharp et al., 2006) and high hydrophobicity and SUVA values indicate high NOM reductions by coagulation. Using SEC (i.e. LC-OCD), Haberkamp et al.,(2007) identified bioplolymers and humic substances to be the main NOM fractions removed during coagulation, whereas low molecular weight acids and neutrals were not affected. NOM removal is, however, not only affected by the constituents of NOM in the raw water, but also substantially impacted by operational parameters such as pH and coagulant type and dose (Edzwald, 1999; Eikebrokk et al., 2006).

NOM removal efficiencies can be as high as 80 % (Crittenden, 2005). However, Haberkamp et al. (2007) reported that high coagulant doses (e.g. 1.3 mmol Fe^{3+}/L), are required for efficient removal (i.e. > 50 %) of biopolymers and humic substances.

The challenges associated with coagulation are the chemicals required and a careful operation with respect to pH adjustment and coagulant dosing, which have to be adjusted based on variations in the raw water characteristics, as well as the disposal of the waste solids generated by coagulation.

2.3.2 Adsorption Processes

Activated carbon is widely used as either granular activated carbon (GAC) or powdered activated carbon (PAC) to remove NOM from source waters, to remove color and to reduce the disinfection by-product formation potential. Activated carbon is a very porous material and adsorption of NOM occurs mainly onto the inner surfaces within the pores and, hence, the pore

size distribution affects the removal of NOM. Velten (2008) reported that the removal efficiency for specific NOM fraction increased as the NOM size decreased. Matilainen (2006) reported that activated carbon most efficiently adsorbed intermediate molecular weight NOM fractions (i.e, between 1,000 to 4,000 Da), while the higher and smaller molar mass fractions were not significantly removed. Hesse et al. (1999) observed only low molecular weight acids and neutrals, which have a molecular weight of a few hundred Daltons (Huber et al., 2011), to be effectively removed during activated carbon treatment. These inconsistencies in the literature with respect to the removal of specific NOM fractions may be related to the interactions between NOM size and the pore sizes of a specific activated carbon product.

The overall removal of NOM in activated carbon systems has been observed to be 80 %. However, activated carbon systems, operated as an adsorption process, are not recommended for raw waters containing high NOM concentrations without pre-treatment because their adsorption capacity is quickly exhausted and regeneration of activated carbon is expensive.

2.3.3 Biological Filtration

Biological filtration is cost effective, easy to operate and has been reported to be suitable for DOC removal, reduction in disinfection by-product formation potential and chlorine demand (Carlson and Amy, 1997; Chaiket et al., 2002; Zhu et al., 2010; Black and Bérubé, 2014). It is also applied because of its ability to control the content of assimilable organic carbon (AOC), a parameter that is closely related to the regrowth potential for microorganism in the distribution system (Haas et al., 1983, van der Kooij, 1992).

During an acclimatization period of approximately 3 months (Velten, 2008; Edzwald, 1999), a biofilm is growing on a filter media. The most commonly used filter media are sand or GAC. Following the acclimatization period, the primary NOM removal mechanism is biological oxidation. Hence, essentially only biodegradable NOM is being removed.
Consistent with the results presented in Apendix A.1, the biopolymers fraction, which has a high molecular weight, has been reported to be well removed by biological filtration (Maeng et al., 2008; Zheng et al., 2010; Halle et al., 2009). Also well removed during biological filtration are low molecular weight acids (see Apendix A.1). Humic substances are, however, typically not well removed (Maeng et al., 2008; Zheng et al., 2010; Halle et al., 2009). This is consistent with the concept that biological filtration is more efficient for waters exhibiting low SUVA (Juhna and Melin, 2006). For this reason, ozonation can be applied as a pre-treatment to decrease SUVA and to improve the biodegradability of NOM (Carlson and Amy, 1997; Juhna and Melin, 2006; Odegaard et al., 2010). However, the increase in overall NOM removal when ozonation is applied prior to biological filtration is limited (Winter et al., 2013).

Biological filtration is cost effective and easy to operate. However, the extent of DOC removal is limited, making biological filtration only suitable for treatment of source waters with low DOC concentrations (Odegaard et al., 2010) or if the removal of specific NOM fractions is of interest (e.g. biopolymers removal during membrane pre-treatment).

2.3.4 Oxidation Processes

The oxidation of water compounds by ozone can occur via two different pathways – direct or indirect. In the direct path, ozone tends to react selectively with compounds containing double

bonds, aromatic systems, amines or sulfides (Gottschalk et al., 2000; von Gunten 2003a). In case of the indirect pathway, hydroxyl radicals are formed which then react with all NOM fractions. Hydroxyl radicals are strong, unselective oxidants and react quickly with NOM. Whereas disinfection occurs predominantly trough ozone, oxidation can be achieved due both hydroxyl radicals or ozone (von Gunten 2003b). The presence of the two pathways depends on pH, alkalinity and type and content of NOM (von Gunten 2003a). At a higher pH, the water contains more hydroxide ions, which increases the formation of hydroxyl radicals. If the pH is lower than 4, the direct pathway dominates (Gottschalk, et al., 2000). However, most source waters to be treated for drinking water purpose have a pH close to 7 or at least between 4 and 10. Hence, both pathways have to be considered.

Advanced oxidation processes (AOP) are defined as processes where hydroxyl radicals are formed that subsequently react with water constituents. As previously discussed, hydroxyl radicals react with NOM as strong and unselective oxidants.

Both ozonation (Chin and Bérubé, 2005; Ko et al., 2000) and AOPs (Sarathy, 2009; Goslan et al., 2006) have been reported to affect NOM by decreasing SUVA. Also, the hydrophobicity decreases during ozone treatment (Westerhoff et al., 1999; Galapate et al. 2001; Chowdhury et al. 2008) and advanced oxidation (Sarathy, 2009). The molecular weight distribution of NOM decreases as well during ozonation (Swietlik et al., 2004) and advanced oxidation (Sarathy, 2009). At doses typically applied in drinking water treatment, the DOC concentration is decreased by 0 % to 16 % by ozone (Chin, Bérubé 2005; Chowdury et al., 2008; Ko et al., 2000; Galapate et al. 2001; Westerhoff et al. 1999) and 36 % to 55 % by advanced oxidation (Sarathy,

2009). Inconsistent results were observed for ozone with respect to disifection by-product formation potential, ranging from an increase by 117 % to a decrease by 50 % (Kleiser and Frimmel, 2000; Galapate et al., 2001; Chin and Bérubé, 2005; Chowdhury et al., 2008). The differences in the observed effect of ozone are most likely related to the NOM characteristics and the ozone dose (Chin and Bérubé, 2005). Inconsistent results were also observed for AOP with respect to disinfection by-product formation potential, ranging from an increase by 41 % to a decrease by 80 % (Kleiser and Frimmel, 2000; Chin and Bérubé, 2005; Sarathy, 2009).

At economically feasible oxidation doses, DOC reduction is limited, as organic components are normally not mineralized but converted into smaller material as a result of partial oxidation. The latter generally leads to an increase in biodegradability of organic matter and results in an increase in AOC (i.e. less biological stable water). Hence, biological filtration is commonly recommended as a post treatment step following oxidation (von Gunten, 2003a; von Gunten et al., 2003b; Hammes et al., 2006).

2.3.5 Ion Exchange

The use of macro-porous anion exchange resins is a promising option to effectively remove NOM from drinking water sources (Cornelissen et al., 2008; Apell and Boyer, 2010). Anion-exchange resins remove NOM by exchanging negatively charged counter ions from its surface with polar, negatively charged dissolved organic matter ions from the solution (Cornelissen et al., 2008). However, adsorption of NOM onto the resins is another significant removal mechanism (Kaeocha, 2008*).* Bolto et al. (2002) observed NOM removal efficiencies ranging from 47 % to 77 % for a wide range of ion exchange resins and surface waters. Humic

substances are predominantly removed by ion exchange (Grefte, 2013; Schultz et al., 2017), whereas biopolymers are poorly removed (Fabris et al., 2007; Huang et al., 2012).

Ion exchange is a promising technology due to its effectiveness in contaminant removal, ease of operation, scalability and low cost (Bolto et al., 2002). However, a major challenge is the regeneration of the resin that is required after the exchange sites of the resins become depleted and the related disposal of the regenerate (McAdam and Judd, 2008), limiting the application of ion exchange in water treatment.

Research, which was conducted in parallel to this thesis, demonstrated that stable NOM removal without regeneration can be achieved when operating anionic ion exchange resins under conditions where biological activity is promoted (BIEx). Over a 10-month test period, corresponding to over 15,000 empty bed volumes, the DOC removal efficiencies were stable in the BIEx system and overall NOM removal efficiencies of 56 ± 7 % were observed (see Appendix A.2). Hence, BIEx appears to be a promising treatment technology with advantages similar to those of conventional biological filtration, but with a substantially higher NOM removal efficiency.

2.3.6 Membrane Filtration

In drinking water treatment, Ultrafiltration (UF) membranes are commonly applied. UF membranes reject NOM typically by less than 40 % (Schäfer, 2007) and do not effectively reduce the disinfection by-product formation potential (Clark and Heneghan, 1991; Laine et al., 1990). This is because the pore size of UF membranes typically used in drinking water treatment

applications is relatively large (see Table 1, Section 2.4.1). However, membranes with a higher selectivity, hereafter referred to as nanofiltration (NF) and tight ultrafiltration (UF) membranes can effectively remove NOM (Lee et al., 2004; Lee et al., 2005a; Odegaard et al., 2010; Patterson et al., 2012). Depending on the membrane selected, removal efficiencies of close to a 100 % can be achieved (Patterson et al., 2012). This is consistent with a reported high reduction in disinfection by-product formation potential (Allgeier and Summers, 1995; Itoh et al., 2001). NOM is rejected by NF and tight UF membranes by size exclusion, but can also be affected by charge effects, hydrophobic interactions, and size exclusion (van der Bruggen et al., 2003; Cho et al. 1999; Jarusutthirak et al., 2002; Yoon et al., 2005). In summary, NF and tight UF can achieve extremely high NOM rejection and the compliance with surface water requirements appear unproblematic (Schäfer, 2007). NF and tight UF membranes with a high selectivity for NOM are particularly well suited for source waters with high concentrations of NOM where other treatments are not able to achieve a sufficient NOM removal.

However, the challenges for the application of NF and tight UF membranes are fouling, CP, system complexity and cost. The present dissertation addresses and discusses these issues and aims to develop frameworks and recommendations for the design and operation of NF and tight UF membrane systems that enable a more widespread application of this technology.

2.4 Nanofiltration and tight Ultrafiltration Membranes

2.4.1 Membrane Classification

Membrane filtration is a physical treatment process for the separation of particulate, macromolecular or dissolved matter. The membrane acts as a selective barrier that retains the

contaminants desired to be removed from the water. In water treatment, membranes are classified as Microfiltration (MF), Ultrafiltration (UF), Nanofiltration (NF), and Reverse Osmosis (RO). This classification is based on the type of materials retained, the trans membrane pressure applied, and on the pore size of the membrane (see Table 1).

Table 1: Characteristics and Applications of Membrane Processes (van der Bruggen et al., 2003; Crittenden, 2005)

	Microfiltration (MF)	**Ultrafiltration (UF)**	**Nanofiltration (NF)**	**Reverse Osmosis (RO)**
Permeability [$Lh^{-1}m^{-2}bar^{-1}$]	>1,000	10 to 1,000	1.5 to 30	0.05 to1.5
Pressure [bar]	0.1 to 2	0.1 to 5	3 to 20	5 to 120
Pore size [nm] (MWCO [Da])	100 to 10,000	2 to 100 (1,000-500,000)	0.5 to 2 (<1,000)	<0.5
Rejection*:				
Monovalent ions	-	-	-	+
Multivalent ions	-	-/+	+	+
Small organics	-	-	-/+	+
Macromolecules	-	+	+	+
Particles	+	+	+	+
Separation mechanism	Sieving	Sieving	Sieving Charge effects	Solution-Diffusion
Applications	Clarification; Pre-treatment; removal of bacteria	Removal of macromolecules, bacteria, viruses	Removal of multivalent ions and small organics	Ultrapure water; desalination

* "-": not effectively removed; "+": effectively removed

In Table 1, the selectivity of the membrane is characterized by pore size, which is defined as the size of the smallest particle that can be retained by the membrane. For UF, NF and RO it is common to characterise the selectivity of the membrane by the molecular weight cut off (MWCO). The MWCO is defined by the molecular weight, with the units [Da], of the components which are rejected by the membrane by more than 90 % (van der Bruggen et al., 2003; Crittenden, 2005).

Membrane processes generally split a feed stream into a retentate or concentrate stream and a permeate stream, as illustrated in Figure 1 (Mulder 1996). A driving force (a gradient in e.g. temperature, energy, concentration or pressure) is essential for the process. In water treatment, a pressure gradient, referred to as trans membrane pressure, is commonly used as the driving force.

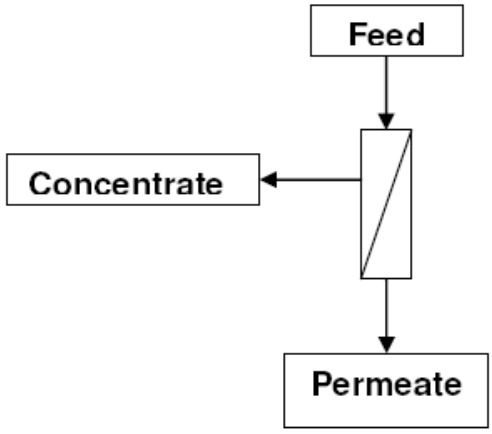

Figure 1: Membrane Process – Feed, Concentrate and Permeate

2.4.2 Contaminant Removal

The removal of NOM by membranes has already been discussed in Section 2.3.6. For comprehension, the current section expands the discussion to other contaminants of potential

interest in drinking water treatment. As previously discussed, in drinking water treatment applications, ultrafiltration membranes (UF) are most widespread. They can effectively remove particulate contaminants such as protozoa and bacteria from raw water sources. However, in addition to the relatively poor removal of NOM, virus removal is also generally limited in commercial UF systems (i.e. virus removal < 4 log) (ElHadidy et al., 2013; Song et al., 2011). This is because the pore sizes of commercially available UF membranes typically range from 0.02 μm to 0.045 μm, which corresponds to a molecular weight cut off (MWCOs) of greater than 100,000 Dalton. In contrast, nanofiltration (NF) membranes and tight UF membranes, hereafter referred as NF and tight UF membranes, which have MWCOs of less than 10,000 Daltons, can effectively remove all pathogens including viruses (i.e. greater than 4 log), and NOM (Lee et al., 2004; Lee et al., 2005a; Odegaard et al., 2010; Patterson et al., 2012) – see Section 2.3.6. Further, they can remove many emerging contaminants (Sadmani et al., 2014; van der Bruggen et al., 1998) and can effectively remove heavy metals, such as arsenic (van der Bruggen and Vandecasteele, 2003; Oh et al., 1998; Sato et al., 2002; Moore et al., 2008).

2.4.3 Membrane Materials

A wide variety of materials are used to manufacture membranes for water and wastewater treatment. The material can significantly affect the chemical and physical properties of membrane and the associated operating conditions such as water permeability, pressure operation range, oxidant tolerance, volatile organic carbon tolerance and pH operation range (Thorsen and Flogstad, 2006; Shon et al., 2013; Patterson et al., 2012). Membrane materials are divided into two major groups, organic and inorganic membranes. Inorganic membranes offer some advantages over organic membranes, such as a higher pressure and temperature tolerance, and

higher chemical and oxidation resistance allowing for more rigorous chemical cleaning protocols (Mulder, 1996; Lee and Cho, 2004). However, the use of ceramic membranes is limited, mainly due to the higher costs and limitations with respect to packing density. Organic membranes are commonly applied in drinking water and wastewater treatment applications. They are typically made of synthetic polymers such as Polyvinylidene Difluoride (PVDF), Polyethylsulfone (PES), Polyethylene (PE), Polyamide (PA), Cellulose Acetate (CA), and Polypropylene (PP) (Meng et al., 2009; Meng et al., 2012), with PES and PVDF being the most commonly used materials. For NF and RO membranes, materials most commonly used are Cellulose Acetate (CA) or Polyamide (PA), which are typically added as a thin layer on top of, for instance, a PES membrane (Schäfer et al., 2005; Schäfer, 2007; Frank et al., 2001; Do et al., 2012). The challenge with NF and RO membranes that are made using CA or PA is a chlorine resistance that is lower than that of, for instance, PES and PVDF membranes, shortening the membrane operational life (Aimar and Chausserand, 2012; Arkhangelsky et al., 2007; Kwon and Leckie, 2006; Levitsky et al., 2011; Yadav et al., 2009; Zondervan et al., 2007).

2.4.4 Membrane Configuration

Membranes are commonly configured into hollow fiber, tubular, flat sheet and spiral wound filtration units. The different membrane configurations differ with respect to packing density, hydrodynamic conditions and hydraulic fouling control measures applicable (see Table 2).

Table 2: Characteristics of Common Membrane Configurations (Crittenden, 2005):

Module geometry	**Packing density [m^2/m^3]**	**Backwashable**	**Common use**
Tubular	10-25	yes	MF, UF (industrial)
Flat sheet	50-200	no	MF/UF (wastewater)
Spiral wound	500-1000	no	NF/RO
Hollow fiber	2000-15,000	yes	MF/UF

Hollow-fiber membranes are either operated with inside-out or outside-in permeate flow. With inside-out permeate flow, feed water flows in the lumen of the membrane and permeates to the outside. With outside-in permeate flow, feed water is outside of the membrane and permeate is collected inside the lumen. Outside-in permeate flow is generally advantageous when the solids concentration in the feed is high.

Spiral wound configurations are most common for NF and tight UF membrane applications (Burbano et al., 2007). Spiral wound configurations consist of flat sheet membranes glued along three sides to form leaves, which are attached to the permeate pipe (i.e. center pipe) along the unsealed edge (see Figure 2). The leaves are wound around the permeate pipe – hence the name spiral wound. The membranes are separated on the permeate side and on the feed side by permeate and feed spacers, respectively. The permeate spacer provides support to the membrane to prevent collapsing under pressure and to help convey the permeate to the permeate pipe (i.e. center pipe). The feed spacer, which is placed in between the leaves, defines the channel height through which the water to be filtered flows. The feed spacer also affects the hydrodynamic

conditions in spiral wound configurations. The flow pattern in spacer filled flow channels (i.e. in spiral wound configurations) is illustrated in Figure 3. In membrane systems with spacer filled flow channels (e.g. spiral wound membranes configurations), the maximum shear stress induced by the liquid flowing along the surface of the membrane is substantially greater than in systems with empty flow channels (e.g. hollow fiber membrane configurations) at a given cross-flow velocity (Koutsou et al., 2007). For this reason, spiral wound configurations are considered to be superior in terms of fouling and CP control compared to hollow fiber configurations (Geraldes et al., 2002; Thorsen and Flogstat, 2006). However, spiral wound configurations generally require extensive pre-treatment to prevent clogging of the spacer filled flow channels, and a high feed pressure is generally required to overcome the headloss that occurs as water flows through the spacer filled flow channel (Sethi and Wiesner, 2000). In addition, fouling and CP control measures, such as backwashing or surface scouring, cannot be applied in spiral wound configurations. More recently, hollow fiber NF/tight UF systems have become commercially available. Unlike spiral wound configurations, hollow fibers can be backwashed and air can be used for fouling and CP control (Bequet et al., 2002; Bonne et al., 2002; Frank et al., 2001; Futselaar et al., 2003; Spruck et al., 2013; Verissimo et al., 2005; Verberk and van Dijk, 2006; Payant et al., 2017).

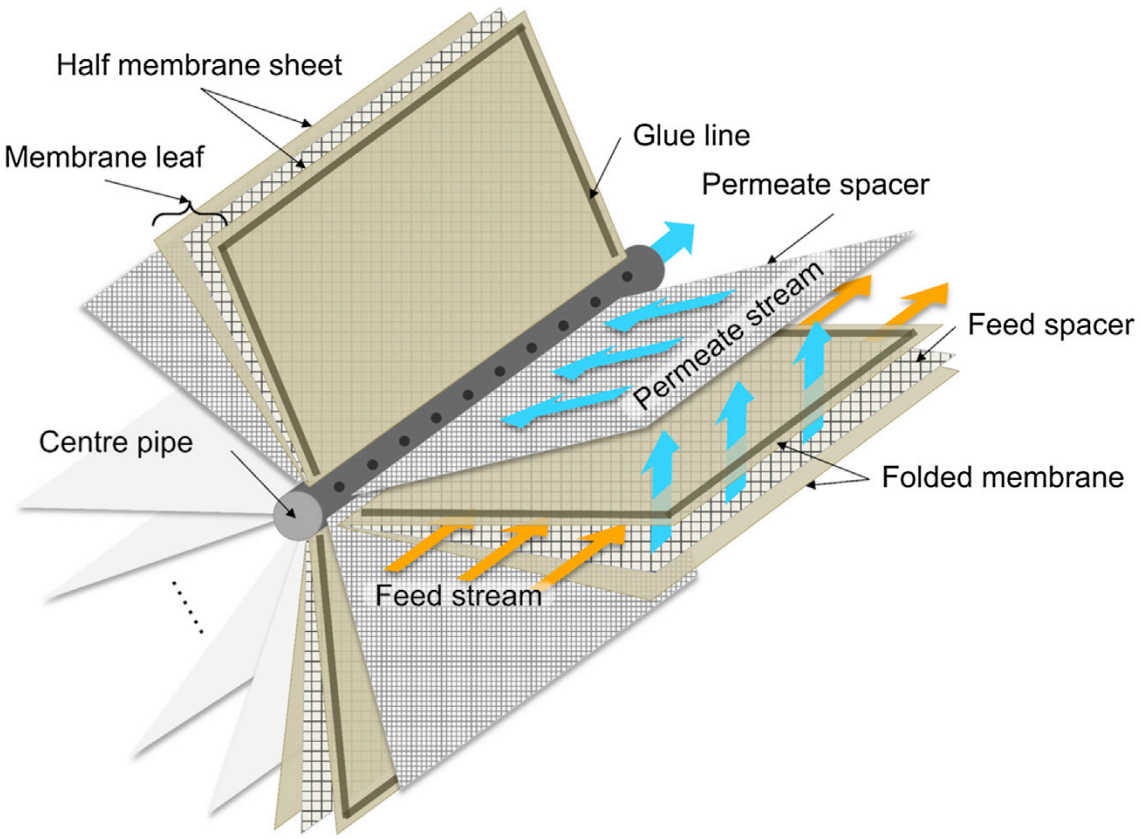

Figure 2: Illustration of the Spiral Wound Configuration (Gu et al., 2017)

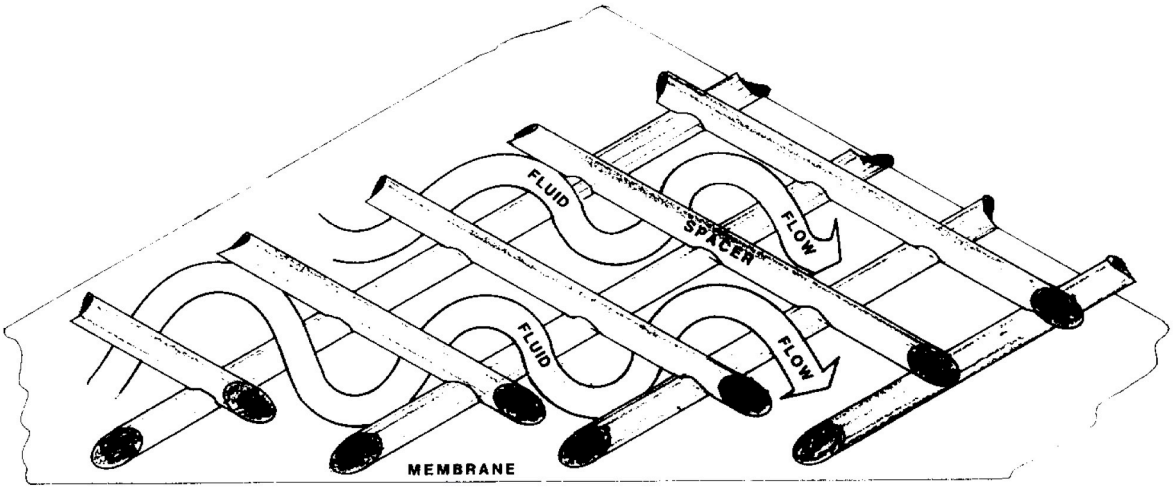

Figure 3: Fluid Flow Streamlines in Spacer Filled Channels (Costa et al., 1994)

2.4.5 Membrane Fouling and Concentration Polarization

Concentration polarization (CP) and fouling are still major challenges in membrane applications. Both CP and fouling increase with resistance to permeate flow and increase the energy demand and/or decrease the volume of water produced by a membrane system. The following discussion focuses on CP and fouling in UF and NF membranes.

No common definition for fouling exists (Melin and Rautenbach, 2004). However, fouling can be classified and characterized as following. Fouling is commonly classified as hydraulically reversible and hydraulically irreversible fouling (Jermann et al., 2007; Jermann et al., 2008; Schäfer et al., 2005). Hydraulically reversible fouling can be controlled by hydraulic control measures, such as backwash or cross-flow, while hydraulically irreversible fouling must generally be controlled through chemical cleaning. Chemically irreversible fouling refers to the long-term accumulation of foulants that can neither be removed hydraulically nor chemically. Hydraulic and chemical fouling control measures are discussed in more detail in Section 2.4.7. With respect to the material that increases the resistance to permeate flow, fouling is differentiated as organic and inorganic fouling, resulting from organic and inorganic matter, scaling (i.e. precipitation) of salts and biofouling caused by the growth of bacteria and the development of a biofilm on the membrane surface. Fouling due to salts (i.e. precipitation) has been reported to not affect fouling in NF applications in drinking water treatment other than through symbiotic fouling with NOM (Nyström et al., 1995; Her et al., 2000). Further information on biofouling in NF applications can be found elsewhere (e.g. Dreszer et al., 2014; Al-Amoudi, 2010). Due to the scope of the present thesis, the following discussion focuses on organic and inorganic fouling.

Fouling occurs as material is retained at the membrane surface or inside the membrane pores, accumulates, and increases the resistance to the permeate flow (Hermia, 1982; Mulder, 1996; Schäfer et al., 2005). Material accumulates when the permeation drag, the force that transports potential foulants towards the membrane, is greater than forces acting in the opposite direction (i.e. away from the membrane) (Song and Elimelech, 1995; Belfort, 1994). NOM is generally considered to be a main contributor to membrane fouling in drinking water treatment applications (Lee et al., 2004; Fonseca et al., 2007; Huang et al., 2007; Jermann et al., 2008; Schäfer et al., 1998; Zheng et al., 2009; Tinghir et al., 2009; Zularisam et al., 2006). The extent of fouling is not necessarily proportional to the total amount of NOM retained, but is rather governed by the retention of specific NOM fractions (Her et al., 2004; Schäfer, 2007; Zularisam et al., 2007; Winter et al., 2016). The NOM fractions that have been reported to be mainly relevant to membrane fouling are biopolymers and humic substances, which are mainly of aquatic and terrestrial origin, respectively (Zumstein and Buffle, 1989; Amy and Her, 2004; Biber et al., 1996).

For UF membranes, the biopolymers fraction of NOM generally contributes most to fouling (Jermann et al., 2007; Laabs et al., 2006; Wray et al., 2013). Fouling due to humic substances is generally not as extensive, although it is more difficult to control hydraulically (e.g. by backwashing) (Jermann et al., 2007; Jermann et al., 2008). Biopolymers have also been reported to substantially contribute to fouling of NF and tight UF membranes (Her et al., 2004; Jarusutthirak et al., 2002; Sari and Chellam, 2013). Humic substances, although effectively rejected, have not been reported to substantially contribute to fouling of NF membranes (Cho et

al., 1999). The limited contribution of humic substances to fouling has been attributed to charge repulsion effects, which enhance the back transport of humic substances in cross-flow systems (Cho et al., 1999; Her et al., 2007). The extent to which electrostatic repulsion contributes to fouling control has been demonstrated to increase with the ratio of cross-flow velocity to permeate flux (Seidel and Elimelech, 2002). Therefore, the effect of electrostatic repulsion on fouling due to humic substances is likely substantially less pronounced in dead end systems (i.e. systems with no cross-flow). Interactions between water constituents can also impact the filtration performance of NF and tight UF membranes. In particular, calcium and particulate matter have been reported to affect the increase in resistance to permeate flow for NF and tight UF membranes (Ahn et al., 2008; Lee et al., 2005a; Contreras et al., 2009; Mahlangu et al., 2015; Li and Elimelech, 2006). Calcium can form bridges between NOM molecules and between the membrane surface and NOM, as well as contribute to the aggregation of NOM by charge destabilization (Jermann et al., 2007; Jermann et al., 2008; Seidel and Elimelech, 2002), increasing the resistance to the permeate flow (Ahn et al., 2008; Listiarini et al., 2009; Mahlangu et al., 2015; Schäfer, 2007; Seidel and Elimelech, 2002). This impact of calcium on the increase in resistance was greatest at intermediate calcium concentrations (i.e. > 1 mM) (Listiarini et al., 2009; Mahlangu et al., 2015). NOM can also adsorb onto colloids and particulate matter resulting in the formation of a dense foulant layer (Jermann et al., 2008; Li and Elimelech, 2006). In addition to contributing to fouling, the presence of a cake layer can also enhance concentration polarization (CP) by hindering the back diffusion of dissolved material (Chong et al., 2008; Hoek and Elimelech, 2003; Tian et al., 2013; Li and Elimelech, 2006; Contreras et al., 2009).

CP, resulting from the accumulation of dissolved material rejected by the membrane, can also increase the resistance to the permeate flow (Schäfer et al., 2005; Mulder, 1996; Van den Berg and Smolders, 1990). Unlike with fouling, material does not deposit on the membrane surface or inside the membrane pores but accumulates in proximity to the membrane surface. CP is characterized by an equilibrium between the convective transport of material towards the membrane and the diffusive transport of retained material away from the membrane, a steady state that is expected to develop within the first minutes of filtration (Schäfer, 2007; Schäfer et al., 2005; Elimelech and Bhattacherjee, 1998). CP can affect the resistance to permeate flow by increasing the viscosity and the osmotic pressure of the solution being filtered, as well as the back-diffusion of retained solutes (Schäfer, 2007; Schäfer et al., 2005). If CP effects become extensive, solutes at the membrane surface can reach a critical concentration (i.e. solubility limit) beyond which they form a cake/gel layer which fouls the membrane surface (Elimelech and Bhattacharje, 1998; Schäfer et al., 1998; Mulder 1996; van den Berg and Smolders, 1990). In the literature, this critical concentration is also referred to as "gel concentration" (Mulder, 1996; Van den Berg and Smolders, 1990). If a material reaches the critical concentration, the back-diffusion of material is limited by the formation of a cake/gel layer. Under such conditions, the convective transport towards the membrane becomes greater than the diffusive transport away from the membrane and fouling occurs, which increases the resistance to permeate flow throughout the filtration phase. According to the Stokes-Einstein equation, the diffusivity and the diffusive transport of material depends on its size. NOM ranges in size from a few hundred Daltons (low molecular weight acids and neutrals) to over 20,000 Da (biopolymers) (Chin et al., 1994; Her et al., 2002; Huber et al., 2011; Jarusutthirak et al., 2002). The size of NOM also generally increases with ionic strength and decreases with pH of a solution due to changes in the shape of

NOM from uncoiled to coiled (Cornel et al., 1986). CP due to the retention of salts in RO and NF systems has been extensively investigated (e.g. Bhattacharjee et al., 2001; Brian, 1965; Hoek and Elimelech, 2003; Rautenbach and Albrecht, 1989; Verberk and van Dijk, 2006). Only a few studies have investigated CP due to retention of NOM in NF membranes. These have indicated that NOM can result in CP and therefore affect system performance (Yoon et al., 2005; Schäfer et al., 1998).

2.4.6 Filtration Laws

Hermia (1982) introduced filtration laws, which aim to model membrane fouling bases on the fouling mechanisms and are commonly applied to characterize membrane fouling (e.g. Schäfer, 2007; Winter et al., 2016; Byun et al., 2011; Ye et al., 2005). Cake or surface fouling is represented by the cake filtration model, which typically takes place when material larger than the membrane pore size is retained. The model for complete and intermediate blocking describes the pore blocking by material with a size approximately equal to that of the membrane pore size. Fouling caused by adsorption of material smaller than the membrane pore size and the tendency to adsorb onto the membrane material is considered by the model for standard blocking.

Cake filtration model: In the cake filtration model the resistance to permeate flow increases linearly with the volume filtered. The permeate flux can be calculated as a function of volume filtered by Equation 1 and filtration time by Equation 2 (Hermia, 1982; Bolton et al., 2006).

$$J = \frac{J_0}{1+k_c \cdot \frac{\mu}{\Delta P} \cdot V \cdot J_0} \qquad \text{Equation 1}$$

$$J = \frac{J_0}{\sqrt{1+2 \cdot k_c \cdot \frac{\mu}{\Delta P} \cdot t \cdot (J_0)^2}}$$ Equation 2

where, J: the permeate flux [ms^{-1}], J_0: the initial permeate flux [ms^{-1}], k_C: the fouling coefficient assuming cake filtration [m^{-2}]; V: specific volume of water filtered [m], μ: the dynamic viscosity [Pa s], ΔP: the trans-membrane pressure [Pa], and t: the filtration time [s].

Complete and intermediate blocking models: When a membrane fouls by complete or intermediate blocking, a portion of the membrane pores become blocked and, hence, impermeable. When the membrane fouls by complete or intermediate blocking, the permeate flux can be modelled using Equations 3 and 4, respectively.

$$J = J_0 \cdot e^{-k_{CB}t}$$ Equation 3

$$J = \frac{J_0}{1+k_{IB} \cdot t \cdot J_0}$$ Equation 4

where, k_{CB}: the fouling coefficient for complete blocking [s^{-1}], and k_{IB}: the fouling coefficient for intermediate blocking [m^{-1}].

Standard blocking model: The standard blocking model considers the accumulation of material on the membrane pore walls, which decreases the radius or the membrane pores. When the membrane fouls by standard blocking, the permeate flux can be modelled using Equation 5.

$$J = J_0 \left(1 - \frac{k_{SB} \cdot V}{2}\right)^2$$ Equation 5

where, k_{SB}: the fouling coefficient for standard blocking [m^{-1}].

2.4.7 Approaches for Mitigating Fouling and Concentration Polarization

Strategies to limit the impact of fouling on membrane process performance include selection or modification of membrane selectivity and material, pre-treatment of the feed solution to lower its fouling potential, the reversal of the accumulation of foulants by membrane cleaning, and the adjustment of operating conditions to limit the mass transport of foulants towards the membrane (e.g. optimizing hydrodynamic conditions, operating at lower flux).

Fouling can be limited through careful selection of the membrane with respect to the pore size and distribution, surface charge, surface roughness, hydrophobicity, and surface charge (Peng and Escobar, 2005; Reiss et al., 1999). Membrane material and surface modification aims to change the membrane surface properties to reduce the adsorption of foulants on the membrane surface by reducing the membrane's hydrophobicity and increase the surface charge to reduce the attracting forces or increase the repulsive forces between foulants (i.e., solute) and the membrane, respectively (Belfort, 1994). Membrane surface roughness has been reported to affect colloidal fouling, in particular with respect so smaller colloids (Boussou et al., 2007). The relationship between fouling and the pore size or MWCO of a membrane is complex, because it is highly dependent on the feed solution characteristics. However, Nyström et al. (1995) and Lin et al. (2009) reported that the fouling potential of NF and UF/tight UF membranes increases as the MWCO increases. Lin et al. (2009) tested UF membranes with MWCOs ranging from 100,000 Da to 1,000 Da and related the higher fouling potential of the membranes with higher MWCOs to an increase in internal fouling (i.e. inner pore adsorption or blocking).

With respect to pre-treatment, a wide range with varying effects on the feed water characteristics can be applied. Coagulation is effective at limiting membrane fouling (van der Bruegge et al., 2003). Coagulation controls fouling by converting colloids, critical for fouling, into larger particles that either exhibit less resistance once deposited onto the membrane surface or are more easily transported away from the membrane (Belfort, 1994). Adsorption processes, such as the application of activated carbon, can remove NOM, which otherwise contributes to fouling (Tatzel et al., 2009). Biological filtration has the ability to degrade NOM and, in particular, the biopolymers fraction of NOM (Maeng et al., 2008; Zheng et al., 2010; Halle et al., 2009), which substantially contributes to NOM fouling (Jermann et al., 2007; Laabs et al., 2006; Wray et al., 2013; Her et al., 2004; Jarusutthirak et al., 2002; Sari and Chellam, 2013). Hence, biological filtration has been reported to effectively reduce fouling in downstream NF and UF (Mosqueda-Jimenez and Huck., 2009; Halle et al., 2009). However, Nguyen and Roddick (2010) and Velten (2008) reported ozonation and subsequent biological filtration to have no effect on the extent of fouling in downstream UF. Several studies have also investigated the effect of oxidation processes on UF and NF fouling. Oxidation processes can effectively reduce membrane fouling by changing the hydrophobicity and the molecular weight distribution of NOM (Kim et al. 2008; Yu et al., 2016; Winter et al., 2016). However, Winter et al. (2016) reported that effective fouling control for NF and tight UF membranes (i.e. MWCOs of 1,000 Da and 8,000 Da) require high oxidant doses, which are not feasible in full scale applications. In addition to the processes discussed above, microfiltration can be applied prior to NF to effectively reduce NF fouling (Sari and Chellam, 2013; Wend et al., 2003).

Once fouling has occurred, it can be controlled by the reversal of the accumulation of foulants, either chemically or physically (i.e. hydraulically). Chemical cleaning is typically used to remove foulants that have been adsorbed to the membrane membranes. A wide range of chemical cleaning agents are commercially available. In general, acid cleaning is suitable for the removal of precipitated salts and alkaline cleaning is good for removing adsorbed organics (van der Bruggen et al., 2003; Liikanen et al., 2002). During chemical cleaning, cleaning agents change the morphology of foulants and alter the surface chemistry of membrane (Li and Elimelech, 2004; Di Martino et al., 2007). The frequency and intensity (i.e., concentration of the cleaning agent and exposure time) of the chemical cleaning varies significantly, depending on the filtration system (Porcelli and Judd, 2010). According to Porcelli and Judd (2010), membrane chemical cleaning can be described as a 5-step process: (i) Bulk reaction (i.e., hydrolysis) of the cleaning agents, (ii) Transport of the cleaning agent to the foulant layers attached to the membrane surfaces and on the membrane pores (iii) transport of the cleaning agent through the foulant layers to the membrane surface, (iv) chemical reactions (i.e., oxidation) that solubilise and detach foulants, and (v) transport of the foulants to the bulk solution. However, while effective at removing foulants from the membrane surface, chemical cleaning deteriorates the membrane and shortens the membrane operational life (Her et al., 2007; Abdullah, 2014). Hence, it is recommended to prevent fouling and apply efficient hydraulic measures to clean membranes to reduce the frequency of chemical cleaning events to limit costs and increase the membranes' operational life. Hydraulic cleaning approaches include permeate flux interruptions (i.e. relaxation phases), backwash, forward flush (i.e. periodic high velocity cross-flow), and air sparging. Forward flush and air sparging induce turbulence at the membrane surface, which enhances the back-transport of foulants (Belfort, 1994). During backwash, water (i.e. commonly

permeate) is permeated through the membrane in inverse direction to loosen the foulant cake layer. Permeate flux interruptions (i.e. relaxation phases) enhance hydraulic cleaning approaches by interrupting the mass-transport of foulants towards the membrane. As previously discussed, the applicability of hydraulic cleaning measures is limited in spiral wound configurations, which are most commonly used for NF and tight UF systems (see Section 2.4.4). For hollow fiber NF, Payant et al. (2016) reported that forward flush was an efficient hydraulic cleaning approach. The cleaning efficiency could be further substantially improved by the addition of a phase with air assisted forward flush. With respect to the mode of operation, Payant et al. (2016) reported a higher overall cleaning efficiency in cross-flow mode than in dead-end mode.

Hydraulic measures to control fouling are commonly applied in NF and tight UF membrane applications. Hydraulic control measures can limit fouling and CP by inducing shear stress at the membrane surface by either cross-flow (i.e. one phase flow) or air sparging (i.e. two phase flow) and enhancing the back-transport of material. It is expected that CP control requires continuous hydraulic measures because it is expected that CP develops rapidly (Schäfer, 2007; Schäfer et al., 2005; Elimelech and Bhattacherjee, 1998), while fouling can be controlled by either continuously or periodic hydraulically with hydraulic cleaning (Payant et al., 2016). In addition to enhancing the back-transport of material, fouling and CP can also be controlled by low permeate flux operation, at which the transport of material towards the membrane is limited.

With respect to balancing the mass transport of material away from the membrane and towards the membrane, which is related to the shear stress induced at the membrane surface and the magnitude of permeate flux, Field et al. (1995) introduced the concept of critical flux to describe

the steady state condition: At critical flux, the transport of foulants towards the membrane surface and away from the membrane are in equilibrium. At permeate flux values above the critical flux fouling occurs, while at permeate flux values at or below the critical flux, in theory, *no fouling occurs*. Due to the complex mixture of foulants, in practice, some fouling still occurs even during operation at or below critical flux values. Bachin et al. (2006) introduced the less restrictive concept of sustainable flux to account for the fact that fouling occurs when operating at a permeate flux that is less than critical. When operating at sustainable flux, *fouling is minimized* (rather than absent), which enables long term operation with limited need for membrane cleaning. Hence, operation at a sustainable flux is recommended and economically beneficial (Bachin et al., 2006; Field and Pierce, 2011). Because the extent of back-transport of potential foulants is proportional to the permeate flux that can be sustained and the back-transport increases with the shear stress induced at the membrane surface, the sustainable flux is a function of the shear stress induced at the membrane surface by hydraulic control measures (Belfort et al., 1994; Field et al., 1995; Bachin et al., 2006).

Several studies have investigated the effect of cross-flow velocity, as a parameter to describe the hydrodynamic conditions in membrane systems, on fouling and CP (e.g. Keucken et al., 2016; Braghetta, 1995; Costa and de Pinho, 2006; Seidel and Elimelech, 2002). However, the extent of fouling and CP is expected to be related to the shear stress induced at the membrane surface (Belfort et al., 1994; Sethi and Wiesner, 1997), which is not only a function of the cross-flow velocity, but also of the configuration and geometry of a membrane system (White, 2003; Koutsou et al., 2007). For this reason, relating the extent of fouling and CP to cross-flow velocity is only relevant when comparing systems with similar geometries. The use of shear stress at the

membrane surface as a parameter to relate the hydrodynamic conditions in a system to the extent of fouling and CP has been considered in applications where two phase flow (i.e. air sparging) is used for fouling and CP control (Tian et al., 2010; Xia et al., 2013; Laborie et al., 1999; Ratkovich et al., 2011; Cabassud et al., 2001; Chan et al., 2011; Jankhah, 2013). These studies indicate that both the magnitude and change in shear stress over time impact the extent of fouling and CP (Chan et al., 2011). Shear stress induced by cross-flow is also expected to impact the extent of fouling and CP in systems with single phase flow. For systems with spacer filled flow channels, typical of spiral wound membranes, hydrodynamic conditions have been characterized in terms of velocity distribution, shear stress induced at the membrane surface and mass transfer expressed by the Sherwood number (Shock and Miquel, 1987; Koutsou et al., 2007; Koutsou et al., 2009; Radu et al., 2014; Bucs et al., 2015). However, these parameters have not been correlated to the extent of fouling and CP that occur in membrane systems.

Chapter 3: Objectives of the Study

3.1 Knowledge Gaps

Nanofiltration (NF) and tight ultrafiltration (UF) membranes are treatment processes that are effective in terms of contaminant removal. The application of NF and tight UF membranes is, however, still limited. This is mainly related to fouling, concentration polarization (CP), as well as the complexity and cost of NF and tight UF systems. Several studies have developed recommendations for improving NF and tight UF system design and operation. However, several knowledge gaps remain that limit a more widespread application of this technology.

Limited knowledge exists with respect to NF and tight UF membrane operation in dead-end mode and in cross-flow mode. Operation in dead-end mode is much simpler than operation in cross-flow mode, and therefore likely less expensive. However, if CP dominates the increase in resistance to permeate flow, continuous measures to mitigate CP, such as operation in cross-flow mode, are required because CP is expected to develop rapidly within minutes of filtration of raw water (Schäfer, 2007; Schäfer et al., 2005; Elimelech and Bhattacherjee, 1998). Mitigating CP is especially important, if CP becomes extensive and induces the formation of a cake/gel layer. Payant et al. (2016) compared dead-end and cross-flow operation of NF membranes. However, in their study only particulate matter (i.e. kaolin) and polysaccharides (i.e. alginate) were considered as potential raw water constituents that may increase the resistance to permeate flow. Humic substances, which also affect the performance of membrane systems and are typically the NOM fraction present at the highest concentration (Zumstein and Buffle, 1989), were not considered and the contribution of CP to the overall increase in resistance was not assessed. The extent of CP due to the retention of salts in RO and NF systems has been extensively

investigated (e.g. Bhattacharjee et al., 2001; Brian, 1965; Hoek and Elimelech, 2003; Rautenbach and Albrecht, 1989). However, only a few studies have investigated CP due to retention of NOM in NF and tight UF membranes. These have indicated that NOM can result in CP and therefore affect system performance (Schäfer et al., 1998; Yoon et al., 2005). However, comprehensive knowledge on the effect of (i) the type of NOM (e.g. polysaccharides and humic substances), (iii) the concentration of NOM, (iv) the presence of particulate matter and calcium, and (v) the membrane MWCO on the contribution of CP to the total increase in resistance to permeate flow is not currently available. As previously discussed, CP is expected to develop rapidly within the first minutes of filtration (Schäfer, 2007; Schäfer et al., 2005; Elimelech and Bhattacharjee, 1998). However, this has never been investigated for NF and tight UF membranes in drinking water applications.

The impact of cross-flow on the material contributing to the increase in resistance to permeate flow by CP or by fouling in drinking water applications using NF and tight UF membranes has not yet been thoroughly investigated. The mechanism responsible for the increase in resistance in NF and tight UF membranes applied for drinking water treatment is of importance, because it directly impacts the effectiveness of hydraulic control measures, such as cross-flow operation. Likely, low velocity cross-flow is sufficient to control (i.e. limit) the increase in resistance to permeate flow resulting from CP and a higher velocity cross-flow is required to control (i.e. limit) the increase in resistance to permeate flow resulting from fouling (Schäfer et al., 2005). Operation with periodic interruption of permeate flow could also decrease the extent of fouling (Hong et al., 1997; Wu et al., 2008). Although commonly used for UF applications, permeate

interruption has not yet been considered for NF and tight UF membranes in drinking water treatment applications.

As previously discussed, the system configuration (e.g. spiral wound and hollow fiber membrane configurations) can have a significant impact on fouling and CP control, energy demand, and cost. Limited knowledge exists regarding the impact of the different membrane configurations and geometries (e.g. size of flow channels) on the extent of fouling and CP. In membrane systems with spacer filled flow channels (e.g. spiral wound membranes configurations), the maximum shear stress is substantially greater than in systems with empty flow channels (e.g. hollow fiber membrane configurations) at a given cross-flow velocity (Koutsou et al., 2007). For this reason, spiral wound configurations are considered to be superior in terms of fouling and CP control compared to hollow fiber configurations (Geraldes et al., 2002; Thorsen and Flogstat, 2006). However, spiral wound configurations generally require extensive pre-treatment to prevent clogging of the spacer filled flow channels, and a high feed pressure is generally required to overcome the headloss that occurs as water flows through the spacer filled flow channel (Sethi and Wiesner, 2000). In addition, fouling and CP control measures, such as backwashing or surface scouring, cannot be applied in spiral wound configurations. More recently, hollow fiber NF systems have become commercially available. Unlike spiral wound configurations, hollow fibers can be backwashed and air can be used for fouling and CP control (Bequet et al., 2002; Frank et al., 2001; Futselaar et al., 2003; Spruck et al., 2013; Verissimo et al., 2005; Verberk and van Dijk, 2006; Payant et al., 2017). Frank et al. (2001) observed less fouling and CP when filtering surface water using a prototype hollow fiber NF membrane than when using commercially available spiral wound NF membranes. However, because the hydrodynamic

conditions in the hollow fiber and spiral wound configurations are expected to differ, it is difficult to comprehensively compare the results obtained with these two configurations. To the best knowledge of the author, no approach has yet been developed to comprehensively compare spiral wound and hollow fiber membrane configurations. Also, the design of cross-flow membrane systems is more complex than the design of dead-end membrane systems and approaches to optimize the design of cross-flow membrane systems with respect to cross-flow velocity and operating permeate flux are still needed for improved designs and more widespread applications.

3.2 Objectives

3.2.1 Contribution of Fouling and CP to the Increase in Resistance to Permeate Flow (Objective 1)

The objective of the first part of the study was to quantify the contribution of fouling and CP to the total increase in resistance during filtration of model raw waters containing polysaccharides, humic substances, and a mixture of both as typical constituents of NOM in natural surface waters and to identify conditions under which extensive increase in resistance to permeate flow occurs. Because it has been reported that particulate matter and calcium can affect fouling and CP, the impact of these raw water constituents was also studied. Also, because fouling and CP are not only expected to depend on the raw water characteristics, but also on the membrane's selectivity, the impact of the MWCO of a membrane on CP and fouling was also investigated.

As previously discussed, CP is expected to develop rapidly within the first minutes of filtration (Schäfer, 2007; Schäfer et al., 2005; Elimelech and Bhattacharjee, 1998). However, this has

never been investigated for NF and tight UF membranes in drinking water applications. Hence, the present study was also to confirm the assumption that CP develops rapidly under conditions typical for drinking water treatment applications.

3.2.2 Mitigation of Fouling and CP (Objective 2)

The objective of the second part of the study was to quantify effect of cross-flow operation and permeate flux interruption (i.e. relaxation phases), as hydraulic control measures, on the extent and control of CP and fouling. Because the MWCO of the NF and tight UF membranes likely affects CP and fouling, membranes with various MWCOs ranging from 300 Da to 8000 Da were considered when assessing hydraulic control measures. The impact of hydraulic control measures was studied by monitoring the flux decline, estimating the permeate flux at steady state, and by characterizing the foulant layer. Based on the results, recommendations are proposed to minimize the resistance to permeate flow when operating NF and tight UF membranes for drinking water treatment.

3.2.3 Hydrodynamics, System Configuration and Geometry (Objective 3)

The objective of the third part of the study was to develop a framework to compare the performance of NF membranes of different configurations and geometries in terms of the permeate flux that can be sustained. To achieve this, the hydrodynamic conditions in spacer filled and empty flow channels of different configurations, representing spiral wound and hollow fiber membrane configurations respectively, were characterized when operating over a range of cross-flow velocities typical of spiral wound and hollow fiber systems. For these conditions, the extent of fouling and CP were quantified in terms of the permeate flux that can be sustained. A

semi-mechanistic relationship was developed to correlate the cross-flow velocity, system configuration and geometry to the average shear stress at the membrane surface and the permeate flux that can be sustained. Only NF membranes were considered because those membranes were found to be better suited for effective NOM removal than tight UF membranes (see Section 5.1).

3.2.4 Cost Analysis and Optimization for Hollow Fiber and Spiral Wound Configurations (Objective 4)

The objective of the fourth part of the study was to apply the framework developed in the previous section to determine operational parameters (i.e. operating permeate flux and cross-flow velocity) resulting in the lowest cost for both, spiral wound and hollow fiber configurations. The impacts of membrane life time and membrane cost on the optimal operation and systems' cost was evaluated. Spiral wound and hollow fiber configurations are comprehensively compared on the basis of capital and operational costs.

Chapter 4: Materials and Methods

4.1 Membrane Test Cells

Three types of membrane systems were considered (see Figure 4): CF042 test cells (Sterlitech, USA), a custom test cell, and a hollow fiber NF mini module (Pentair, X-Flow, Netherlands). The length and the width of the flow channel of the CF042 test cell were 85.5 mm and 39.2 mm respectively, corresponding to a total membrane surface area of 0.0034 m^2. If not specified otherwise, the height of the CF042 test cell was 2.3 mm. For the shear measurements and filtration tests discussed in Chapter 7, different flow channel heights were considered by adding shims to the CF042 test cells (see Table 3). Both conditions with and without spacers in the flow channel of the CF042 test cell were considered. The width of the flow channel of the custom test cell was similar to that of the CF042 test cell (i.e. 40 mm). However, the length of the custom test cell was greater (i.e. 910 mm), and only one flow channel height was considered for the custom test cell (see Table 3). The total equivalent membrane surface area of the custom test cell was 0.0364 m^2. For tests with spacer filled flow channels, diamond shaped spacers with filaments crossing in 90 degree angles were used for the CF042 test cells (Sterlitech, USA) and the custom test cell (Hydranautics, USA). The length and the inner diameter of the hollow mini module (Pentair, X-Flow, Netherlands) were 300 mm and 0.8 mm respectively. The total membrane surface area of the hollow fiber mini module was 0.07 m^2.

a)

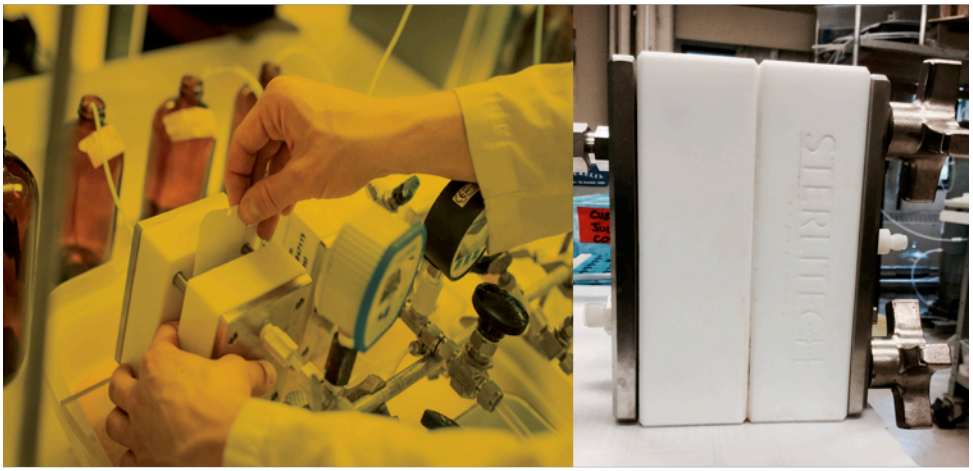

b)

c)

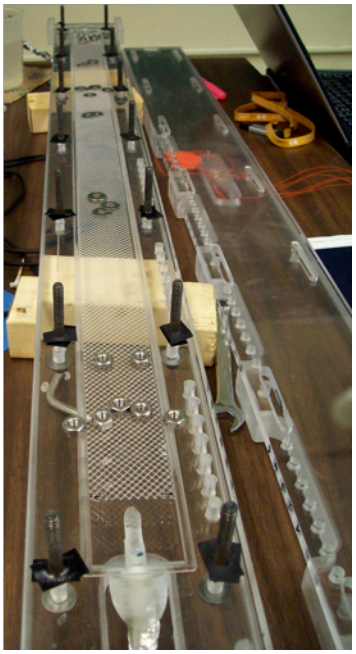

Figure 4: Membrane Test Cells (a: CF042 test cell; b: hollow fiber mini module; c: custom test cell)

Table 3: Configurations of the Membrane Test Cells

Flow channel height	Spacer thickness	Void Volume	Hydraulic diameter [mm]
CF042 test cell			
2.3 mm	none	1.00	4.2
0.78 mm	none	1.00	1.5
1.03 mm	none	1.00	1.1
1.84 mm	none	1.00	1.9
0.78 mm	0.43 mm	0.90	1.2
1.03 mm	0.78 mm	0.96	3.3
1.84 mm	1.65 mm	0.94	2.3
Custom test cell			
0.75 mm	0.78 mm	0.86	2.6
Hollow fiber mini module			
N/A	N/A	1.00	0.8

4.2 Model Raw Water Preparation

Model raw waters of various compositions were considered. The biopolymer and humic material content of the raw waters represent aquagenic (autochthonous) and pedogenic (allochthonous) or

microbial derived and terrestrial NOM, respectively (Amy and Her, 2004; Biber et al., 1996). In the model raw waters considered, the biopolymer and humic material were modelled using the polysaccharide alginate derived from brown algae (Sodium Alginate, Sigma Aldrich, Canada) and Suwannee River NOM (Suwannee River NOM 2R101N, International Humic Substances Society, United States of America), respectively. Note that, Suwannee River NOM 2R101N consists predominantly of humic substances. However, in contrast to humic acid and fulvic acid isolates, Suwannee River NOM 2R101N also contains lower molecular weight NOM fractions that are present in terrestrial NOM. Hence, Suwannee River NOM 2R101N was considered a good surrogate for terrestrial NOM. In the following, Suwannee River NOM 2R101N is discussed as a representative of humic substances, because they are the main constituent of this model NOM. More details on Suwannee River NOM 2R101N can be found elsewhere (Green et al., 2015).

To prepare the model raw waters, NOM surrogates (i.e. the polysaccharide alginate and/or Suwannee River NOM) were dissolved in Milli-Q laboratory water. Sodium bicarbonate at a concentration of 1 mM was added as a buffer. This concentration of bicarbonate also corresponds to an alkalinity that is within a range typical of that present in natural source waters (Hincks and Mackie, 1997). The retention of alkalinity during filtration ranged from approximately 2 % to 40 % (depending on the membrane MWCO) and the impact of alkalinity rejection on CP and resistance during filtration was calculated (Schäfer, 2007) to be negligible relative to the overall increases in resistance observed in the present study (see Appendix B.1) and, hence, is not further discussed. The pH was then adjusted to 7.0 (± 0.1) using sodium hydroxide or hydrochloric acid as needed. Prior to all filtration tests, all model raw water

solutions were filtered through a 0.45 μm filter (nitrocellulose). For tests with calcium and particulate matter, particulate matter and calcium were added to the model raw water as kaolin and calcium chloride, respectively, after the model raw water solutions were filtered through a 0.45 μm filter. The turbidity was adjusted to approximately 15 NTU by adding 15 mgL^{-1} of kaolin. The calcium concentration was set to 0.5 mM (50 mgL^{-1} as $CaCO_3$).

4.3 Analyses

4.3.1 DOC and UV Absorbance at 254 nm

Prior to analysis, samples were filtered through 0.45 μm filters (nitrocellulose). UVA absorbance at 254 nm (UVA_{254}) was measured using a UV 300, UV-Vis Visible Spectrometer (Spectronic Unicam, USA). DOC was analyzed using a Phoenix 8000 TOC analyzer (Teledyne Tekmar, USA).

4.3.2 Total Suspended Solids

Total suspended solids were analyzed in conformity the Standard Methods 2540D (AWWA, 2005).

4.3.3 Size Exclusion Chromatography

Prior to analysis, samples were filtered through 0.45 μm filters (nitrocellulose). Size exclusion chromatography (SEC) was performed using a High Performance Liquid Chromatography (HPLC) (Perkin Elmer, Canada) with DOC detection for the analysis of NOM in the feed and permeate. The method used was adopted from Huber et al. (2011). A TSK HW-50S column (Tosoh, Japan) was used as the stationary phase and a phosphate buffer (2.5 g/L KH_2PO_4 + 1.5 g/L Na_2HPO_4 x H_2O) was used as the mobile phase. The sample injection volume and flow rate

were 1 mL and 1 $mLmin^{-1}$, respectively. A GE Sievers 900 Turbo Portable TOC Analyzer (GE Sievers, Canada) with a sampling rate of 4 s and a detection range of 0.2 mg C/L to 10 mg C/L was used as the DOC detector.

4.4 Evaluation of Data from Filtration Tests

4.4.1 Dead End Filtration

For the filtration tests conducted in dead-end mode, as described in Section 4.5, fouling was quantified by the rate of fouling, quantified based on fouling coefficients obtained from standard filtration laws fitted to the experimental data collected during the filtration of model raw water (Hermia, 1982; Bolton et al., 2006) (see Section 2.4.6). Based on the minimum chi-square value, for all conditions investigated in the present study, the permeate flux could be best modeled by assuming that fouling was predominantly due to the formation of a cake layer on the membrane surface (see Equation 6), which is consistent with the results from Lin et al. (2009), which suggest that external fouling (i.e. gel formation) dominates for membranes with MWCOs of less than 10,000 Da. Therefore, the results are presented in terms of cake fouling coefficient (k_c). Typical results showing the model fitted to experimental data is presented in Figure 10 (Section 5.2). Note that, likely more than one fouling mechanism occur in parallel (Bolton et al., 2006). In the present study, the fouling behavior was modelled based on the dominant fouling mechanism, which allows to quantify the rate of fouling using a single fouling coefficient.

$$J = \frac{J_0^{'}}{1+k_c \cdot \frac{\mu}{\Delta P} \cdot V \cdot J_0^{'}} \qquad \text{Equation 6}$$

where, J: the permeate flux [ms^{-1}], J'_0: the initial permeate flux; k_C: the fouling coefficient assuming cake filtration [m^{-2}]; V: specific volume of water filtered [m], μ: dynamic viscosity [Pa s] and ΔP: trans-membrane pressure [Pa].

The initial permeate flux J'_0, which was a fitted parameter, was defined as the measured clean water flux (J_0) less the rapid decrease in the flux within the first few minutes of a filtration test (see Figure 10, Section 5.2). Because CP is expected to develop within the first minutes of filtration, the difference between J_0 and J'_0 was assumed to be due to CP (Schäfer, 2007; Schäfer et al., 2005; Elimelech and Bhattacharjee, 1998). Note that the validity of this assumption is further discussed in Section 5.2.2.

4.4.2 Cross-Flow Filtration

For the filtration tests considering cross-flow operation (see Sections 4.6 and 4.7), fouling was assessed based on the permeate flux the can be sustained. Cross-flow enhances the back-transport of material that accumulates at or on the membrane surface and the extent of back-transport is proportional to the permeate flux that can be sustained (Belfort et al., 1994; Field et al., 1995; Bachin et al., 2006). For this reason, the extent of fouling and concentration polarization (CP) was quantified based on the permeate flux at steady state, which corresponds to the sustainable and recommended operational flux (Bachin et al., 2006; Field and Pearce, 2011). The permeate flux at steady state was estimated by fitting standard filtration laws (Hermia, 1982; Bolton et al., 2006) (see Section 2.4.6) – i.e. a modified version of Equation 6 to account for the steady state flux during cross-flow operation (see Equation 7) - to the experimental data. Again, based on the minimum chi-square value, for all conditions investigated in the present study, the permeate flux could be best modelled by assuming that fouling was predominantly due to the

formation of a cake layer on the membrane surface. Note that, likely multiple fouling mechanisms can occur in parallel (Bolton et al., 2006). In the present study, the fouling behavior was modelled based on the dominant fouling mechanism (i.e. cake fouling) and the rate of fouling was quantified using the estimated cake fouling coefficient (k_C).

$$J = \frac{J_0 - J_{SS}}{\sqrt{1+2 \cdot k_c \cdot \frac{\mu}{\Delta P} \cdot t \cdot (J_0 - J_{SS})^2}} + J_{SS} \qquad \text{Equation 7}$$

where, J: instantaneous permeate flux [ms^{-1}], J_0: initial permeate flux, J_{SS}: steady state permeate flux [ms^{-1}], μ: dynamic viscosity [Pa s], ΔP: trans-membrane pressure [Pa], and t: filtration time [s]; when fitting Equation 7 to the data, the fitted parameter (i.e. steady state flux) was constrained to values greater than or equal to zero.

4.5 Contribution of Fouling and CP to the Increase in Resistance to Permeate Flow (Objective 1)

4.5.1 Membrane Filtration Tests

The experimental setup, illustrated in Figure 5, was operated with 3 CF042 test cells in parallel (note, no shims or spacers were used to alter the channel height or configuration of the CF042 test cells). The experimental setup consisted of feed vessels, membrane cells, bleed lines and permeate collection systems. Two feed vessels were used, one containing clean water and the other containing a model raw water. The pressure applied to both vessels was equal, enabling the feed to the membrane to be switched between model raw water and clean water without causing any pressure variation in the membrane cells. The transmembrane pressure applied to the vessels was kept constant at 2.8 ± 0.1 bar (i.e. 40.0 ± 1.0 psi). The membrane filtration experiments were

conducted as constant pressure and variable flux tests. The tests were conducted at room temperature (23°C ± 1 °C). The CF042 test cells were operated in a pseudo dead-end mode with a continuous bleed that introduced a very low and constant cross-flow of less than 0.0001 m/s. The bleed line allowed the liquid to be purged from the membrane cell when the feed was switched, while still providing pseudo dead-end operation. The corresponding residence time in the flow channel of the membrane test cell was approximately 14 minutes. All filtration tests were conducted in triplicate in three sequential phases:

1. pre-clean water filtration phase (for a minimum of 3 hours)
2. filtration phase with model raw waters (for approximately 3 hours)
3. post-clean water filtration phase (for a minimum of 45 minutes)

The filtration tests were conducted in these three sequential phases to quantify the contribution of CP and fouling to the increase in the resistance to permeate flow as discussed in more detail in Section 5.2.2. Immediately prior to the start of the filtration phase with model raw water, the drain valve was opened and the content of the flow cell was purged, ensuring that the concentration of NOM in the flow cell at the start of the filtration of model raw water was equivalent to that of the model raw water. The drain was then partially closed to generate a low and constant low cross-flow velocity of 0.0001 m/s.

Milli-Q laboratory water was used for clean water flux tests prior and post filtration of model raw waters. The pH of the Milli-Q laboratory water used for clean water flux tests was also adjusted to 7.0 (± 0.1) using sodium hydroxide.

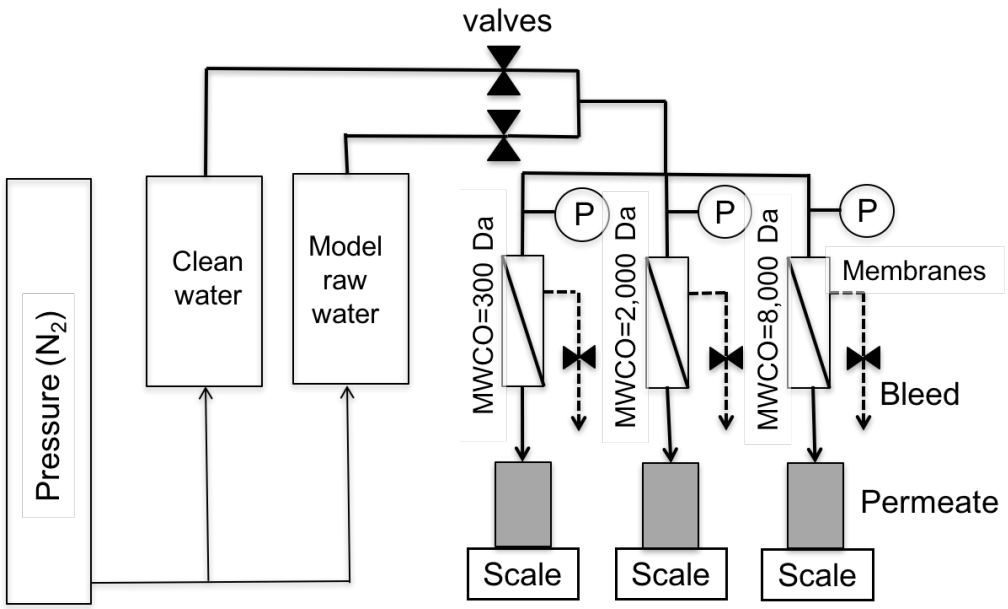

Figure 5: Experimental Setup I for Dead-End Filtration
(setup illustrated with 3 parallel membrane test cells)

Flat sheet, thin film composite polyamide (PA) membranes with nominal molecular weight cut offs (MWCOs) of approximately 300 Da (DK series, GE Osmonics), 2000 Da (GH series, GE Osmonics) and 8000 Da (GM series, GE Osmonics) were considered as a representative range for NF and tight UF membranes. The intrinsic membrane resistances for the 300 Da, 2,000 Da and 8,000 Da MWCO membranes were 9.0 10^{13} ± 1.1 10^{13} m^{-1}, 8.1 10^{13} ± 1.1 10^{13} m^{-1} and 2.2 10^{13} ± 2.0 10^{12} m^{-1}, respectively.

4.5.2 Model Raw Water Composition

Model raw waters with 3 different NOM compositions were considered: (i) alginate, (ii) Suwannee River NOM (SRNOM) and (iii) mixtures of SRNOM and alginate at a carbon mass ratio of 4:1. The ratio of 4:1 in the mixtures of SRNOM and alginate were selected based on

humic substances to biopolymers ratios obtained from size exclusion chromatography (SEC) analyses of a local surface water (Jericho Pond, Vancouver, Canada) and is also consistent with the ratios reported in literature, which indicates that humic substances account for 70-80 % of the NOM in many natural waters (Zumstein and Buffle, 1989). All three model raw water compositions considered were tested at two DOC concentrations: 5 mgL^{-1} and 10 mgL^{-1}. To assess the interactions between different NOM fractions, calcium and particulate matter on the contribution of CP and fouling to the total increase in Resistance to permeate flow, particulate matter and calcium were added to the model raw water as kaolin and calcium chloride, respectively. The compositions of the model raw waters used for the different filtration tests are summarized in Table 4.

Table 4: List of Different Model Raw Water Compositions Considered

SRNOM[a] [$mg_C L^{-1}$]	Alginate [$mg_C L^{-1}$]	Calcium [$mg_{CaCO3} L^{-1}$]	Particulate Matter[b] [$mg L^{-1}$]
5	0	0	0
5	0	50	0
5	0	50	15
0	5	0	0
0	5	50	0
4	1	0	0

a: Suwannee River NOM
b: Added to model turbidity

4.6 Mitigation of Fouling and CP (Objective 2)

4.6.1 Membrane Filtration Tests

The experimental setup (see Figure 6) was operated with three CF042 test cells in parallel (note, no shims or spacers were used to alter the channel height or configuration of the CF042 test cells). The experimental setup consisted of a feed tank, membrane cells, back-pressure valves, permeate collection systems and a variable speed pump. The variable speed pump (Hydra-Cell, USA), the back-pressure valves, and the by-pass, were used to control the trans membrane pressure and the cross-flow velocities. The experimental setup was operated under constant pressure and variable flux. Cross-flow velocities of approximately 0 (i.e. approximately 10^{-4} m/s; corresponding to dead end operation), 0.05 ms^{-1} and 0.25 ms^{-1} were considered. A cross-flow velocity of 0.25 ms^{-1} was chosen as the upper limit because no significant fouling was observed for this cross-flow velocity during initial tests with the membranes with MWCOs of 300 Da and

2,000 Da. Also, 0.05 ms^{-1} and 0.25 ms^{-1} correspond to the lower and upper limit of cross-flow velocities commonly used in practice (Bucs et al., 2015; Malek et al., 1996). The permeate was returned into the feed-tank by a peristaltic pump during a 10-minute period every hour to minimize the volume of model raw water used and to maintain a constant concentration of NOM in the system. Permeate interruption (i.e. relaxation) phases were introduced by closing solenoid valves on the permeate line for 10 minutes every hour. All experiments were conducted in duplicate in two sequential phases: pre-clean water filtration, and filtration of model raw waters. The transmembrane pressure applied during the filtration tests was kept constant at 2.8 ± 0.1 bar (i.e. 40.0 ± 1.0 psi). For dead end operation, the temperature of the raw waters was 23 ±1 ºC (i.e. room temperature). For cross-flow operation, the temperature ranged from 23 ºC to 26 ºC, depending on operating conditions. For all conditions, the measured permeate flux was normalized to a temperature of 20 ºC by accounting for the impact of temperature on the viscosity.

Milli-Q laboratory water was used for clean water flux tests prior and post filtration of model raw waters. The pH of the Milli-Q laboratory water used for clean water flux tests was also adjusted to 7.0 (± 0.1) using sodium hydroxide.

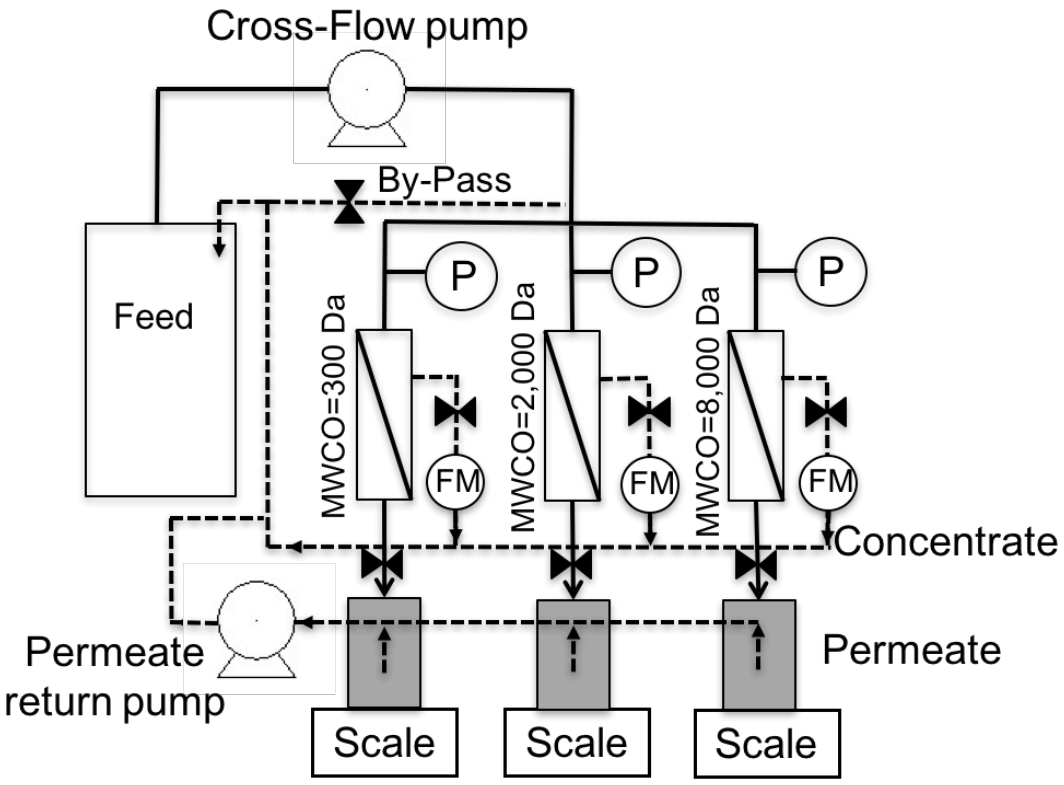

Figure 6: Experimental Setup II for Cross-Flow Filtration
(setup illustrated with 3 parallel membrane test cells)

Flat sheet, thin film composite polyamide (PA) membranes with nominal molecular weight cut offs (MWCOs) of approximately 300 Da (DK series, GE Osmonics), 2000 Da (GH series, GE Osmonics) and 8000 Da (GM series, GE Osmonics) were considered as a representative range for NF and tight UF membranes. The intrinsic membrane resistances for the 300 Da, 2000 Da and 8000 Da MWCO membranes were $9.0\ 10^{13} \pm 1.1\ 10^{13}\ m^{-1}$, $8.1\ 10^{13} \pm 1.1\ 10^{13}\ m^{-1}$ and $2.2\ 10^{13} \pm 2.0\ 10^{12}\ m^{-1}$, respectively.

4.6.2 Model Raw Water Composition

The model raw water contained a mixture of SRNOM and alginate, a 4:1 (SRNOM:alginate) and were adjusted to a DOC concentration of 5 mg C/L. The turbidity was adjusted to 15 NTU by adding 15 mgL^{-1} of kaolin and the calcium concentration was set to 0.5 mM (50 mgL^{-1} as $CaCO_3$).

4.6.3 Characterization of Foulant Layer

The foulant layer composition was assessed by first extracting the foulants from the membrane surface and then characterizing the extracted material. For extraction, membranes were placed in beakers with a 20 ppm hypochlorite solution and sonicated for 30 minutes following the completion of a filtration test. The membranes were then removed and the solution filtered through a 1.2 μm glass filter (Fisher Scientific, USA). A filter pore size of 1.2 μm was selected to separate the kaolin particles from the other model raw water constituents. The retained material was analyzed for total suspended solids, while the filtered solution was analyzed for DOC and UV absorbance at 254 nm. The retention of kaolin by the 1.2 μm filter was greater than 96 %. Adsorption of calcium onto kaolin is expected to be negligible (Atesok et al., 1988) and, hence, calcium is expected to pass through the 1.2 μm filter and not expected to affect the TSS measurements. The results are presented in terms of normalized mass, which corresponds to the ratio of mass of material extracted from the membrane surface to the mass of material present in the volume of model raw water permeated through the membrane during filtration tests. For the material where transport towards the membrane is governed by convection (i.e. polysaccharides and particulate matter) and under conditions without cross-flow (i.e. without enhanced back-transport), values lower than unity for the normalized mass were attributed to

incomplete recoveries during the extraction of the foulant layer. The recovery efficiencies were 68 % to 71 % and 88 % to 91 % for particulate matter (i.e. kaolin) and polysaccharides (i.e. alginate), respectively. For the material where the diffusive transport away from the membrane is significant (i.e. humic substances), values lower than unity were attributed to incomplete recoveries and to the diffusive back transport. An additional filtration test was conducted where the concentration of particulate matter, polysaccharides and humic substances in the water exiting the membrane test cell through the slow drain were monitored. The corresponding mass balance confirmed that values for normalized mass of less than one for particulate matter and polysaccharides were indeed due to loss of particulate matter and polysaccharides during sampling and/or extraction and that values for normalized mass of less than one for humic substances were predominantly related to the diffusive back-transport (see Appendix D1).

4.7 Hydrodynamics, System Configuration and Geometry (Objective 3)

4.7.1 Membrane Filtration Tests

The experimental setup (see Figure 7) was operated with two CF042 test cells in parallel, with a hollow fiber NF mini module and a custom test cell. The setup was similar to the experimental setup II (see Section 4.6.1). However, permeate was not returned into the feed reservoir. The cross-flow was generated using peristaltic pumps (Masterflex, USA) for the CF042 test cell and the custom test cell and a piston pump (Hydra-Cell, USA) for the hollow fiber mini module. For all filtration tests, the temperature of the solution in the cross-flow system was monitored. During the filtration tests, the feed reservoir was pressurized using compressed nitrogen to generate the trans-membrane pressure required for permeation. The pressure was measured at the inlet and the outlet of the membrane test cells.

Laboratory water was used for clean water flux tests prior and post filtration of model raw waters. The pH of the laboratory water used for clean water flux tests was also adjusted to 7.0 (± 0.1) using sodium hydroxide.

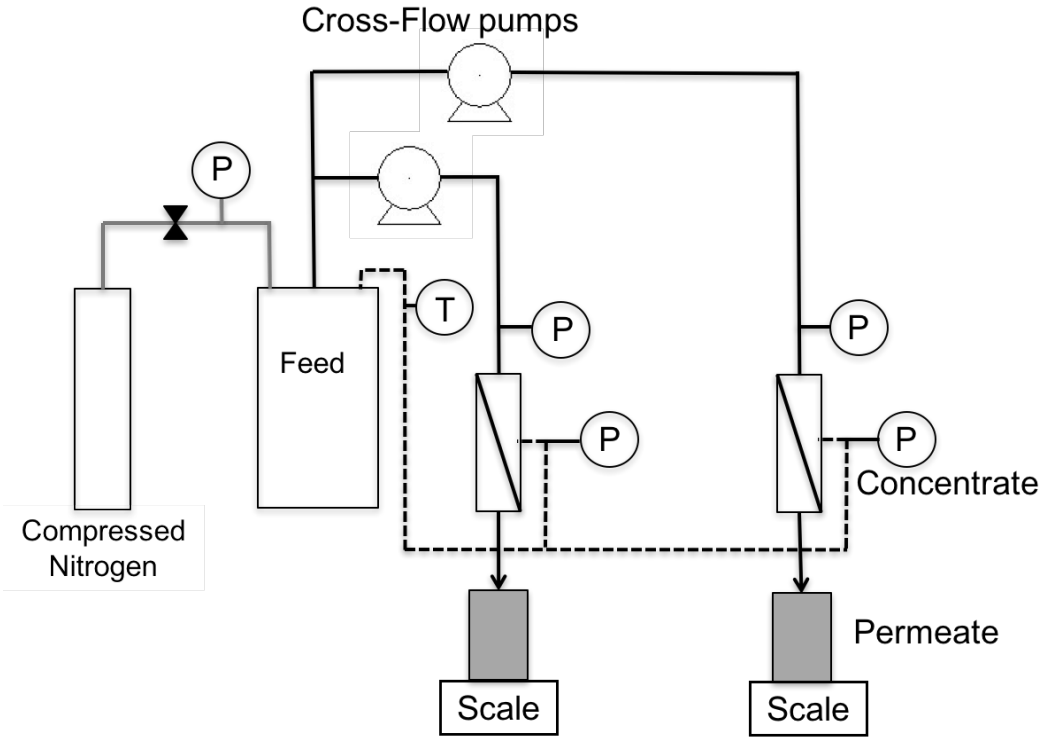

Figure 7: Experimental Setup III for Cross-Flow Filtration
(setup illustrated with 2 parallel membrane test cells, one operated with a spacer filled flow channel and one with an empty flow channel configuration)

Two series of filtration tests were performed with the CF042 cells, operated with NF membranes with a nominal molecular weight cut off (MWCO) of 600 to 800 Da (NFG series, Synder Filtration, USA). A third series of filtration tests was performed with the inside-out hollow fiber mini module operated with NF membranes with a nominal MWCO of 1000 Da (Pentair, X-Flow,

Netherlands). Results of the present study demonstrated that membranes with a MWCO of < 2,000 Da could be used to effectively remove NOM (see Section 5.1).

The recovery was kept below 50 % (i.e. limiting the maximum DOC concentration of the water to be filtered to 20 mgL^{-1}). The permeate flux was normalized to a temperature of 20 ºC by accounting for the impact of temperature on the viscosity. Due to variations in the room temperature, tests were conducted at temperatures ranging from 19.1 °C to 25.0°C with the variation in temperature within a single filtration test being less than 2.7°C

The first series of filtration tests, performed with CF042 test cells, were conducted at a relatively high initial permeate flux and for a duration of approximately 20 hrs. The high initial permeate flux resulted in substantial flux decline during filtration tests. The extent of fouling and CP in spacer filled and empty flow channels were assessed based on the permeate flux decline and estimated steady state permeate flux values. The geometries (i.e. flow channel height) and cross-flow velocities were adjusted to achieve average shear stress values of 0.5 Pa, 2.5 Pa and 5.0 Pa at the membrane surface.

The second series of filtration tests, performed with the CF042 test cells, were identical to the first series with the exception that the tests were conducted with an initial permeate flux equivalent to the maximum steady state permeate flux estimated as part of the first series of filtration tests, for a given set of experimental conditions, to validate the steady state flux estimated during the first series of filtration tests.

The third series of filtration tests, performed with the hollow fiber mini module, were to confirm if the results obtained using CF042 membrane test cells with empty flow channel configurations (i.e. without spacers) were representative of systems with hollow fiber configurations with inside-out permeate flow. The test was performed at a cross-flow velocity adjusted to achieve a sear stress value of 5.0 Pa at the membrane surface.

The experimental conditions (i.e. average shear stress, initial permeate flux, flow channel height and cross-flow velocity) for all filtration tests are summarized in Table 5.

Table 5: Experimental Conditions for Filtration Tests

Average shear stress [Pa]	Initial permeate flux [$Lm^{-2}h^{-1}$]	Spacer	Flow channel height [mm]	Cross-flow velocity [ms^{-1}]
CF042 cell – Series 1				
0.5	37.0	No	1.08	0.08
	39.8	Yes	1.84	0.09
	38.7	No	1.08	0.23
	38.7	Yes	1.84	0.16
2.5	38.3	No	1.08	0.60
	39.2	Yes	1.84	0.46
	41.3	No	1.84	1.04
	41.3	Yes	1.08	0.24
5.0	43.2	No	0.78	0.92
	45.2	Yes	1.08	0.62
	38.5	No	1.08	1.20
	38.6	Yes	0.78	0.53
CF042 cell – Series 2				
0.5	9.2	No	1.08	0.12
	8.9	Yes	1.84	0.09
2.5	16.0	No	1.84	1.04
	16.2	Yes	1.08	0.24
5.0	24.2	No	0.78	0.92
	25.2	Yes	1.08	0.62
Hollow fiber mini module – Series 3				
5.0	25.0	No	0.8	0.50

4.7.2 Raw Water

The raw water being filtered was a natural surface water (Jericho Pond, Vancouver, BC) diluted with tap water to a constant DOC concentration of 10 (± 0.3) mgL^{-1} . Jericho Pond water contains a broad spectrum of NOM fractions of aquagenic and terrestrial origin, predominantly consisting of humic substances and containing a substantial amount of biopolymers (see Appendix B1). Prior to the filtration tests, the raw water was pre-filtered with a 5 µm cartridge filter (Mc-MasterCarr, USA). Filtration with a 5 µm filter is typically applied as pre-treatment in full scale spiral wound NF applications (Shetty and Chellam, 2003).

4.7.3 Shear stress Measurements

For shear stress measurements, the solution was not pressurized and no permeation took place. The shear stress at the membrane surface was measured in the CF042 test cells with various channel heights and configurations (see Table 3) and the custom test cell with a spacer filled channel configuration using an electrochemical method (Fulton et al., 2011; Böhm et al., 2014; Jankhah, 2013). The shear probes, consisting of platinum wire with a diameter of 0.5 mm, were installed into a Plexiglas sheet such that they sat flush with the inside surface and positioned where a membrane would otherwise be located. The shear stress was measured at different locations using multiple shear probes installed next to each other in a row on a Plexiglas sheet, orthogonal to the direction of flow. In the direction of flow, the shear stress at different locations was measured by sliding the Plexiglas sheet, containing the row of shear probes, along length of the flow channel. The setup for the shear measurements using the CF042 test cell is shown in Figure 8. For the CF042 membrane test cell, the shear stress was measured every 5 mm in the direction of flow and orthogonal to the direction of flow. For the custom test cell, the shear stress

was measured every 1 mm in the direction of flow and orthogonal to the direction of flow, providing greater resolution into the distribution of shear stress in the test cell. For the custom test cell, shear stress was measured over a length of 35 mm, halfway along the custom test cell, from 470-505 mm. Radu et al. (2014) and Bucs et al. (2015) reported that hydrodynamic conditions are similar throughout spacer filled flow channels. The shear stress values in the CF042 membrane test cells were measured for cross-flow flows of 300 $mLmin^{-1}$, 540 $mLmin^{-1}$ and 1360 $mLmin^{-1}$, which corresponds to cross-flow velocities ranging from 0.06 ms^{-1} to 0.79 ms^{-1}. The shear stress values in the custom test cell was measured at a cross-flow of 270 $mLmin^{-1}$, which corresponds to a cross-flow velocity of 0.18 ms^{-1}.

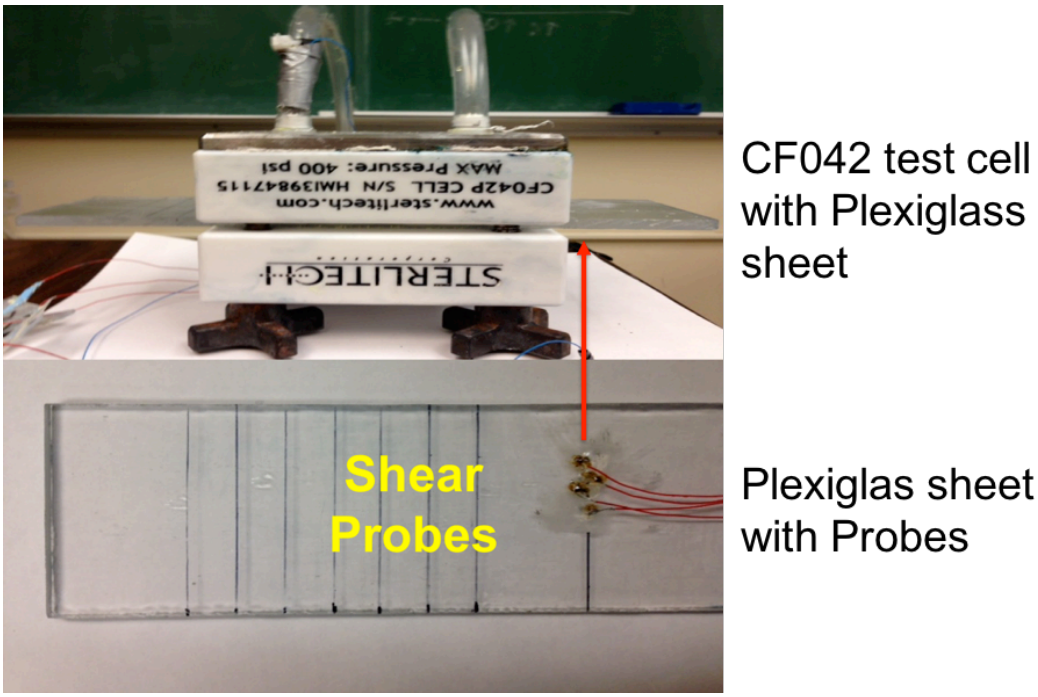

Figure 8: Test Setup for Shear Measurements – CF042 Test Cell

4.8 Cost Comparison and Optimization (Objective 4)

The costs considered in the present study are the cost for purchasing membrane modules, replacing membrane modules and the energy costs related to cross-flow operation and permeation to operate the membrane system over the design life.

The total energy costs were calculated as the sum of the power required for cross-flow operation and the power required for permeation, multiplied by the time of operation and the specific energy cost.

The power required for cross-flow is calculated as the product of the pressure loss at a given membrane module at a given cross-flow velocity, the flow through the membrane module and the number of modules required for the design flow (see Equation 8) (White, 2003). The friction factors for spiral wound and hollow fiber configurations were calculated using Equations 9 and 10, respectively (White, 2003; Koutsou et al., 2007). The decrease in permeate flux due to the pressure drop inside the flow channels was considered by calculating the average pressure in the module using Equations 11-12 (White, 2003), which was used to calculate the average permeate flux over the module length (see Equation 13) (Schäfer, 2007; Mellevialle et al., 1996). The change in cross-flow velocity over the length of the modules due to permeation was less than 3 % for the range of conditions considered. Hence, the effect of the change in cross-flow velocity over the length of the modules on the pressure loss along the length of the modules was negligible. The average permeate flux obtained was used for the cost evaluation. The cross-flow velocity used to calculate the energy demand was chosen to be sufficient to prevent fouling at the point of the highest permeate flux (i.e. at the inlet of the module).

$$P_{cross\text{-}flow} = \frac{f \cdot \frac{L_{Module}}{d_h} \cdot \delta \cdot \frac{(v_{cross\text{-}flow})^3}{2} \cdot A_{cross\text{-}section,Module} \cdot Q_{Permeate}}{A_{Membrane,Module} \cdot J_{SS} \cdot \eta}$$

Equation 8

$$f = \frac{64}{Re} = \frac{64 \cdot \mu}{v_{cross\text{-}flow} \cdot d_h \cdot \delta}$$

Equation 9

$$f = 2.3 \cdot Re^{-0.31} = 2.3 \left(\frac{v_{cross\text{-}flow} \cdot d_h \cdot \delta}{\mu} \right)^{-0.31}$$

Equation 10

$$TMP = \frac{J_{SS}}{L_P}$$

Equation 11

$$TMP_{Avg} = TMP\text{-}f \cdot \frac{L}{2d_h} \cdot \frac{v_{cross\text{-}flow}^2}{2} \cdot \delta$$

Equation 12

$$J_{SS,Avg} = TMP_{Avg} \cdot L_P$$

Equation 13

where, $P_{cross\text{-}flow}$: power required for cross-flow operation [W], f: the friction factor [/], L_{Module}: the length of the membrane module [m], d_h: the hydrodynamic diameter [m], δ: density of water [kgm^{-3}], $v_{cross\text{-}flow}$: the cross-flow velocity [ms^{-1}], $A_{Cross\text{-}Section,\ Module}$: cross-sectional area of the membrane module's flow channel [m^2], $A_{Membrane,Module}$: the total membrane surface area of the membrane module [m^2], $Q_{Permeate}$: the total permeate (i.e. design) flow [m^3s^{-1}], J_{SS}: the operating

flux, which is approximated by the estimated as the steady state flux [ms^{-1}], η: pump efficiency, μ: dynamic viscosity [Pa s], TMP: trans-membrane pressure [Pa], L_P: the permeability of the membrane [$Lm^{-2}Pa^{-1}$], TMP_{Avg}: average trans-membrane pressure over the whole module length, and $J_{SS,Avg}$: average permeate flux over the whole module length.

The power required for permeation was calculated using Equation 14 (White, 2003; Schäfer, 2007).

$$P_{Permeation} = \frac{J_{SS}}{L_P} \cdot Q_{Permeate} \qquad \text{Equation 14}$$

where, $P_{Permeation}$: power required for permeation [W].

The cost for purchasing and replacing the membrane modules, considering full scale application, was calculated as the product of the membrane area required and the cost per unit of membrane area. The replacement of the membrane was based on the assumed membrane lifetime (the assumed membrane lifetime is listed in Table 8, Section 8.1). The membrane area required was calculated using Equation 15.

$$A_{Membrane,total} = \frac{Q_{Permeate}}{J_{SS}} \qquad \text{Equation 15}$$

All costs are presented as net present value. The net present value for purchasing and replacing membranes was calculated using Equation 16 and for the energy required to operate the system in Equation 17 (http://www.rechnungswesen-verstehen.de/investition-finanzierung/Kapitalwertmethode.php) (the assumed rate of return is listed in Table 8, Section 8.1).

$$MC = \sum_{n=\frac{DL}{ML}\text{-}1}^{n=0} MC_j \cdot (1+i)^{n \cdot ML}$$

Equation 16

$$EC = EC_a \frac{(1+i)^{DL}\text{-}1}{i \cdot (1+i)^{DL}}$$

Equation 17

where, MC: the total cost for purchasing and replacing the membranes [$], DL: the design life [a], ML: the membrane lifetime [a], MC_j: the cost for each membrane purchase and replacement [$], i: rate of return [/], EC: the total energy costs over the design life [$], and EC: the annual energy costs [$].

Chapter 5: Contribution of Fouling and CP to the Increase in Resistance to Permeate Flow (Objective 1)

The objective of the first part of the study was to quantify the contribution of fouling and CP to the total increase in resistance during filtration of model raw waters containing polysaccharides, humic substances, and a mixture of both as typical constituents of NOM in natural surface waters and to identify conditions under which extensive increase in resistance to permeate flow occurs. Because it has been reported that particulate matter and calcium can affect fouling and CP, the impact of these raw water constituents was also studied. Also, because fouling and CP are not only expected to depend on the raw water characteristics, but also on the membrane's selectivity, the impact of the MWCO of a membrane on CP and fouling was also investigated.

As previously discussed, CP is expected to develop rapidly within the first minutes of filtration (Schäfer, 2007; Schäfer et al., 2005; Elimelech and Bhattacharjee, 1998). However, this has never been investigated for NF and tight UF membranes in drinking water applications.

5.1 Rejection of Natural Organic Matter

The amount of material rejected by the membranes was defined based on the difference between that present in the feed (i.e. the model raw water) and that present in the permeate. As illustrated in Figure 9, the membranes with MWCOs of 300 Da and 2000 Da could effectively reject all of the alginate present in model raw waters, and the membrane with a MWCO of 8000 Da could reject most of the alginate present in model raw waters. This was expected because the molecular weight of alginate is greater than 10,000 Da (Jarusutthirak et al., 2002; Huber et al., 2011) and the MWCOs of all the membranes considered are lower than 10,000 Da (i.e. ranging from 300

Da to 8,000 Da). Only a small amount of the larger constituents in SRNOM was rejected by the membrane with a MWCO of 8000 Da. The extent of the rejection increased as the MWCO of the membranes decreased, with all of the organic material being rejected by the membrane with a MWCO of 300 Da. Again, this was expected, because most of the constituents of SRNOM have a molecular weight in between 300 Da and 8,000 Da (Chin et al., 1994; Her et al., 2002).

Note, that NOM in most surface waters consists mainly of humic substances (i.e. lower molecular weight NOM) (Zumstein and Buffle, 1989). Because effective NOM removal is one of the main motivation to implement NF and tight UF membranes in drinking water treatment, membranes with lower MWCOs (i.e. < 2,000 Da) are recommended for this application.

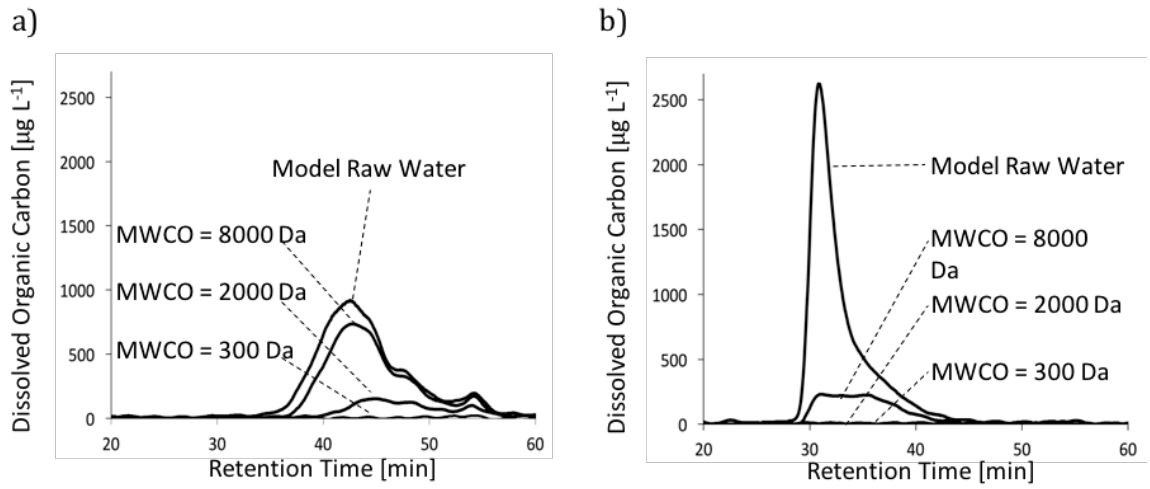

Figure 9: Typical Size Exclusion Chromatograms of Model Raw Water and Permeate Samples (a: model raw water containing SRNOM at 10 mgL^{-1} ; b: model raw water containing alginate at 10 mgL^{-1} ; Dalton values correspond to the MWCOs of the different membranes; note that the retention time of the chromatograms is inversely proportional to the log of the molecular weight)

5.2 NOM fouling and Concentration Polarization

Typical results from the filtration tests are presented in Figure 10. For all conditions investigated, the permeate flux remained constant during the pre-clean water filtration phase, then decreased over time (i.e. volume filtered) when filtering model raw waters, and increased during the post clean water filtration phase.

As previously discussed, CP is characterized by an equilibrium between the convective transport of material towards the membrane and the diffusive transport of retained material away from the membrane. Steady state is expected to be established within minutes once filtration of model raw water begins (Schäfer, 2007; Schäfer et al., 2005; Elimelech and Bhattacharjee, 1998). Hence, the rapid initial decrease in the permeate flux when filtering model raw waters was attributed to CP (this assumption is further discussed in Section 5.2.2). The subsequent slower longer term decrease in permeate flux was attributed to fouling.

Fouling occurs if the permeation drag is greater than the forces acting on potential foulants away from the membrane (Song and Elimelech, 1995). Because the permeation drag remains constant when switching from the model raw water filtration phase to the post clean water filtration phase, no back transport and no recovery in resistance due to fouling is expected during post clean water filtration. However, a recovery in resistance due to CP is expected during post clean water filtration. This is because a concentration gradient of retained material is still present, for a relatively short period of time, after switching from the model raw water filtration phase to the post clean water filtration phase. During this time, the convective transport of material towards the membrane is zero (i.e. clean water filtration), while the diffusive transport of retained material away from the membrane surface is greater than zero, resulting in a reduction (i.e.

recovery) in resistance. Note, that if CP becomes extensive, and a cake/gel layer is formed, the recovery in resistance during post clean water resistance will be limited (Schäfer et al., 1998; Mulder, 1996; van den Berg and Smolders, 1990; Elimelech and Bhattacharjee, 1998). Therefore, although a high recovery during post clean water filtration suggests that CP likely dominates, the increase in resistance due to permeate flow, other indicators of fouling and CP must be considered when interpreting the results.

As previously discussed, for all conditions investigated, the permeate flux could be best modeled assuming fouling was predominantly due to the formation of a cake layer on the membrane surface (see Section 4.4). The fit of the cake fouling model (Equation 6, Section 4.4) to typical data is presented in Figure 10. For all conditions investigated, the extent of fouling was quantified with respect to the fouling coefficient, as discussed in Section 5.2.1, and the contributions of CP and fouling to the increase in resistance to permeate flow was analyzed as discussed in Section 5.2.2.

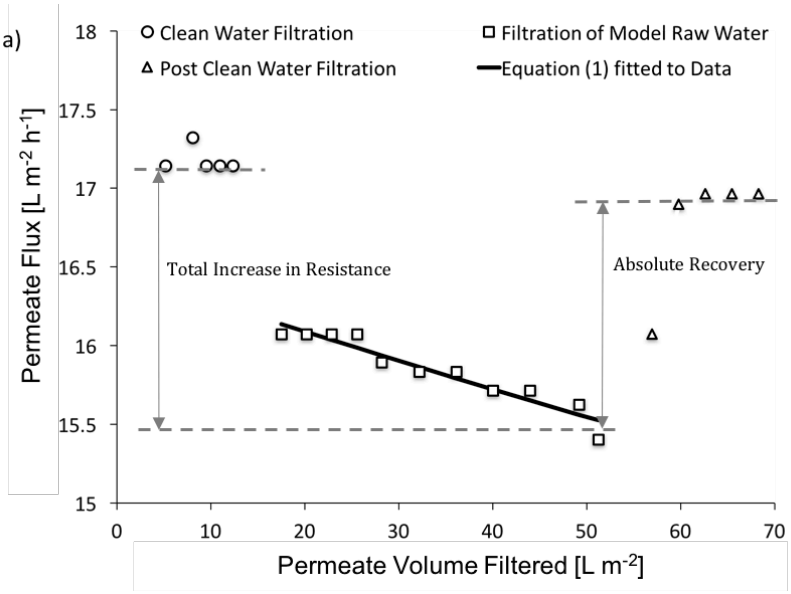

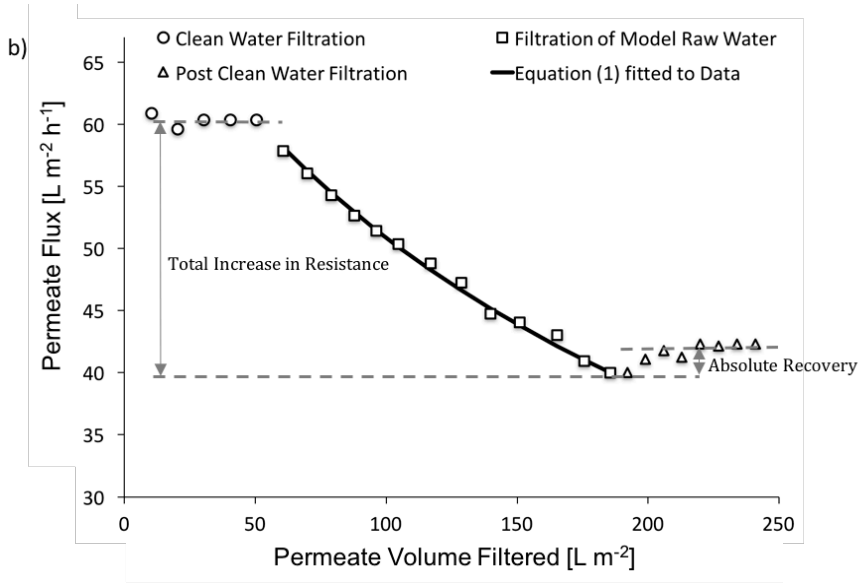

Figure 10: Typical Results from Filtration Tests
(a: MWCO = 300 Da and SRNOM at 5 mgL^{-1} of DOC; b: MWCO = 8000 Da and Alginate at 5 mgL^{-1} of DOC)

5.2.1 Contribution of Fouling to the Increase in Resistance to Permeate Flow

The fouling coefficients (k_c) for the different experimental conditions investigated are summarized in Figure 11. When filtering model raw waters containing alginate, the fouling coefficients were similar for the membranes with MWCOs of 300 and 2,000 Da and only slightly lower (not statistically different) for the membrane with the MWCO of 8,000 Da. These results are consistent with those presented in Section 5.1, where the rejection of alginate was similar when filtering with membranes with MWCOs of 300 Da and 2,000 Da MWCO, and slightly lower when filtering with the membrane with a MWCO of 8,000 Da. Considering the substantially different initial permeate fluxes for the membranes with different MWCOs and the similar fouling coefficients observed for all membranes, it can be concluded that the fouling coefficient was independent of the initial permeate flux. Further, the fouling coefficient was

proportional to the concentration of alginate in the model raw water filtered (i.e. the fouling coefficient doubled when the concentration of alginate in the raw water was twice as high), suggesting that for all membranes, fouling was similar and predominantly due to convective transport and the accumulation of a cake layer with similar characteristics for all membranes. These results are also consistent with the fact that the molecular weight of alginate is greater than the MWCO of all membranes considered (see Section 5.1).

When filtering model raw waters containing SRNOM, the fouling coefficient was substantially higher for the membrane with a MWCO of 300 Da than for the membranes with MWCOs of 2,000 Da and 8,000 Da. This is again consistent with the higher rejection of SRNOM by the membrane with a MWCO of 300 Da than the membranes with MWCOs of 2,000 and 8,000 Da. It should be noted that the fouling coefficients were similar for the membranes with MWCOs of 2,000 and 8,000 Da even though the rejection of organic material present in SRNOM was greater for the membrane with a MWCO of 2,000 Da than for the membrane with a MWCO of 8,000 Da. For the membrane with a MWCO of 8,000 Da, the fouling coefficient was proportional to the concentration of SRNOM in the model raw water. However, for the membranes with MWCOs of 300 and 2,000 Da, the fouling coefficient was not proportional to the concentration of SRNOM in the model raw water. The deviation from proportionality increased as the MWCO of the membrane decreased. These results indicate that unlike those observed when filtering model raw water containing alginate, when filtering model raw water containing SRNOM with high rejection (i.e. using membranes with low MWCOs), fouling was not only governed by the convective transport of material towards the membrane, but also likely by the formation of a CP induced cake/gel layer at the membrane surface as discussed in Section 5.2.2.

When filtering model raw waters containing a mixture of SRNOM and alginate, the fouling behavior was similar to that of model raw water containing SRNOM, suggesting that the higher percentage of low molecular weight NOM (i.e. 80 % low molecular weight NOM versus 20 % high molecular weight NOM) governed the fouling behavior.

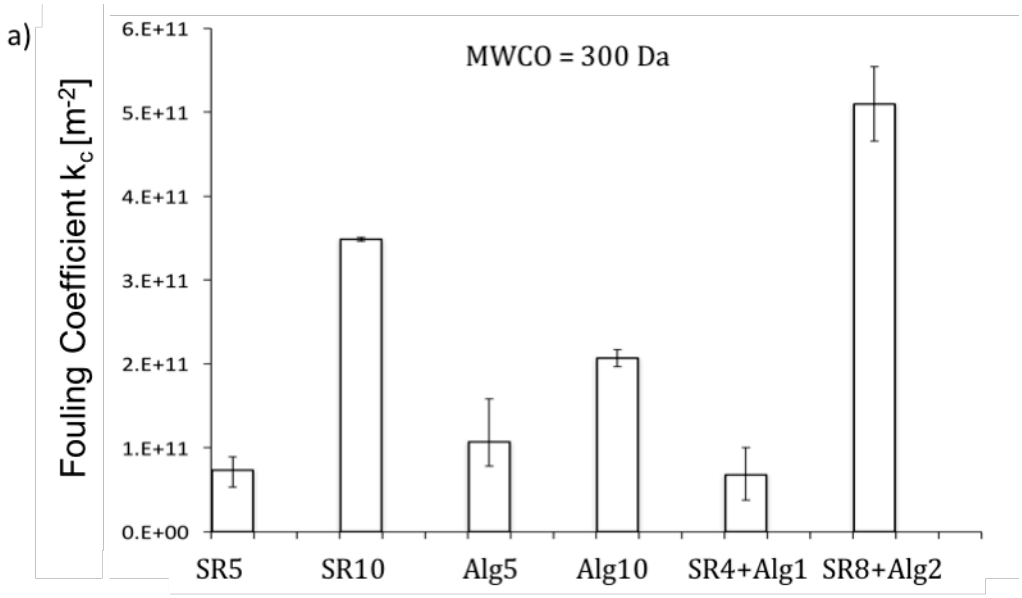

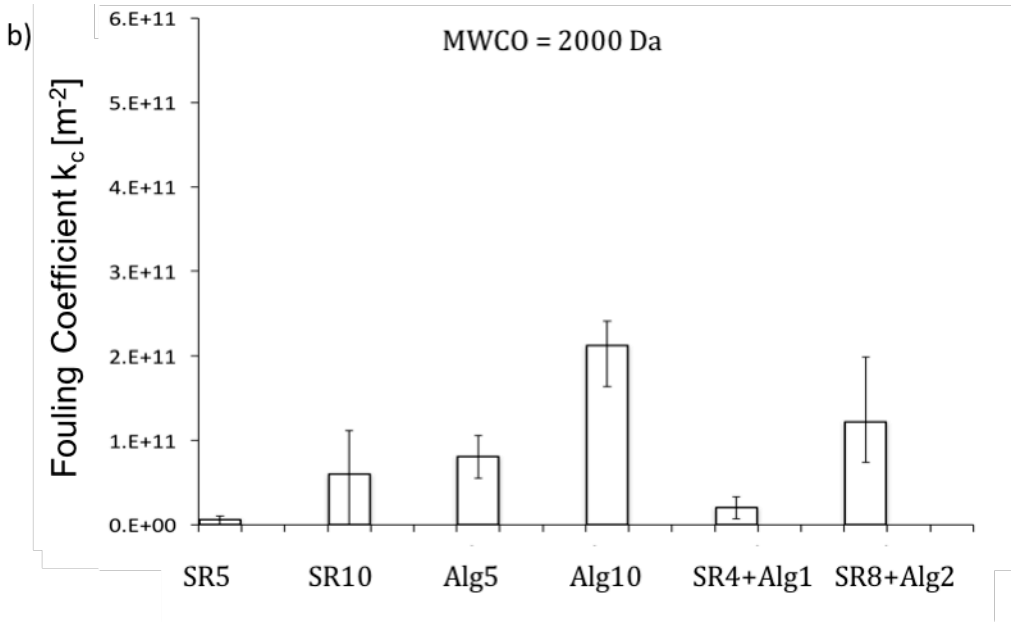

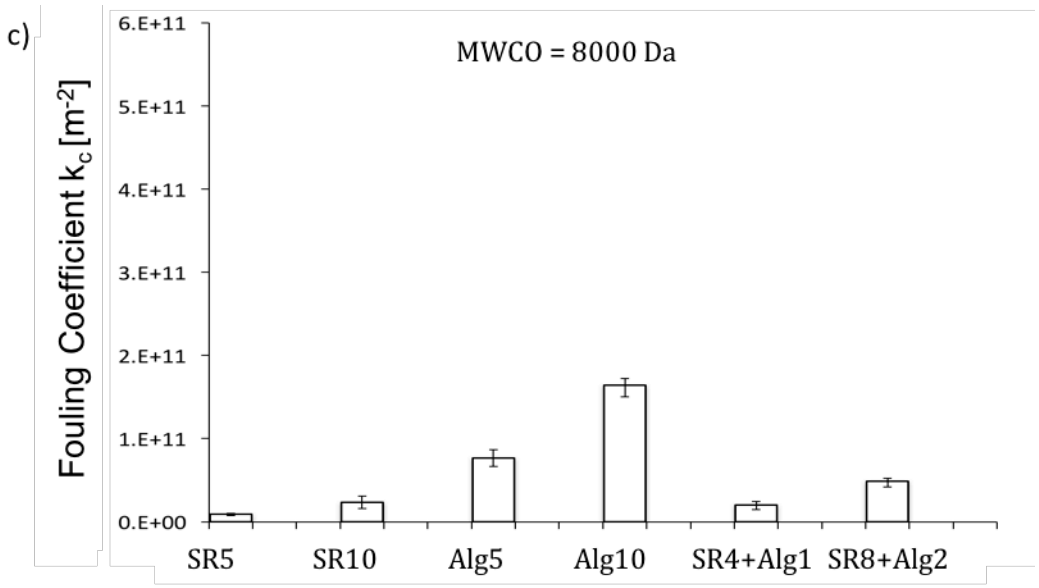

Figure 11: Fouling Coefficient k_c for Different Filtration Tests
(a: MWCO = 300 Da; b: MWCO = 2000 Da; c: MWCO = 8000 Da; SR5: SRNOM at 5 mgL^{-1} ; SR10: SRNOM at 10 mgL^{-1} ; Alg5: Alginate at 5 mgL^{-1} ; Alg10: Alginate at 10 mgL^{-1} ; SR4+Alg1: SRNOM at 4 mgL^{-1} + alginate at 1 mgL^{-1} ; SR8+Alg2: SRNOM at 8 mgL^{-1} + alginate at 2 mgL^{-1} ; error bars correspond to observed minimum/maximum values)

5.2.2 Contribution of CP to the Increase in Resistance to Permeate Flow

The contribution of CP to the total increase in resistance during filtration of the model raw waters was quantified by the relative recovery. The relative recovery was defined as the ratio of the absolute recovery to the total increase in resistance during filtration of model raw water (see Figure 12). The total increase in resistance was calculated based on the difference between the permeate flux during a pre-clean water filtration phase and at the end of a filtration of model raw water phase. The absolute recovery was calculated based on the difference between the permeate flux at the end of a filtration of model raw water phase and at the end of a post clean water filtration phase. Figure 12 illustrates the relative recoveries for the different conditions investigated.

The relative recovery generally increased as the MWCO of the membrane decreased. Also, the relative recovery generally increased when the concentration of NOM in the raw water increased. When filtering model raw water containing alginate, the relative recoveries were low, ranging from approximately 10 % to 40 %. Also, the fouling coefficient increased proportionally with the concentration of alginate in the model raw water (see Section 5.2.1). This, combined with the low relative recoveries, suggest that the increase in resistance to permeate flow was dominated by fouling when filtering model raw waters containing alginate at all concentrations considered (i.e. 5 mgL^{-1} and 10 mgL-1). However, when filtering model raw waters containing SRNOM, the relative recoveries were higher, ranging from approximately 50 % to 100 %. The greater relative recoveries when filtering model raw waters containing SRNOM rather than when filtering alginate was attributed to the differences in the diffusion coefficients of these types of NOM. Diffusion coefficients of 2.2×10^{-10} to 3.8×10^{-10} m^2s^{-1} have been reported for humic substances

(Schäfer, 2007), which account for most of the organic material in SRNOM, while that for alginate is in the order of 9.4×10^{-11} m^2s^{-1}, an estimate based on Dextran T-70 (Schäfer, 2007). The diffusive transport of retained material from the membrane back into solution is expected to increase relative to the molecular diffusion (Schäfer, 2007). Also, the permeation drag is expected to be greater for alginate than for SRNOM because of the larger size of alginate compared to SRNOM (Belfort, 1994). The relative recovery for the membrane with a MWCO of 300 Da was lower when the concentration of SRNOM in the model raw water increased (i.e. from 5 mgL^{-1} to 10 mgL^{-1}). Under these conditions, the concentration at the membrane surface is expected to be high, and likely resulted in the formation of a cake/gel layer at the membrane surface (Schäfer et al., 1998; Mulder, 1996; van den Berg and Smolders, 1990; Elimelech and Bhattacharjee, 1998). Once formed, the resistance offered by the cake/gel layer could not be reversed during post clean water filtration, which is consistent with previous research where humic substances fouling was observed to by irreversible (Jermann et al., 2007; Jermann et al., 2008; Schäfer et al., 1998; Schäfer, 2007).

When filtering model raw waters containing a mixture of SRNOM and alginate, the relative recovery was similar to that of model raw waters containing SRNOM, again suggesting that the higher percentage of low molecular weight NOM (i.e. 80 % low molecular weight NOM versus 20 % high molecular weight NOM) was mainly responsible for the observed changes in permeate flux.

a)

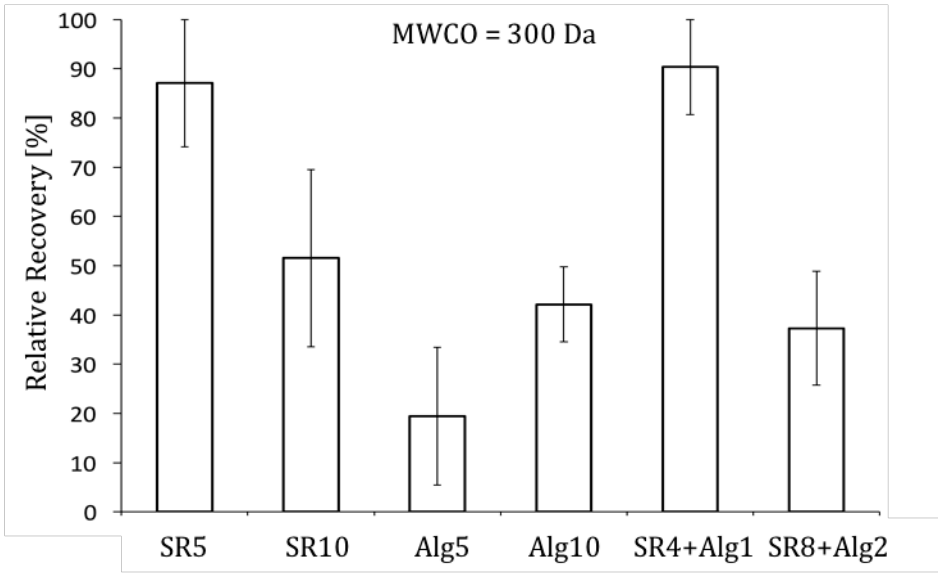
MWCO = 300 Da
Relative Recovery [%]
100
90
80
70
60
50
40
30
20
10
0
SR5
SR10
Alg5
Alg10
SR4+Alg1
SR8+Alg2

b)

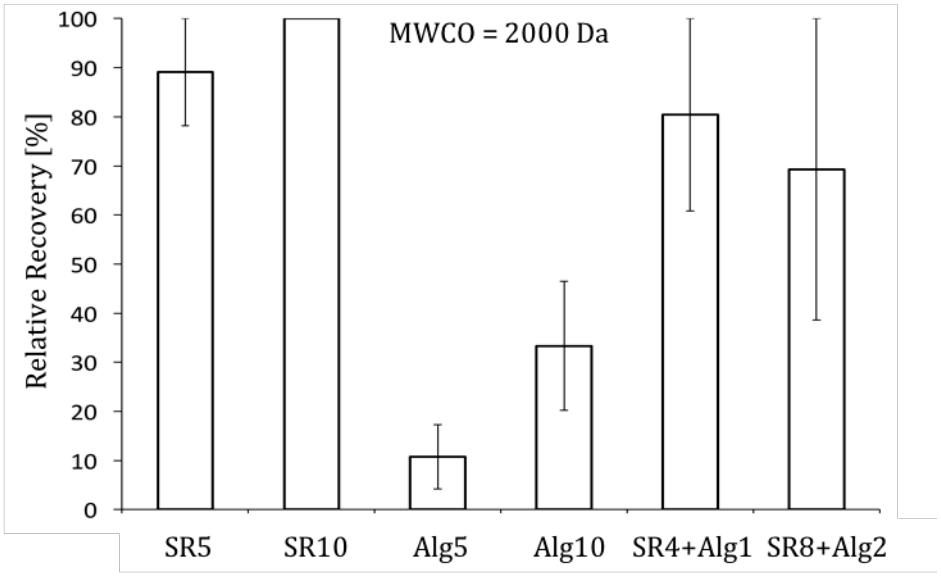
MWCO = 2000 Da
Relative Recovery [%]
100
90
80
70
60
50
40
30
20
10
0
SR5
SR10
Alg5
Alg10
SR4+Alg1
SR8+Alg2

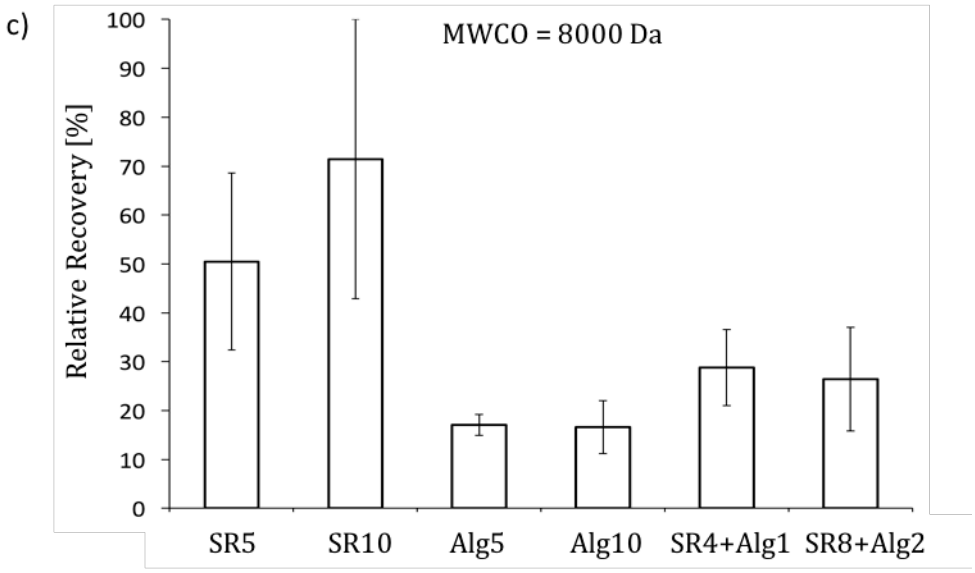

Figure 12: Relative Recovery During Post-Clean Water Filtration
(a: MWCO = 300 Da; b: MWCO = 2000 Da; c: MWCO = 8000 Da; SR5: SRNOM at 5 mgL^{-1} ; SR10: SRNOM at 10 mgL^{-1} ; Alg5: Alginate at 5 mgL^{-1} ; Alg10: Alginate at 10 mgL^{-1} ; SR4+Alg1: SRNOM at 4 mgL^{-1} + alginate at 1 mgL^{-1} ; SR8+Alg2: SRNOM at 8 mgL^{-1} + alginate at 2 mgL^{-1} ; error bars correspond to observed minimum/maximum values)

As illustrated in Figure 13, when filtering model raw waters containing SRNOM or a mixture of SRNOM and alginate, a linear correlation was observed between the initial rapid increase in resistance during model raw water filtration and the absolute recovery during post clean water filtration (R^2=0.97). When filtering model raw waters containing alginate, no correlation was observed (R^2 =0.04, see Appendix C1). The correlation supports the assumption that the initial rapid increase in resistance is due to CP rather than fouling, that CP develops rapidly within the first minutes of filtration when filtering raw waters containing NOM, and confirms that the relative recovery observed when filtering model raw waters containing SRNOM can be attributed to CP. In addition, these results confirm that the total increase in resistance to the permeate flow is mainly impacted by CP when filtering model raw waters containing SRNOM.

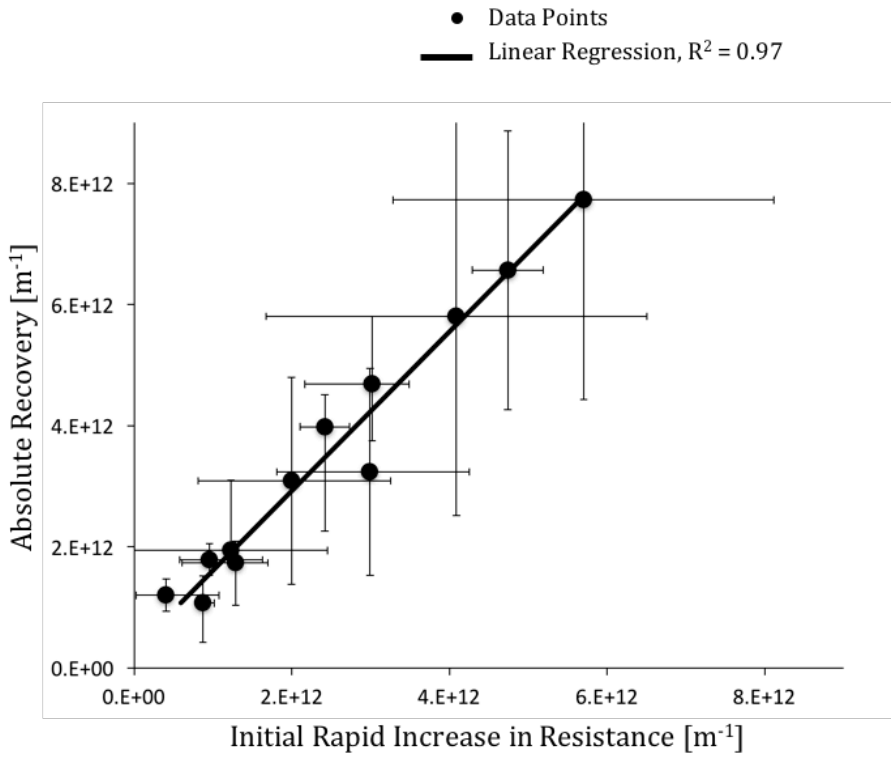

Figure 13: Correlation between Absolute Recovery and Initial Rapid Increase in Resistance (model raw waters containing SRNOM and a mixture of SRNOM + alginate; solid line: linear regression, R^2=0.97, slope = 1.31 ± 0.35, Intercept = 3 10^{11}; p = 0.05; error bars correspond to minimum/maximum values)

5.3 Effect of Calcium and Particulate Matter on CP and Fouling

When adding calcium to model raw waters containing polysaccharides, the relative recovery of 28 ±13 % did not change noticeably, indicating that the contribution of CP to the total increase in resistance was not affected by calcium at the concentration considered (50 mgL^{-1} as $CaCO_3$) (see Figure 14). However, when calcium was added to model raw waters containing humic

substances, the relative recovery of 87 ±13 % decreased to 20 ±10 % indicating that calcium decreased the contribution of CP to the increase in resistance. This is consistent with the results reported by Schäfer (2007), which suggest that NOM deposition onto the membrane surface increases in the presence of calcium. Jermann et al. (2007 and 2008) and Seidel and Elimelech (2002) reported that calcium increases the size of humic substances by enhancing aggregation and impeding charge repulsion, which likely decreased the diffusive back-transport of humic substances resulting in the observed decrease in CP. Also, Tipping et al. (1988) reported that the solubility of humic substances decreases with its charge and, hence, calcium might decrease the solubility of humic substances and enhance their deposition by the formation of a gel/cake layer. Adding particulate matter (i.e. kaolin) to the model raw water containing humic substances and calcium further decreased the relative recovery (4.4 % ± 4.4 %) (note, no filtration tests were conducted with raw water containing simultaneously polysaccharides, calcium and particulate matter). Chong et al. (2008), Hoek and Elimelech (2003), Tian et al. (2013) and Li and Elimelech (2006) attributed the increase in resistance due to the presence of a cake layer, as would be expected when filtering raw waters containing kaolin, to hindered back-diffusion of dissolved material and/or to the adsorption and aggregation of humic substances and particulate matter. The adsorption of humic substances onto particles has been reported to be greater in the presence of calcium (Jermann et al., 2008). Hindered back diffusion, adsorption and aggregation would be expected to decrease the relative recovery.

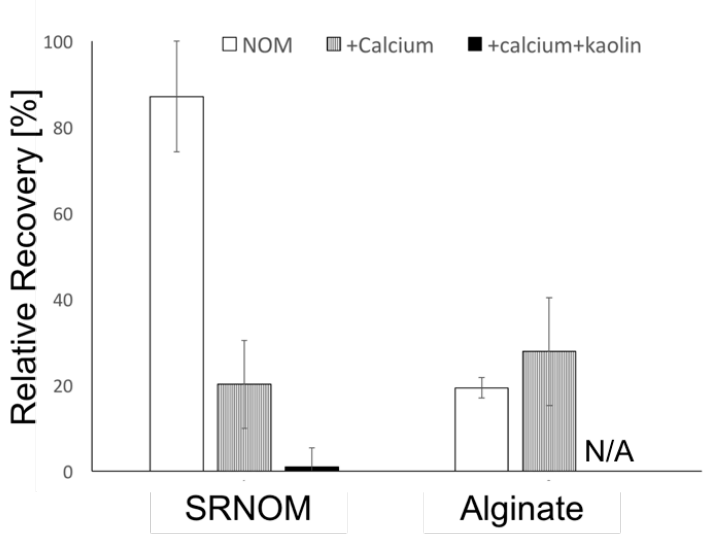

Figure 14: Relative Recovery in the Presence of Calcium and Particulate Matter (model raw water with various compositions including humic substances (i.e. SRNOM), polysaccharides (i.e. alginate) calcium and particulate matter (i.e. kaolin), membrane's MWCO = 300 Da; n = 2, error bars correspond to minimum and maximum values)

5.4 Overall Impact of Fouling and CP to the Increase in Resistance to Permeate Flow

Overall, the results suggest that, when filtering model raw waters containing alginate, the total increases in resistance to permeate flow is dominated by fouling, while the total increase in resistance to permeate flow is dominated by CP when filtering model raw waters containing SRNOM (i.e. humic substances, lower molecular weight NOM). The impact of CP is greatest for membranes with a lower MWCOs (i.e. < 2,000 Da), which are recommended for the effective removal of NOM in drinking water treatment applications. Filtration using membranes with higher MWCOs (e.g. 8,000 Da) is not prone to CP because the lower molecular weight NOM, responsible for CP, is not effectively retained.

It should be noted that when the impact of CP is extensive (i.e. filtration of raw waters containing mainly humic substances / low molecular weight NOM with low MWCO membranes), the increase in resistance is much greater than when filtration was dominated by fouling. For this reason, and because NOM in surface waters consists predominantly of humic substances (Zumstein and Buffle, 1989), operation with control measures to continuously limit CP, such as cross-flow operation, should be considered for drinking water treatment using NF and tight UF membranes. Dead end operation, which is typically used for drinking water production using UF is not recommended because it cannot continuously limit CP.

When filtering model raw water containing humic substances in the presence of calcium and particulate matter, the increase in resistance is dominated by fouling rather than CP, which differs from the results observed in the absence of calcium and particulate matter. Therefore, it is likely that measures commonly used to minimize CP, such as low velocity cross-flow, would not be effective to limit the increase in resistance during filtration of raw waters containing humic substances as well as calcium and particulate matter. Higher velocity cross-flow, which can be used to minimize fouling would likely be required.

Future research, presented in Chapters 6 and 7, will investigate the impact of control measures (e.g. cross-flow) and different membrane configurations (i.e. hollow fiber versus spiral wound membrane configurations) to mitigate CP and fouling in NF and tight UF membrane systems applied for drinking water treatment.

5.5 Conclusions

The following five main conclusions can be made based on the results of the present study.

- Because NOM in most surface waters consists mainly of humic substances (i.e. lower molecular weight NOM) and because effective NOM removal is likely one of the main motivation to implement NF and tight UF membranes in drinking water treatment, membranes with lower MWCOs (i.e. < 2,000 Da) are recommended, if the NOM is to be removed in a single step.

- When filtering raw waters containing high concentrations of alginate (i.e. polysaccharides, high molecular weight NOM), the total increase in the increase in resistance to permeate flow is mainly dominated by fouling; when filtering raw waters containing predominantly humic substances (i.e. lower molecular weight NOM), the total increase in resistance to permeate flow is mainly dominated by CP. The impact of CP is greatest for membranes with low MWCOs (i.e. < 2,000 Da).

- When filtering raw waters containing high concentrations of humic substances (i.e. 10 mgL^{-1}) with the membrane with the lowest MWCO (i.e. 300 Da), the impact of CP became extensive and the increase in resistance was greater than observed for any other experimental condition considered, likely due to the formation of a CP induced cake/gel layer.

- Operation with control measures to continuously limit CP, such as cross-flow operation, should be considered in drinking water applications using NF and tight UF membranes. Dead end operation, which is typically used for drinking water production using UF, is not recommended because it cannot continuously limit CP.

- The results suggest that calcium and particulate matter decreased the diffusive back-transport of humic substances (i.e. SRNOM) away from the membrane into the bulk solution; hence, when filtering model raw water containing humic substances, calcium and particulate matter, the increase in resistance is dominated by fouling rather than CP, which differs from the results observed in the absence of calcium and particulate matter; further research (see Chapters 6 and 7) assesses what hydraulic control measures are best suited for these conditions.

Chapter 6: Mitigation of Fouling and Concentration Polarization (Objective 2)

As discussed in the previous chapter, operation with control measures to continuously limit CP, such as cross-flow operation, should be considered for drinking water treatment using NF and tight UF membranes. Also, it is likely that measures commonly used to minimize CP, such as low velocity cross-flow, would not be effective to limit the increase in resistance during filtration of raw waters containing humic substances as well as calcium and particulate matter.

The objective of the second part of the study was to quantify effect of cross-flow operation and permeate flux interruption (i.e. relaxation phases), as hydraulic control measures, on the extent and control of CP and fouling. Because the MWCO of the NF and tight UF membranes likely affects CP and fouling, membranes with various MWCOs ranging from 300 Da to 8000 Da were considered when assessing hydraulic control measures. The impact of hydraulic control measures was studied by monitoring the flux decline, estimating the permeate flux at steady state, and by characterizing the foulant layer. Based on the results, recommendations are proposed to minimize the resistance to permeate flow when operating NF and tight UF membranes for drinking water treatment.

6.1 Impact of Hydraulic Control Measures

Typical results from filtration tests with cross-flow velocities of 0 ms^{-1}, 0.05 ms^{-1} and 0.25 ms^{-1}, when using membranes with MWCOs of 300 Da, 2000 Da and 8000 Da and model raw water containing humic substances (i.e. SRNOM), polysaccharides (i.e. alginate), calcium and particulate matter (i.e. kaolin) are presented in Figure 15. A model raw water containing calcium and turbidity was considered, because these constituents are commonly present in natural raw

waters and fouling control is expected to be more challenging in their presence. As expected, for all membranes considered, the rate of the flux decline increased as the cross-flow velocity decreased (Seidel and Elimelech, 2002). When using membranes with MWCOs of 2,000 Da and 8,000 Da, no flux decline was observed during the tests with the highest cross-flow velocity considered (0.25 ms^{-1}).

All filtration tests were performed with membranes of different MWCOs, operated at a similar trans-membrane pressure. As a result, the permeate flux differed substantially for the different filtration tests. It was therefore not possible to directly compare the fouling rates observed for membranes with different MWCOs (Seidel and Elimelech, 2002). As previously discussed, the permeate flux at steady state provides an estimate of the back-transport of the material that would otherwise accumulate at the membrane surface (Section 4.4.2). For this reason, the impact of the different hydraulic control measures was assessed based on the permeate flux that could be sustained at steady state, estimated by fitting Equation 7 to the filtration data. To account for slight variations in initial permeate flux between filtration tests, the results were normalized to the initial permeate flux.

a)

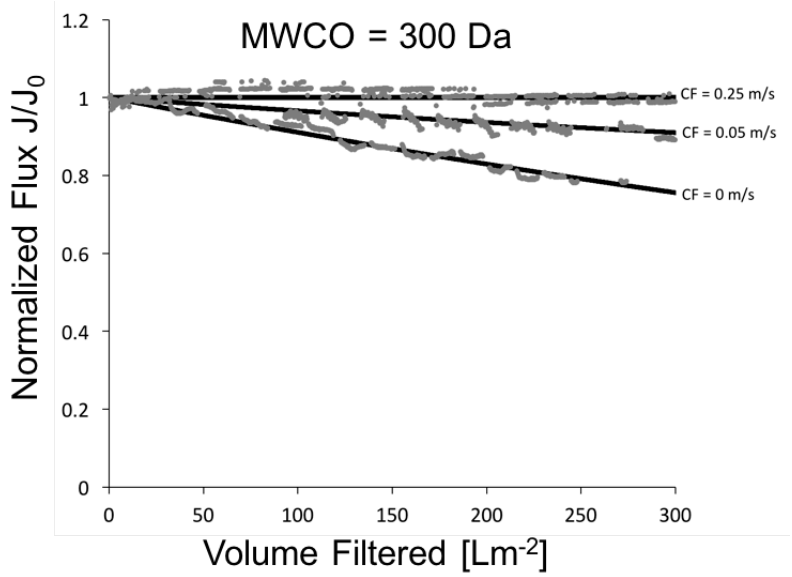
MWCO = 300 Da
Normalized Flux J/J0
Volume Filtered [Lm-2]
CF = 0.25 m/s
CF = 0.05 m/s
CF = 0 m/s
1.2
1
0.8
0.6
0.4
0.2
0
0
50
100
150
200
250
300

b)

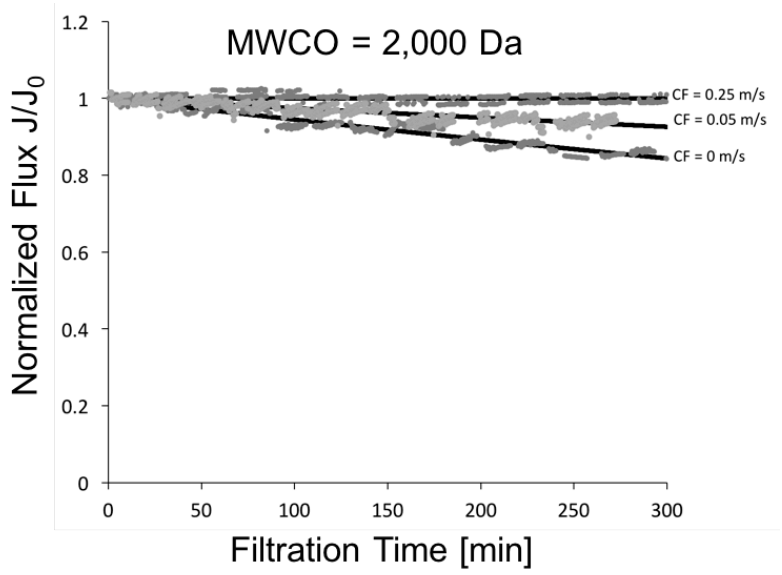
MWCO = 2,000 Da
Normalized Flux J/J0
Filtration Time [min]
CF = 0.25 m/s
CF = 0.05 m/s
CF = 0 m/s
1.2
1
0.8
0.6
0.4
0.2
0
0
50
100
150
200
250
300

c)

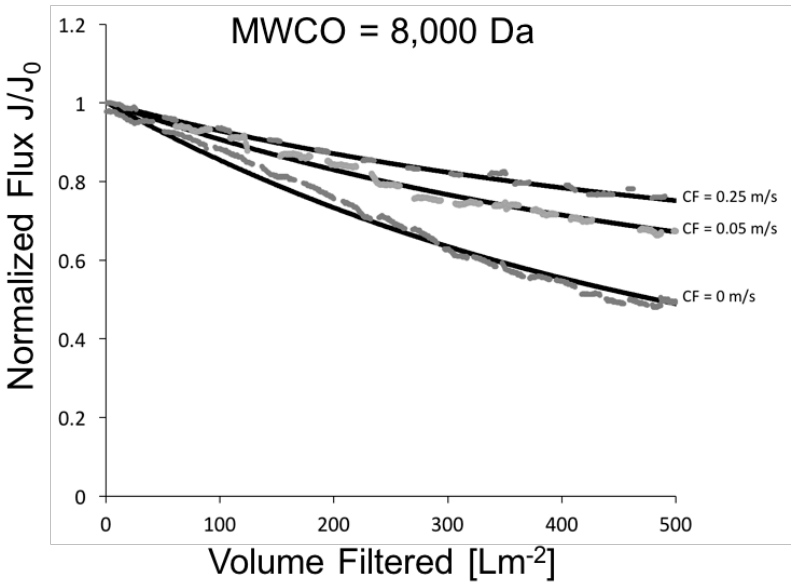

Figure 15: Typical Filtration Test Results
(model NOM with calcium and particulate matter; a: membrane with a MWCO of 300 Da; b: membrane with a MWCO of 2000 Da; c: membrane with a MWCO of 8000 Da)

The estimated permeate flux at steady state for the different conditions investigated are summarized in Figure 16. As expected, for a cross-flow velocity of 0 ms^{-1} (i.e. dead end operation), the permeate flux eventually reached a value of 0 $Lm^{-2}h^{-1}$ (Song, 1998). For the medium cross-flow velocity of 0.05 ms^{-1}, the average steady state permeate flux values ranged from 2.7 – 6.4 $Lm^{-2}h^{-1}$, depending on the MWCO of the membrane. A consistent, but not significant, positive trend was observed between the permeate flux at steady state and the MWCO of the membranes. The lower steady state permeate flux at lower membrane MWCOs was attributed to the greater retention of smaller NOM by these membranes (see Section 5.1). For the highest cross-flow velocity of 0.25 ms^{-1}, the average steady state fluxes varied over a narrow range from 14.8 $Lm^{-2}h^{-1}$ to 18.6 $Lm^{-2}h^{-1}$, depending on the MWCO of the membranes.

No decline in permeate flux was observed when using the membranes with MWCOs of 300 Da and 2000 Da.

These results confirm that measures commonly used to minimize CP (i.e. low cross-flow velocity) are not effective in limiting the increase in resistance during filtration of raw waters containing humic substances as well as calcium and particulate matter. However, higher velocity cross-flow can be used to minimize the increase in resistance to permeate flow.

Introducing permeate flux interruptions (i.e. relaxation) periods of 10 minutes every hour did not result in less fouling or higher steady state fluxes (see Figure 16), suggesting that, once a foulant layer has been formed, it is difficult to remove it hydraulically. This is consistent with previous work on NF membranes fouled with polysaccharides (i.e. alginate) and particulate matter (i.e. kaolin) where Payant et al. (2017) observed that less foulants were recovered overall, when applying rigorous hydraulic cleaning consisting of air-scouring, forward flush and backwash in a dead-end system compared to a cross-flow system. The formation of a hydraulically less reversible foulant layer is enhanced by the presence of humic substances (i.e. SRNOM) in the cake layer (Jermann et al., 2007; Jermann et al., 2008).

a)

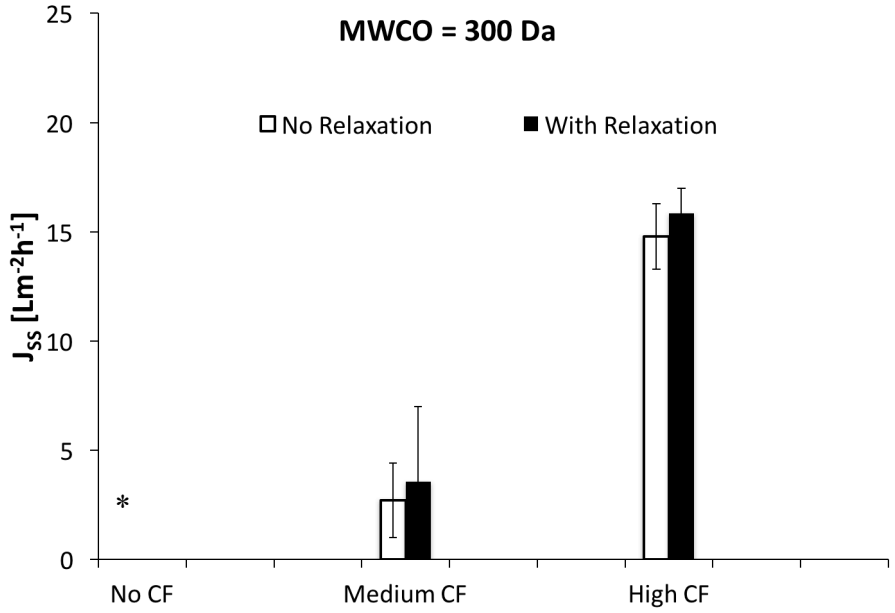
MWCO = 300 Da
No Relaxation
With Relaxation
J_{ss} [$Lm^{-2}h^{-1}$]
25
20
15
10
5
0
*
No CF
Medium CF
High CF

b)

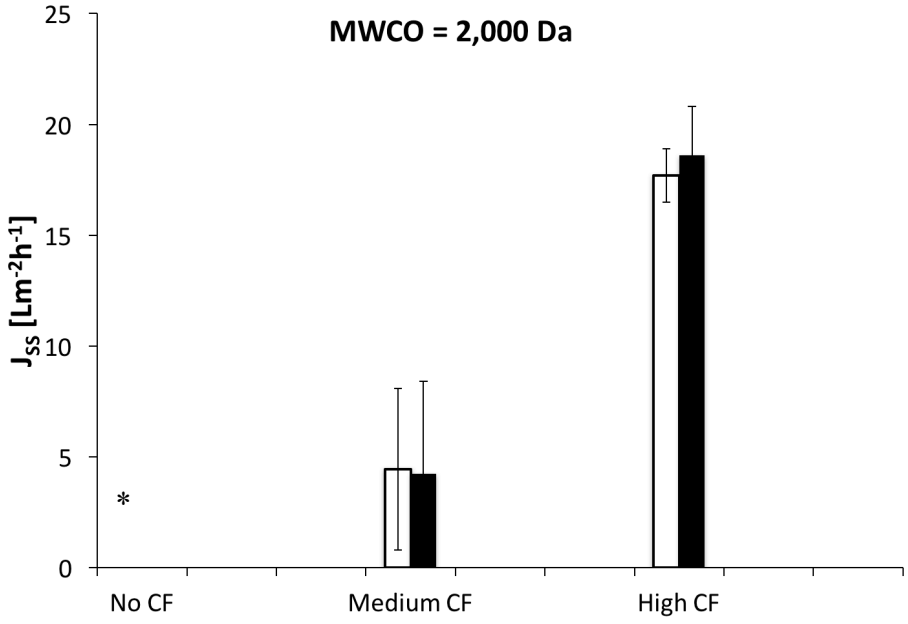
MWCO = 2,000 Da
J_{ss} [$Lm^{-2}h^{-1}$]
25
20
15
10
5
0
*
No CF
Medium CF
High CF

c)

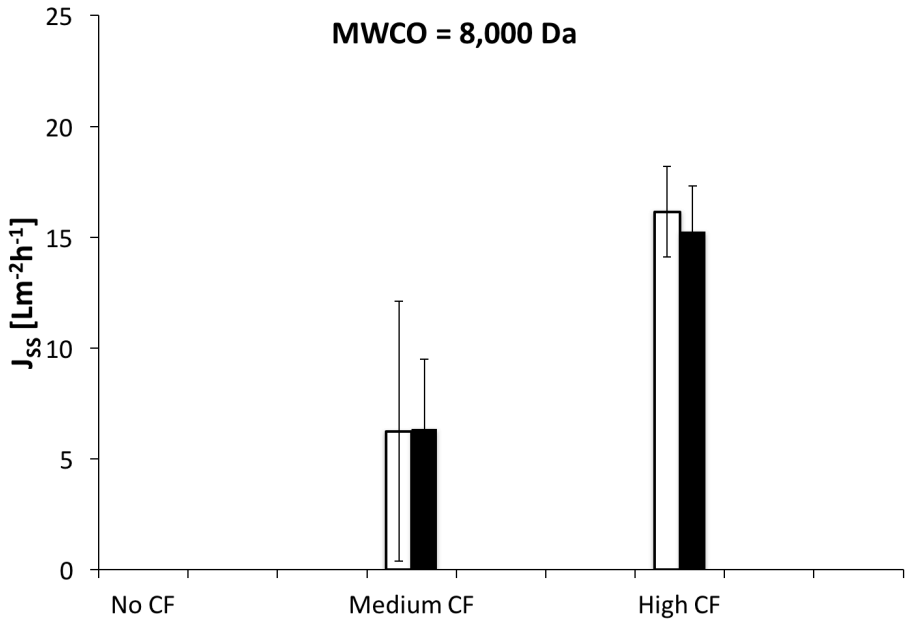

Figure 16: Steady State Permeate Flux (J_{SS}) versus Cross-Flow Velocity
(model NOM with calcium and particulate matter; a: membrane with a MWCO of 300 Da; b: membrane with a MWCO of 2000 Da; c: membrane with a MWCO of 8000 Da; error bars correspond to minimum and maximum values; * steady state permeate flux of 0 L m^{-2} h^{-1}; n=2)

6.2 Foulant Layer Composition

To gain insight into the impact of hydraulic control measures on the resistance to permeate flow, the composition of the foulant layer was characterized. As previously discussed (see Section 4.6.3), the results are presented in terms of normalized mass (see Figure 17), which corresponds to the ratio of mass of material extracted from the membrane surface to the mass of material present in the volume of model raw water permeated through the membrane, during filtration tests.

6.2.1 Retention of Material at the Membrane Surface

When no hydraulic control measures (i.e. cross-flow) were applied, the normalized mass for polysaccharides (i.e. alginate) and particulate matter (i.e. kaolin) in the foulant layer were high and similar for all membrane MWCOs considered. A high normalized mass was expected because these are effectively retained by all of the membranes considered (see Section 5.1). In contrast, a low normalized mass was observed for humic substances (i.e. SRNOM) when no hydraulic control measures were applied. The low normalized recovery is consistent with results by others (Cho et al., 1999; Her et al., 2007) and is likely due to the back transport of humic substances into bulk solution during filtration even in the absence of a cross-flow (see Section 5.2.2). An additional filtration test was conducted where the concentration of humic substances in the water exiting the membrane test cell through the slow drain was monitored. The corresponding mass balance suggests that the observed lower values for normalized mass for humic substances were indeed due to effective back-transport of humic substances into bulk solution (see Appendix D1). This is also consistent with the results reported by Schäfer (2007), which suggest that the mass of humic substances that deposited on the membrane was relatively small relative to the mass of material present in the volume of model raw water permeated through the membrane during filtration tests.

The normalized mass recovered decreased as the MWCO of the membranes increased, which is consistent with the apparent molecular weight distribution of the humic substances used during this study. To exclude the impact of retention on the normalized mass, only results from filtration tests conducted with low MWCO (i.e. 300 Da) membranes were further considered when discussing the impact of hydraulic control measures (i.e. cross-flow). These membranes

effectively retain essentially all of the foulants present in the model raw water including humic substances (i.e. particulate matter, polysaccharides and humic substances).

6.2.2 Impact of Fouling Control Measures on Membranes with Low MWCO

When cross-flow was applied as a hydraulic control measure, the normalized mass of polysaccharides and particulate matter in the foulant layer decreased as the cross-flow velocity increased. This was expected because shear induced back-transport increases with cross-flow velocity (Belfort et al., 1994; Sethi and Wiesner, 1997). However, the normalized mass of humic substances remained constant for all cross-flow velocities considered. Because of the relatively small size of humic substances, the magnitude of the shear induced back-transport was likely too small to affect the normalized mass. As reported by Li and Elimelech (2006), these results suggest that humic substances accumulated in the foulant layer through hindered back-diffusion, rather than adsorption onto the particulate matter, in the presence calcium and particulate matter. Had the latter be dominant, a reduction in the normalized mass of humic substances would have been expected when the normalized mass of particulate matter in the foulant layer decreased. Considering that cross-flow velocity does not impact the normalized mass of humic substances in the foulant layer, the observed increase in steady state flux with cross-flow velocity (discussed in Section 6.1) likely resulted from greater shear induced back-transport of polysaccharides and particulate matter at higher cross-flow velocities. Note that, even when no fouling was observed based on changes in normalized flux (i.e. cross-flow velocity of 0.25 ms^{-1} and membranes with lower MWCOs of 300 Da and 2000 Da), some polysaccharides (i.e. alginate), humic substances (i.e. SRNOM) and particulate material (i.e. kaolin) could be extracted from the membrane

surface, indicating that foulants can be present even when they cannot be perceived based on permeate flux measurements.

a)

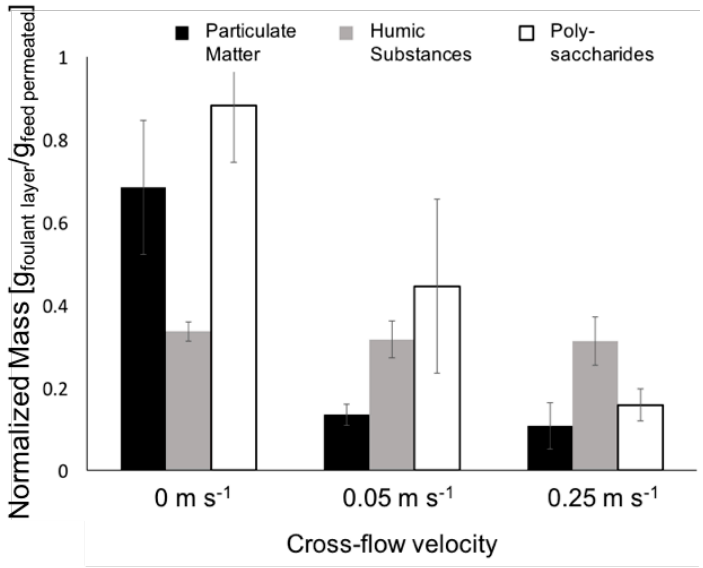

b)

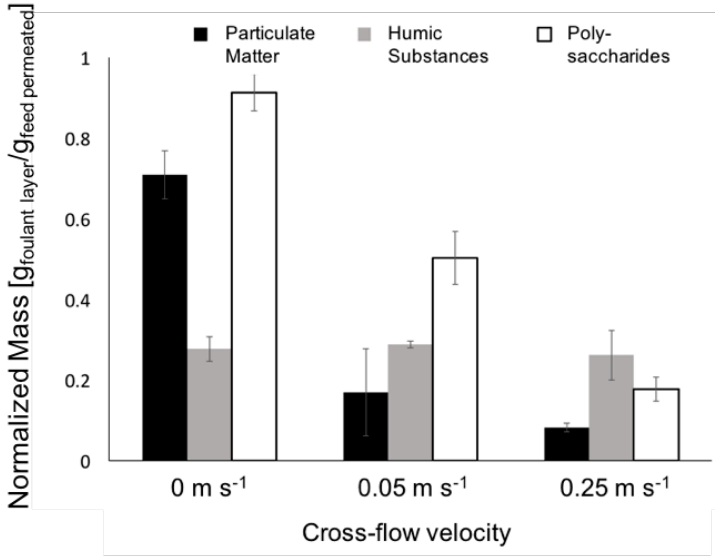

c)

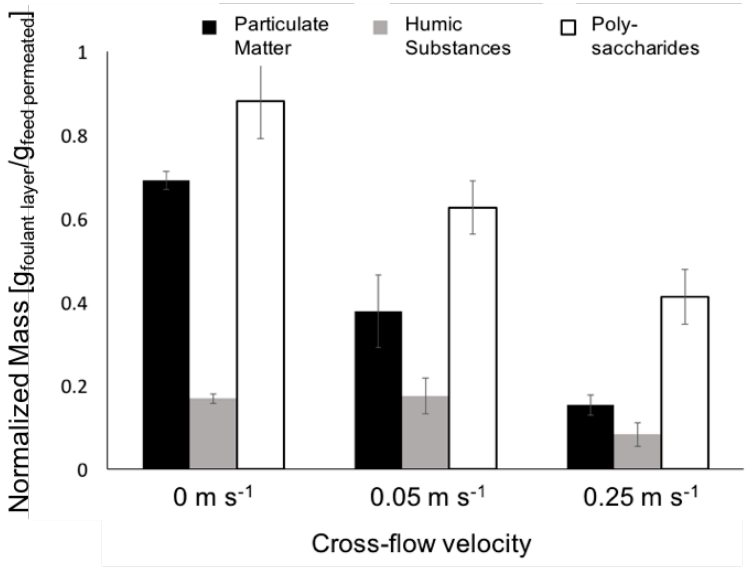

Figure 17: Normalized Mass of Material in the Foulant Layer
(model NOM with calcium and particulate matter; a: membrane with a MWCO of 300 Da; b: membrane with a MWCO of 2000 Da; c: membrane with a MWCO of 8000 Da; error bars correspond to minimum and maximum values; n=2)

6.3 Summary and Implications

When filtering model raw water containing only humic substances (i.e. SRNOM), the extent of diffusive back-transport was high and the increase in resistance to permeate flow, which was dominated by CP, could be limited using low intensity hydraulic control measures (i.e. low cross-flow velocity) (see Figures 18a-b and 19a-b). Based on previous work, low intensity hydraulic control measures are recommended to be applied continuously to effectively control CP, which dominates when filtering raw waters containing predominantly smaller NOM, such as humic substances (see Section 5.4). However, when calcium and particulate matter (i.e. kaolin) were present in the raw water containing humic substances and polysaccharides, and fouling dominates the increase in resistance to permeate flow (see Section 5.3), hydraulic control measures primarily affected the accumulation of polysaccharides and particulate matter (see

Figures 18c-e and 19c-e). The back-transport of polysaccharides and particulate matter for conditions where cross-flow is applied is related to shear induced diffusion or inertial lift (Belfort, 1994; Sethi and Wiesner, 1997). A further discussion on the predominant back-transport mechanism (i.e. shear induced diffusion or inertial lift) is provided in Section 7.3. For the range of cross-flow velocities considered, the amount of polysaccharides and particulate matter accumulating at the membrane surface decreased as the cross-flow velocity increased. Therefore, a high intensity hydraulic control measure is recommended to minimize the increases in resistance to permeate flow during filtration using NF and tight UF membranes. As reported by Payant et al. (2017), periodic back-wash and air scouring could also enhance the effectiveness of cross-flow. The filtration tests using permeate flux interruptions (i.e. relaxation) indicated that it was difficult to hydraulically remove the accumulated material, once a foulant layer had been formed. Therefore, it is recommended to apply the high intensity hydraulic control measure continuously (i.e. apply high velocity cross-flow), to prevent the accumulation of polysaccharides and particulate matter at the membrane surface.

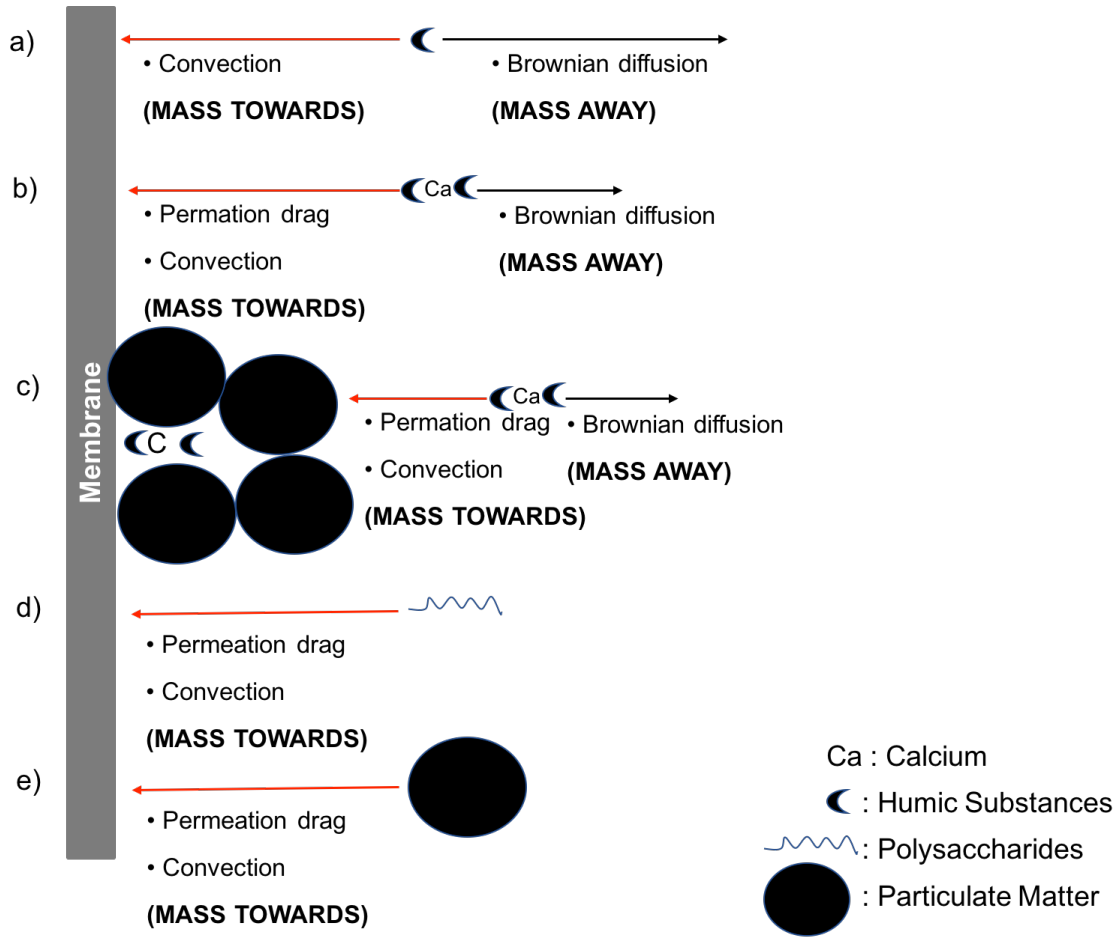

Figure 18: Illustration of Mass-Transport Mechanisms for Conditions without Cross-Flow (for raw waters containing a: humic substances; b: humic substances and calcium; c: humic substances, calcium, and particulate matter; d: polysaccharides; e: particulate matter)

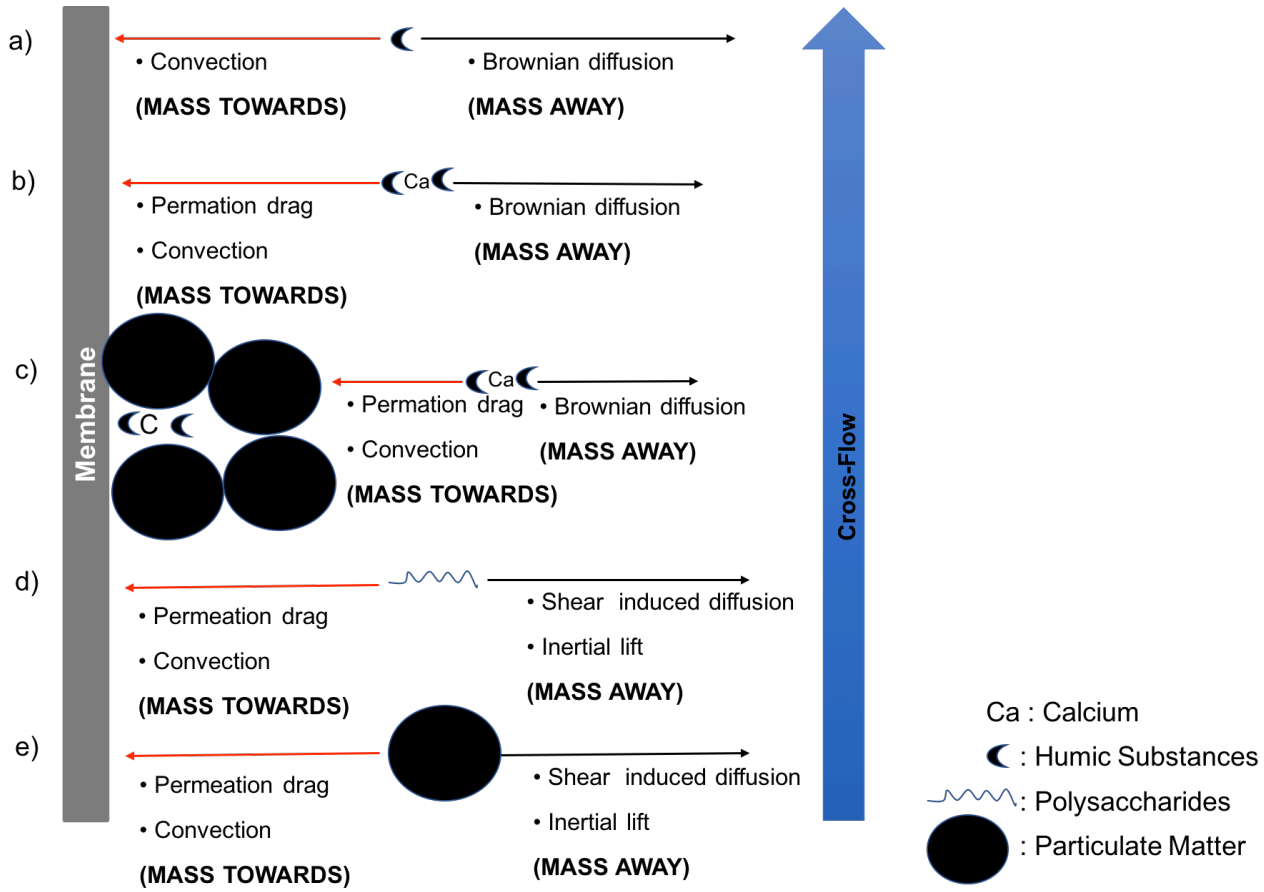

Figure 19: Illustration of Mass-Transport Mechanisms for Conditions witht Cross-Flow (for raw waters containing a: humic substances; b: humic substances and calcium; c: humic substances, calcium, and particulate matter; d: polysaccharides; e: particulate matter)

6.4 Conclusions

The effect of cross-flow operation and permeate flux interruption as hydraulic control measures on the increase in resistance to permeate flow resulting from CP and fouling were assessed. Listed below are the main outcomes from the present study:

- The extent of the increase in resistance to permeate flow resulting from fouling and CP decreased as the cross flow-velocity increased.

- When calcium and particulate matter (i.e. kaolin) were present in the raw water containing humic substances and polysaccharides (i.e. alginate), hydraulic control measures primarily affected the accumulation of polysaccharides and particulate matter.

- For the range of cross-flow velocities considered, the amount of polysaccharides and particulate matter accumulating at the membrane surface decreased as the cross-flow velocity increased. For this reason, high intensity hydraulic control measures (i.e. high velocity cross-flow) are recommended to minimize the increase in resistance to permeate flow when filtering raw waters containing humic substances (i.e. SRNOM), polysaccharides (i.e. alginate), calcium and particulate matter (i.e. kaolin).

- Because it is difficult to hydraulically remove the accumulated material once a foulant layer has been formed, it is recommended to apply the high intensity hydraulic control measure (i.e. high velocity cross-flow) continuously.

Chapter 7: Hydrodynamics, System Configuration and Geometry (Objective 3)

The objective of the third part of the study was to develop a framework to compare the performance of NF membranes of different configurations and geometries in terms of the permeate flux that can be sustained. To achieve this, the hydrodynamic conditions in spacer filled and empty flow channels of different configurations, representing spiral wound and hollow fiber membrane configurations respectively, were characterized when operating over a range of cross-flow velocities typical of spiral wound and hollow fiber systems. For these conditions, the extent of fouling and CP were quantified in terms of the permeate flux that can be sustained. A semi-mechanistic relationship was developed to correlate the cross-flow velocity, system configuration and geometry to the average shear stress at the membrane surface and the permeate flux that can be sustained. Only NF membranes were considered because those membranes were found to be better suited for effective NOM removal than tight UF membranes.

7.1 Hydrodynamic Conditions in Spacer Filled and Empty Flow Channels

Figure 18 illustrates typical results obtained for the distribution of shear stress at the membrane surface in the spacer filled and empty flow channels of the CF042 test cell and the custom test cell. The spatial variation of shear stress in the spacer filled flow channels was high (see Figure 20 a and c). The location of the shear stress maxima could be accurately identified with the custom test cell, which provided greater spatial resolution for the shear measurements. As illustrated in Figure Figure 20 c, reoccurring local shear stress maxima were observed. Using Computational Fluid Mechanics, Koutsou et al. (2007) also reported reoccurring local shear stress maxima and the maxima were located close to the narrow region between the spacer filaments and the flow channel walls. The Reynolds numbers for the spacer filled flow channels

ranged from 180 to 830 for the conditions investigated. In spacer filled flow channels, the flow transitions from laminar to transient, unsteady flow at Reynolds numbers above 200 (Bucs et al., 2015; Radu et al., 2014). In the empty flow channels, no pronounced spatial variation of shear stress was observed (see Figure 20 b). For the conditions investigated, the Reynolds numbers were less than 1200 for empty flow channels, indicating laminar flow conditions prevailed. For empty flow channels, the flow is laminar and steady for Reynolds numbers below 2200 (White, 2003). Table 6 lists the average and range (i.e. standard deviation) of shear stress values for the different conditions investigated.

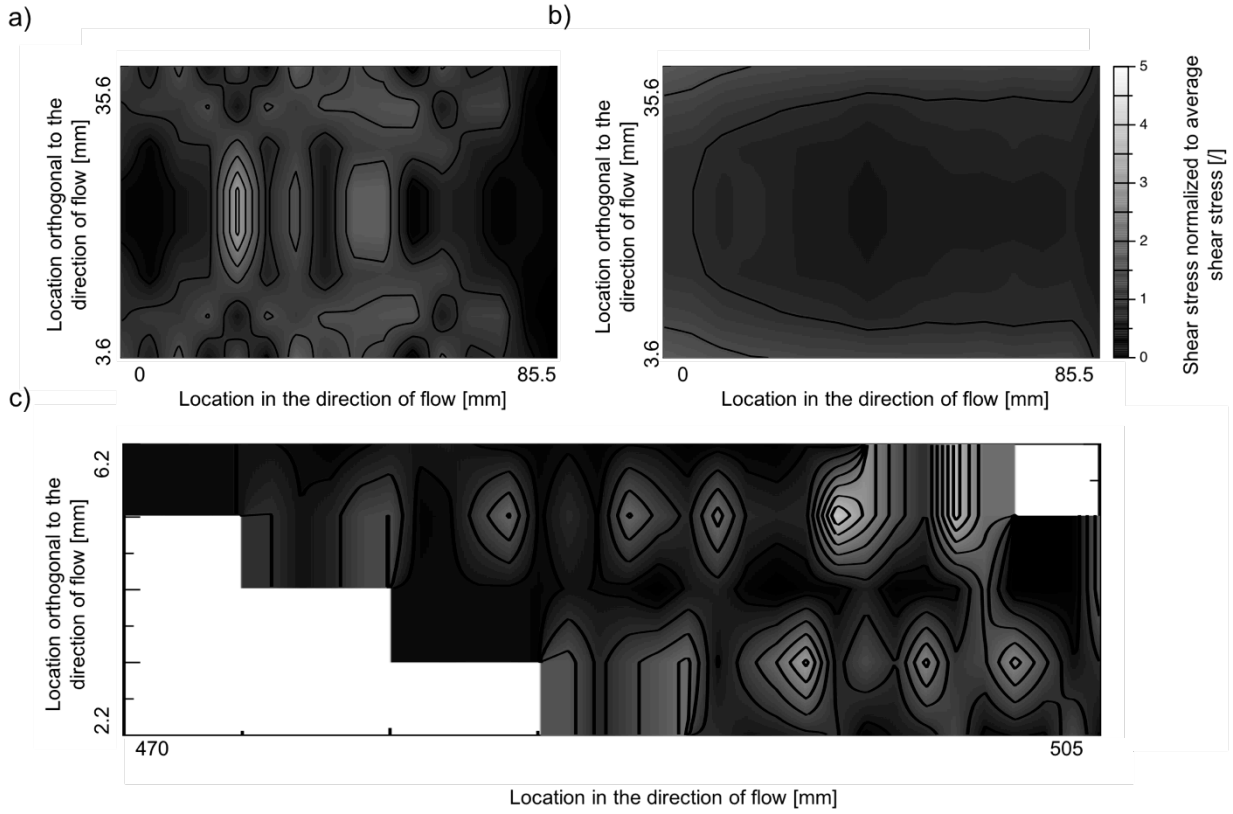

Figure 20: Typical Shear Stress at the Membrane Surface
(a: CF042 with spacer filled flow channel, cross-flow velocity = 0.79 ms^{-1}, average shear stress=6.0 ±3.6 Pa; b: CF042 with empty flow channel, cross-flow velocity of 0.76 ms^{-1}, average shear stress=4.7 ±1.4 Pa; c: custom cell with spacer filled flow channel, cross-flow velocity=0.18 ms^{-1}; average shear stress=5.6 ±4.3 Pa; ± corresponds to the standard deviation of the local shear stress values; note, for the custom test cell, shear stress was only measured over a length of 35 mm, halfway along the custom test cell, from 470-505 mm)

Table 6: Average, Minimum and Maximum Shear Stress
for the conditions investigated (CF042 test cell)

Flow channel height [mm]	**Cross flow velocity [ms^{-1}]**	Average shear stress [Pa]	Standard deviation (spatial variation)	**Cross flow velocity [ms^{-1}]**	Average shear stress [Pa]	Standard deviation (spatial variation)
	Spacer filled flow channel configuration			Empty flow channel configuration		
0.78	**0.17**	1.9	1.24	**0.17**	0.7	0.26
1.03	**0.14**	1.5	1.44	**0.13**	1.4	0.33
1.84	**0.07**	0.7	0.31	**0.08**	0.4	0.07
2.3	**N/A**	N/A	N/A	**0.06**	0.1	0.05
0.78	**0.31**	3	1.81	**0.30**	1.6	0.74
1.03	**0.25**	2.5	1.62	**0.23**	1.7	0.37
1.84	**0.13**	1.3	0.53	**0.14**	0.6	0.11
2.3	**N/A**	N/A	N/A	**0.1**	0.2	0.11
0.78	**0.79**	6.0	3.58	**0.76**	4.7	1.44
1.03	**0.63**	4.3	2.57	**0.57**	3.2	0.57
1.84	**0.32**	2.8	1.33	**0.34**	1.25	0.35
2.3	**N/A**	N/A	N/A	**0.25**	0.5	0.23

For two phase flow (i.e. with air sparging), in addition to the shear stress, the time variable characteristics of the shear stress have been documented to significantly contribute to fouling and

CP control (Chan et al., 2011). However, for single phase flow, the shear stress remains relatively constant over time. For empty flow channels, the shear stress is spatially relatively constant, while it varies considerably for spacer filled flow channels. It has been hypothesized that the high spatial variability in spacer filled flow channels substantially affects the extent of fouling and CP for single phase flow (i.e. cross-flow) systems (Koutsou et al., 2007; Thorsen and Flogstat, 2006). However, the impact of the overall magnitude of the shear stress and the spatially variable characteristics of the shear stress on the extent of fouling and CP have not been investigated.

Regression analysis indicated that the measured shear stress, averaged over time and the locations considered, for any module configuration and geometry, could be expressed using a simple linear equation (Equation 18), for which a and b are fitted parameters (see Figure 21). The R^2 values for configurations with spacer filled flow channel and empty flow channel were 0.95 and 0.93 respectively.

$$\tau_{Avg} = a \cdot \mu \cdot \frac{v_{cross\text{-}flow}}{d_h} + b \qquad \text{Equation 18}$$

where, τ_{Avg}: average shear stress at the membrane surface [Pa], μ: dynamic viscosity [Pa s], $v_{cross\text{-}flow}$: cross-flow velocity [ms^{-1}], d_h: hydrodynamic diameter [m], a and b: fitted parameters. For spacer filled flow channels the hydrodynamic diameter was calculated according to Schock and Miquel (1987) and for the empty flow channels according to White (2003).

For the configuration with spacer filled flow channels, the parameters a and b were 7.44 ± 1.36 and 0.93 ± 0.43, while for the configuration with empty flow channels they were 9.28 ± 1.76 and

0.20 ± 0.32, respectively (± corresponds to the 95 % confidence interval of the estimated parameters). The regression equation was characterized as semi-mechanistic because the average shear stress, quantified based on the momentum equation, yields a relationship similar to that presented in Equation 18, but for which parameters a and b are 8 and 0, respectively (White, 2003). These results indicate that a simple semi-mechanistic relationship can be used to quantify the impact of the system configuration and system geometry on the average shear stress induced by cross-flow.

The discrepancy between the average shear stress measured for the spacer filled channel and the shear stress calculated using the momentum equation is likely because the momentum equation assumes laminar flow while for spacer filled channels, more turbulent flow prevailed (Bucs et al., 2015; Radu et al., 2014), especially at the intermediate and high cross-flow velocities considered. Also, at a cross-flow velocity of zero, the shear stress is expected to be zero. However, for the system with spacer filled channels, the regression analysis suggests that at a cross-flow velocity of zero, the average sear stress is greater than zero. It should be noted that for the lowest cross-flow velocity considered, the average shear stress appears to deviate from the regression line and trends towards zero at a cross-flow velocity of zero. Further research, beyond the scope of the present study, would be required to investigate the impact of low cross-flow velocities, and non-laminar conditions on the average shear stress. Nonetheless, for the range of conditions investigated, Equation 18 provides a good estimate of the average shear stress induced onto the surface of a membrane by-cross-flow.

a) b)

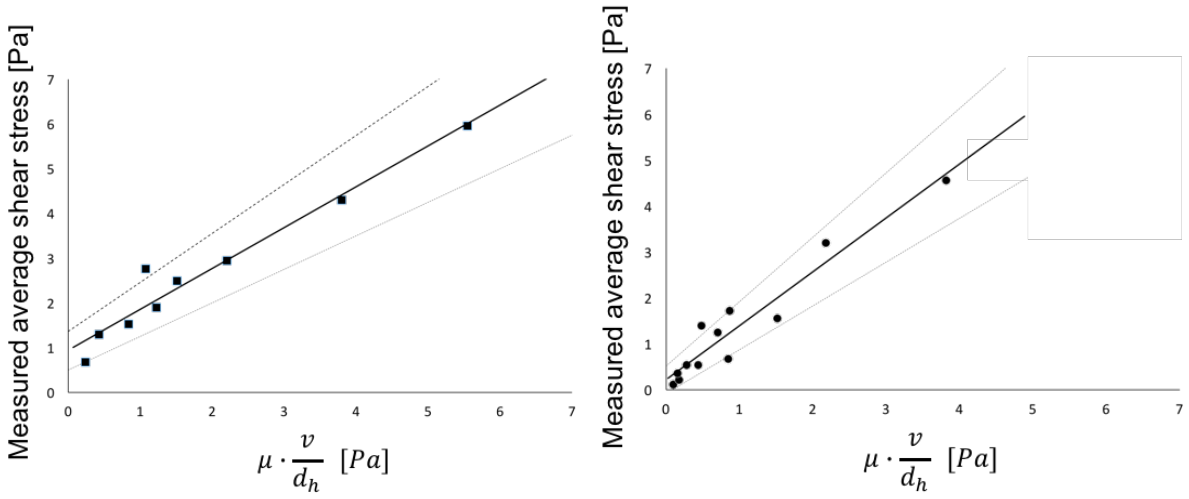

Figure 21: Average Shear Stress for Different Configurations and Geometries
(a: spacer filled flow channel, R^2=0.95; b: empty flow channel, R^2=0.92; dotted lines correspond to the 95 % confidence interval boundaries)

7.2 Permeate Flux Decline and Steady State Permeate Flux

If the extent of fouling and CP depends on the average shear stress at the membrane surface, regardless of the system configuration and spatial variability of the shear stress, the extent of fouling and CP observed for spacer filled and empty flow channels are expected to be similar at a given average shear stress.

To assess the importance of the average as well as the spatial variability of shear stress on CP and fouling, filtration tests were conducted under conditions with similar average shear stress, but different spatial variabilities (i.e. configurations with spacer filled and empty flow channels). The cross-flow velocities required to induce an average shear stress of 0.5 Pa, 2.5 Pa and 5.0 Pa

were determined using Equation 18 and the corresponding estimated parameters a and b, for systems with different configurations and geometries, except for an average shear stress of 0.5 Pa in the spacer filled flow channel configuration. The cross-flow velocities required to induce an average shear stress of 0.5 Pa in the spacer filled flow channel configuration was estimated by interpolating between the data point with the lowest measured shear stress (i.e. 0.68 Pa) (see Figure 21) and zero (see discussion Section 7.1).

For the first series of filtration tests, which were performed with the CF042 test cell, the initial permeate flux was set to 42 (± 3) L m^{-2} h^{-1}. The initial permeate flux was selected such that significant flux decline could be observed during the filtration tests. To account for slight variations in initial permeate flux between filtration tests, the results were normalized to the initial permeate flux.

For all conditions investigated, a significant decrease in normalized permeate flux was observed (see Figure 22). As expected, the decrease in normalized permeate flux was higher at lower average shear stress values (Belfort, 1994, Sethi and Wiesner, 1997). For the filtration tests for which the shear stress was set at 0.5 Pa, 2.5 Pa and 5.0 Pa, the normalized flux decreased to 65-71 %, 78-84 % and 85-87 % of the initial value, respectively, after filtering 600 Lm^{-2} of raw water. However, for a given average shear stress, no difference in permeate flux decline was observed for test cells with different configurations (i.e. spacer filled and empty flow channels) and geometries (i.e. flow channel heights). These results indicate that the extent of fouling and CP was dependent on the average shear stress at the membrane surface and independent of the spatial variability of the shear stress.

a)

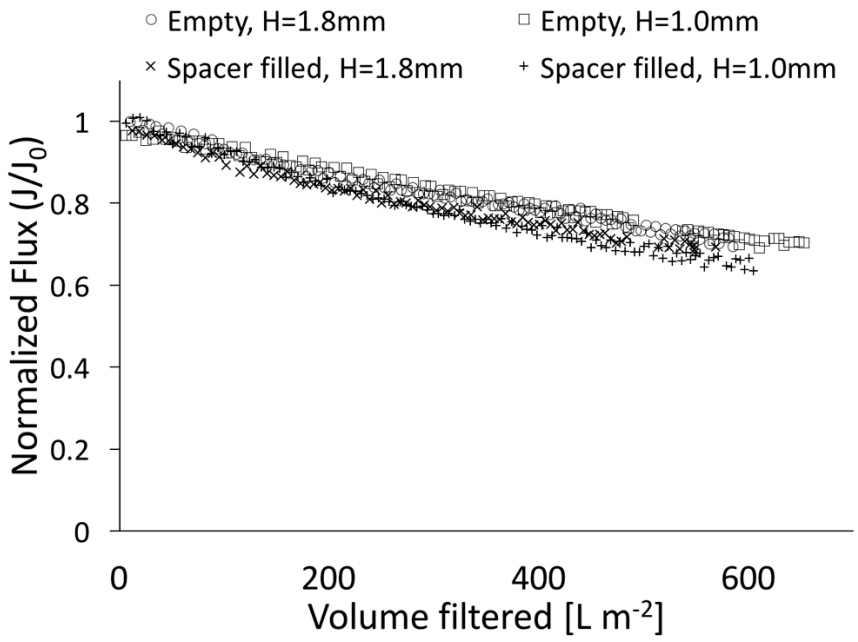
Empty, H=1.8mm
Empty, H=1.0mm
Spacer filled, H=1.8mm
Spacer filled, H=1.0mm
Normalized Flux (J/J0)
1
0.8
0.6
0.4
0.2
0
0
200
400
600
Volume filtered [L m-2]

b)

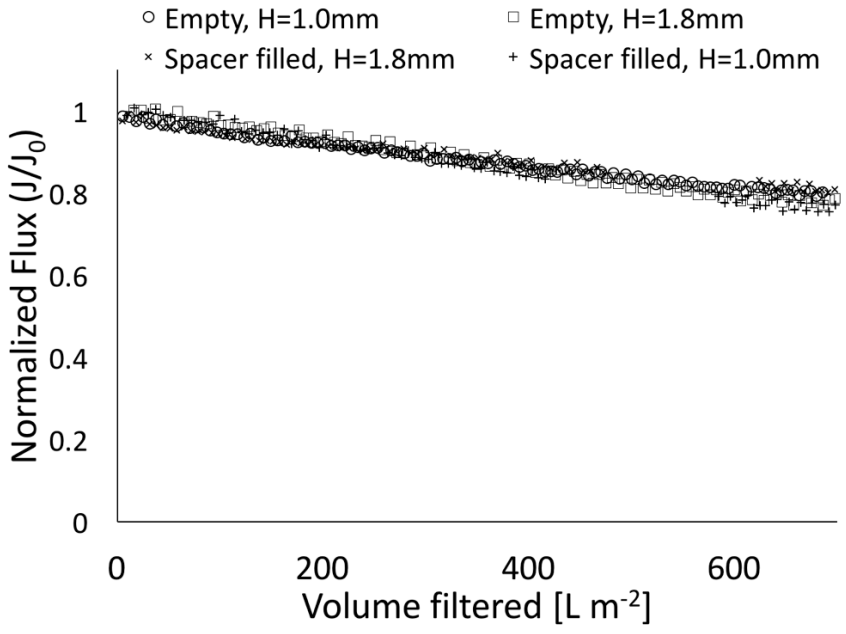
Empty, H=1.0mm
Empty, H=1.8mm
Spacer filled, H=1.8mm
Spacer filled, H=1.0mm
Normalized Flux (J/J0)
1
0.8
0.6
0.4
0.2
0
0
200
400
600
Volume filtered [L m-2]

c)

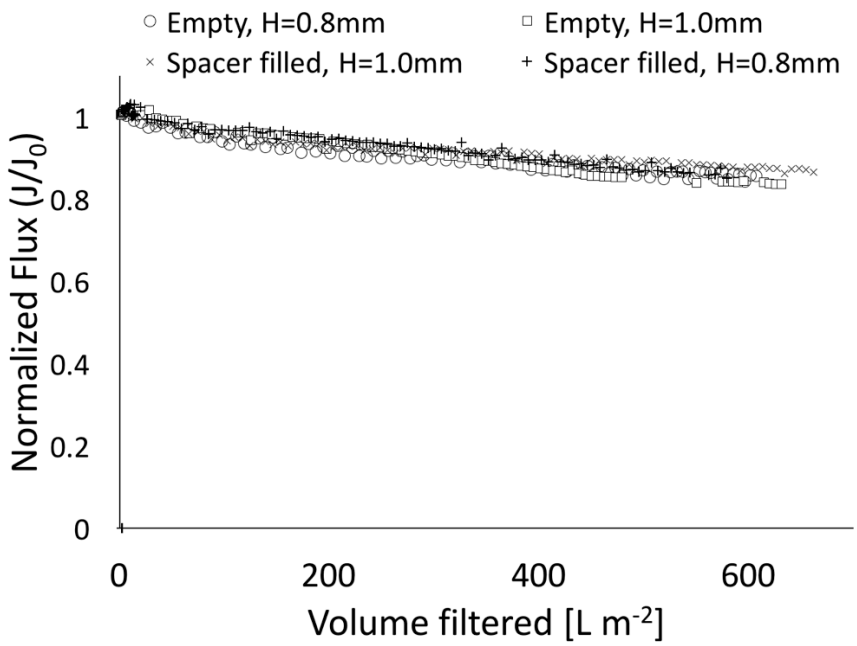

Figure 22: The Impact of Average Shear Stress on the Normalized Permeate Flux – First Series of Filtration Tests (a: average shear stress = 0.5 Pa, b: average shear stress = 2.5 Pa, c: average shear stress = 5.0 Pa; H corresponds to the flow channel height)

As previously discussed, the permeate flux at steady state provides an estimate of the back-transport of the material that would otherwise accumulate at the membrane surface (see Section 4.4.2). For this reason, the impact of the different hydraulic control measures was assessed based on the permeate flux that could be sustained at steady state, estimated by fitting Equation 7 to the filtration data.

The estimated permeate flux values at steady state for the different conditions investigated are summarized in Figure 24. As expected, the estimated steady state flux increased with the average shear stress induced by the cross-flow at the membrane surface. Similar steady state flux values

were observed for the test cells with spacer filled and empty flow channels at a given average shear stress, again indicating that the extent of fouling and CP was dependent on the average shear stress at the membrane surface and independent the spatial variability of the shear stress.

Although the steady state permeate flux could be estimated by fitting Equation 7 (see Section 4.4.2) to the filtration data from the first series of filtration tests, steady state conditions were never actually reached during these experiments. For this reason, a second series of filtration tests was also conducted with CF042 test cells to validate the steady state flux estimated during the first series of filtration tests. For the second series of filtration tests, the initial permeate flux was set to a value equivalent to the maximum steady state flux estimated from the first series of filtration tests for a given set of experimental conditions (see Figure 24). Since the magnitude of the steady state flux was of interest, absolute values are presented in Figure 23.

As illustrated in Figure 24 and Table 7, the steady state flux estimated in the second series of filtration tests are consistent with those estimated in the first series of filtration tests. These results once again indicated that the extent of fouling and CP was dependent on the average shear stress at the membrane surface and independent of the spatial variability of the shear stress. Because the steady state conditions estimated during the first and second series of filtration tests are similar, the results also indicate that the permeate flux that can be sustained, and therefore the extent of back-transport, is not impacted by the initial permeate flux.

A third series of filtration tests, performed with the hollow fiber mini module, was conducted to confirm if the results obtained using CF042 membrane test cells with empty flow channel

configurations (i.e. without spacers) were representative of systems with hollow fiber configurations with inside-out permeate flow. The average shear stress induced at the membrane surface for the hollow fiber mini module was calculated using the momentum equation (i.e. Equation 18 with a = 8 and b = 0), where the hydraulic diameter corresponding to the inner diameter of the hollow fiber (White, 2003, Payant et al., 2017). The cross-flow velocity was adjusted to induce an average shear stress of 5.0 Pa at the membrane surface and the initial permeate flux was adjusted to be equal to the maximum estimated steady state flux for configurations with empty flow channels. No difference in the steady state permeate flux was observed for the test with the CF042 test cell with empty flow channel configuration and the hollow fiber NF mini module (see Figure 23 c, Figure 24, and Table 7), indicating that the results for empty flow channels are representative of these for inside out hollow fiber mini modules.

Consistent with the outcomes of a study conducting computational fluid dynamics modelling of a laboratory membrane filtration cell (Tarabara and Wiesner, 2003), Radu et al. (2014) and Bucs et al. (2015) reported that the hydrodynamic conditions in smaller membrane test cells with spacer filled flow channels are representative of those in full scale spiral wound configurations. Therefore, the results for the CF042 test cell with spacer filled and empty flow channel configurations from the present study are expected to be representative of full scale spiral wound and hollow fiber membrane configurations, respectively.

a)

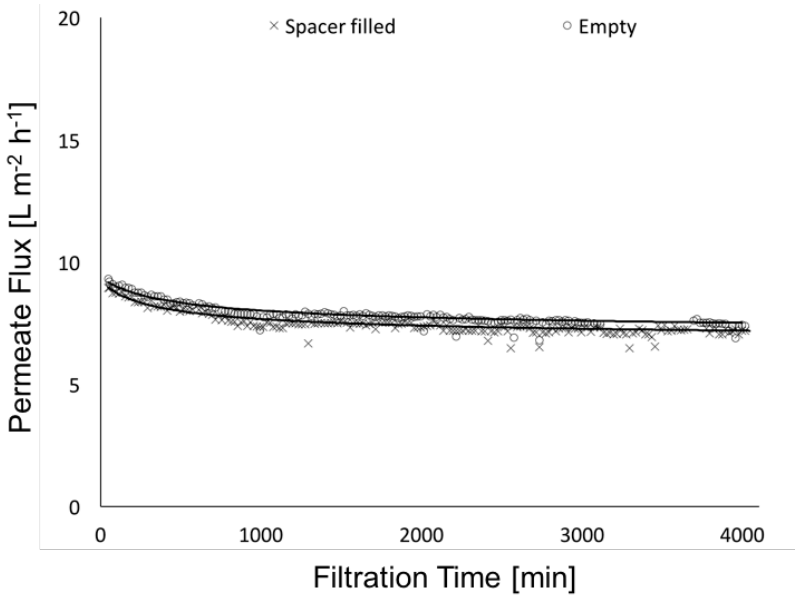
Spacer filled
Empty
Permeate Flux [L m-2 h-1]
Filtration Time [min]
0
5
10
15
20
0
1000
2000
3000
4000

b)

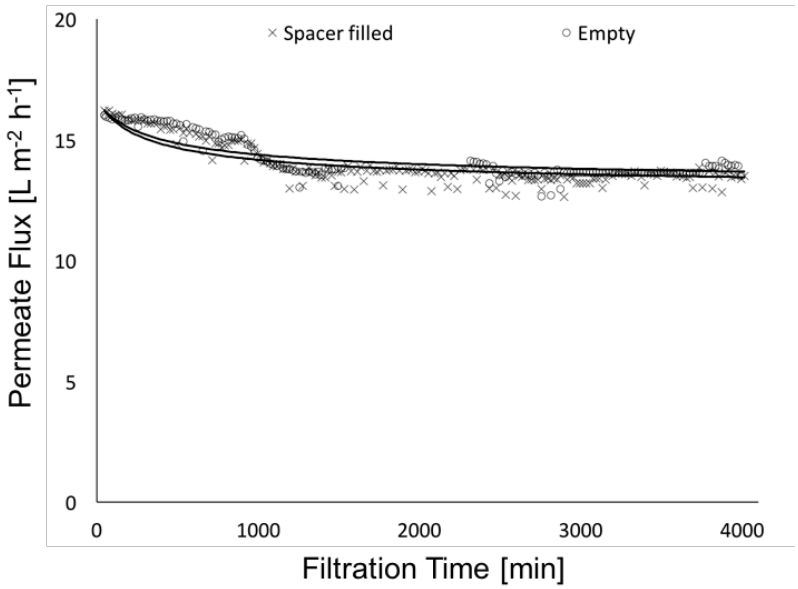
Spacer filled
Empty
Permeate Flux [L m-2 h-1]
Filtration Time [min]
0
5
10
15
20
0
1000
2000
3000
4000

c)

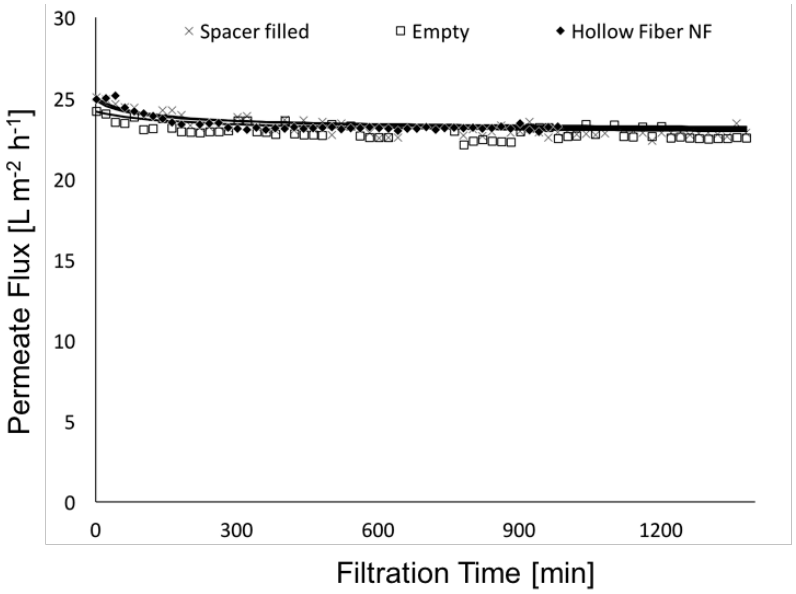

Figure 23: Impact of Average Shear Stress on the Permeate Flux – Second Series of Filtration Tests (a: average shear stress = 0.5 Pa, b: average shear stress = 2.5 Pa, c: average shear stress = 5.0 Pa; solid lines represent fitted filtration model – i.e. Equation 7, see Section 4.4.2)

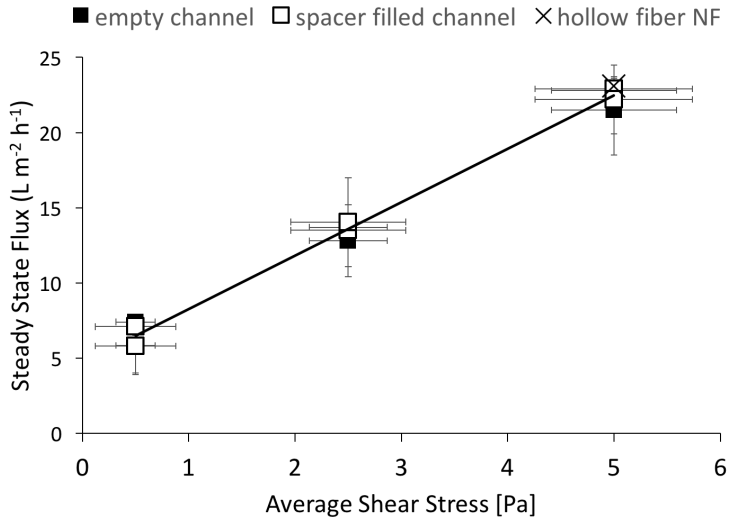

Figure 24: Estimated Steady State Permeate Flux versus Average Shear Stress (linear regression: $R^2 = 0.99$; x-axis: error bars correspond to the confidence interval boundaries defined by the standard error of the fitted parameters; y-axis: error bars correspond to minimum and maximum value)

Table 7: Estimated Steady State Permeate Flux Values

		First Series of Filtration Tests (CF042 Test Cell)	Second Series of Filtration Tests (CF042 Test Cell)	Third Series of Filtration Tests (Hollow Fiber Mini Module)
Average Shear Stress [Pa]*	Configuration	J_{SS} ** $[Lm^{-1}h^{-1}]$	J_{SS} $[Lm^{-1}h^{-1}]$	J_{SS} $[Lm^{-1}h^{-1}]$
0.5 (± 0.2)	With spacer	5.8 (± 1.9)	6.64	N/A
0.5 (± 0.4)	Without spacer	5.9 (± 1.9)	6.85	N/A
2.5 (± 0.4)	With spacer	14.1 (± 3.0)	11.85	N/A
2.5 (± 0.5)	Without spacer	12.8 (± 2.4)	12.07	N/A
5.0 (± 0.6)	With spacer	22.2 (± 2.3)	22.14	N/A
5.0 (± 0.7)	Without spacer	21.5 (± 3.0)	22.70	N/A
5.0	N/A	N/A	N/A	22.50 (± 0.02)

* ± corresponds to the confidence interval boundaries defined by the standard error of the fitted parameters

** ± corresponds to minimum and maximum value

7.3 Framework to Compare the Performance of NF Membranes of Different Configurations and Geometries

The increase in the steady state permeate flux with the increase in average shear stress at the membrane surface is most likely related to the back-transport of biopolymers, such as polysaccharides, and particulate matter (see Sections 6.2.2-6.3). Neither the back-transport of particulate matter nor the back-transport of biopolymers, such as polysaccharides, are substantially affected by Brownian diffusion (see Sections 5.2-5.3). Hence, it was hypothesized that shear induced diffusion is the dominant back-transport mechanism affecting the steady state permeate flux. If shear induced diffusion is the dominant back-transport mechanism affecting the steady state permeate flux, a linear relationship would be expected between those two parameters

(Belfort, 1994; Sethi and Wiesner, 1997). The hypothesis that shear induced diffusion is the dominant back-transport mechanism affecting the steady state permeate flux was confirmed by regression analysis, which indicated that the estimated steady state permeate flux values from the first, the second, and the third series of filtration tests could be expressed using a simple linear equation (see Equation 19), for which c and d are fitted parameters (see Figure 24). Inserting Equation 18 into Equation 19, yields in a relationship for the steady state flux as a function of cross-flow velocity and hydrodynamic diameter (see Equation 20). The fitted parameters c and d were 3.56 ± 0.24 and 4.27 ± 0.83, respectively, for both spacer filled and empty flow channels (± corresponds to the 95 % confidence interval of the estimated parameters). The fitted parameters a and b are presented in Section 7.1 for spacer filled and empty flow channel configurations.

$$J_{SS} = c \cdot \tau_{Avg} + d \qquad \text{Equation 19}$$

$$J_{SS} = a \cdot c \cdot \mu \cdot \frac{v_{cross\text{-}flow}}{d_h} + c \cdot b + d \qquad \text{Equation 20}$$

where J_{SS}: steady state flux, τ_{Avg}: average shear stress at the membrane surface [Pa], μ: dynamic viscosity [Pa s], $v_{cross\text{-}flow}$: cross-flow velocity [ms-1], dh: hydrodynamic diameter [m], a, b, c, and d: fitted parameters.

Equation 20 provides a framework to compare the performance of NF membranes of different configurations and geometries in terms of the permeate flux that can be sustained.

At an average shear stress of zero the sustainable permeate flux is expected to be zero. However, the regression analysis suggests that at an average shear stress of zero, the permeate flux that can

be sustained is greater than zero. Further research, beyond the scope of the present study, would be required to investigate the impact of low average shear stress on the permeate flux that can be sustained. Nonetheless, for the range of conditions investigated, Equations 20 and 21 provide a good estimate of the permeate flux that can be sustained for a given cross-flow velocity, system configuration and system geometry.

It should be noted that additional research is also needed to assess the input of raw water characteristics on the correlation relating the parameters obtained during the present study.

7.4 Conclusions

The following three main conclusions can be made based on the results of the present study.

- A semi-mechanistic relationship, based on the momentum equation, can be used to estimate the average shear stress induced by cross-flow at the membrane surface for different configurations and geometries.

- The extent of fouling and CP was dependent on the average shear stress at the membrane surface and independent of the spatial variability of the shear stress, and with that independent of the system configuration (i.e. spacer filled versus empty flow channel), as well as independent of the system geometry (i.e. hydrodynamic diameter).

- A relationship was developed that provides a framework to compare the performance of NF membranes of different configurations and geometries in terms of the permeate flux

that can be sustained, and to optimize the operating set point of NF membranes with respect to system configuration, cross-flow velocity and operating flux.

Chapter 8: Cost Comparison and Optimization of Hollow Fiber and Spiral Wound NF Systems (Objective 4)

The objective of the fourth part of the study was to apply the framework developed in the previous section to determine operational parameters (i.e. operating permeate flux and cross-flow velocity) resulting in the lowest cost for both, spiral wound and hollow fiber configurations. The impacts of membrane life time and membrane cost on the optimal operation and systems' cost was evaluated. Spiral wound and hollow fiber configurations are comprehensively compared on the basis of capital and operational costs.

8.1 Cost Optimization

A relationship was developed that relates the cross-flow velocity to the steady state flux (see Section 7.3), which corresponds to the permeate flux that can be sustained and is, hence, recommended as the operating flux (Bachin et al., 2006; Field and Pearce, 2011). Using this relationship, the cross-flow required to operate at a given sustainable flux can be calculated using Equations 18 (Section 7.1) and 19 (Section 7.3) – the corresponding parameters a, b, c and d are presented in Sections 7.1 and 7.3. With this information, it is possible to estimate the capital and operating costs associated with the sustained operation of NF membranes, at a given cross-flow velocity (as presented in Section 4.8). The assumptions for the cost estimation and optimization are presented in Table 8.

A summary of the results for the cost estimation and optimization for the hollow fiber NF and spiral wound NF system are presented in Figure 25. The cost for purchasing and replacing the membranes decreases as the operating flux (i.e. J_{SS}) increases (see Equation 15, Section 4.8)

because less total membrane area is required to produce a given volume of treated water when operating at a higher permeate flux. The energy costs increase as the operating flux (i.e. J_{SS}) increases because the cross-flow required for operation at a higher sustainable flux increases according to Equation 20, and the power required increases with increasing cross-flow (Equations 8-10) and permeate flow (Equation 14) (see Section 4.8). Combined, the membrane costs and the energy costs result in a minimum total cost at a given operating permeate flux, depending on the system configuration, the geometry, the specific membrane cost, the membrane permeability, and membrane operational life of a membrane system. The specific membrane costs and the permeability depend on the membrane being considered. The pressure drop due to cross-flow is specific to the module configuration and geometry (see Equations 9-10, Section 4.8). Also, the relationship between cross-flow velocity and operating flux is expected to be affected by the raw water characteristics; as such, additional research is needed to assess the input of raw water characteristics on the correlation relating the parameters obtained during the present study (see Section 7.3).

Table 8: Parameters for Cost Estimation and Optimization

Parameter	Assumption	Reference
Design life	20 years	Costa and de Pinho, 2006 Sethi and Wiesner, 2000
Annual interest rate	2 %	
Membrane lifetime	5 years	Costa and de Pinho, 2006 Sethi and Wiesner, 2000
Membrane cost	Hollow Fiber NF: 140 $USm^{-2} Spiral wound NF: 35 $USm^{-2}	Costa and de Pinho, 2006 Samhaber and Nguyen, 2014 Sethi and Wiesner, 2000
Module geometry specifications considered	Hollow Fiber: Pentair HFW1000 (membrane area of 40 m^2 per module) Spiral Wound: 8" element with 31 mil spacer (membrane area of 42.4 m^2 per module)	
Permeability	10.4 $Lm^{-2}h^{-1}$	Pentair X-Flow HFW1000 Data Sheet
Wire to water efficiency	70 %	Sethi and Wiesner, 2000
Energy cost	0.0875 US(kWh)^{-1}$	Samhaber and Nguyen, 2014 USIEA, 2017
Temperature	20ºC	
Raw Water	Jericho Pond Water	Present study (see Sections 4.7.2 and 7.2-7.3)

a)

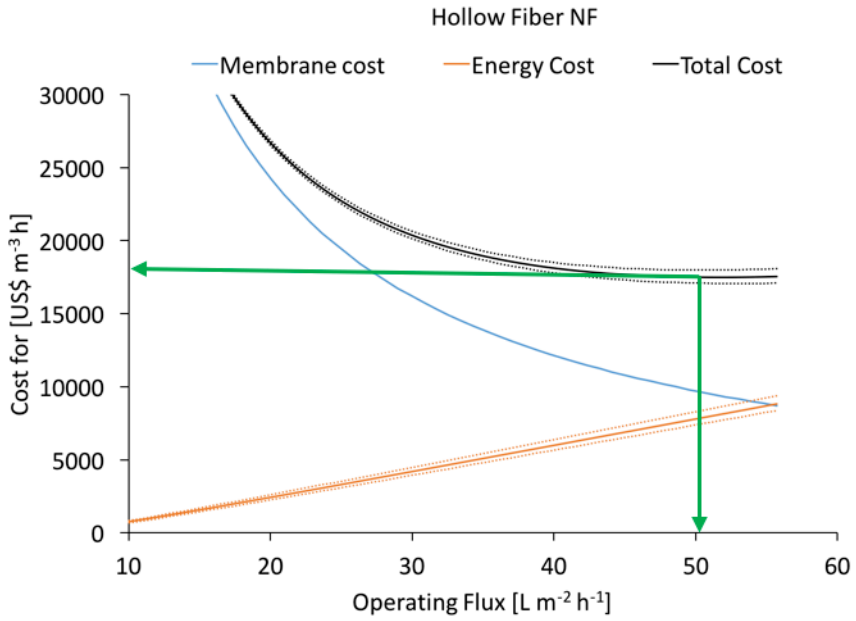

b)

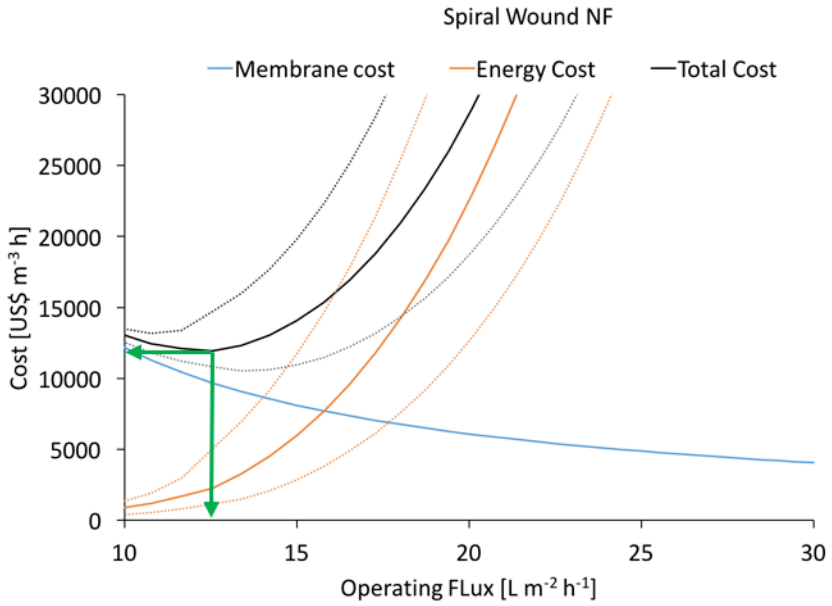

Figure 25: Cost Estimation and Optimization
(a: hollow fiber NF; b: spiral wound NF; dotted lines correspond to the confidence interval boundaries defined by the standard error of the fitted parameters; arrow presents optimal operating permeate flux corresponding to minimal total cost)

The operational set point corresponding to the lowest overall cost for the hollow fiber NF was operation at a permeate flux of approximately 50 $Lm^{-2}h^{-1}$. Sustained operation at this permeate flux requires a cross-flow velocity of approximately 1.3 ms^{-1}, and an inlet pressure of approximately 4.8 bar. Under these conditions, pressure drop along the length of the membrane module (module length = 1.5 m) is approximately 1.0 bar. The overall cost associated with hollow fiber NF operated at 50 $Lm^{-2}h^{-1}$ is approximately 17,500 $ per m^3h^{-1} produced for 20 years (i.e. approximately 0.1 $\$m^{-3}$). Note that the optimal operating flux determined in the present study is substantially higher than that commonly applied in spiral wound NF systems (i.e. 15-20 $Lm^{-2}h^{-1}$) (Keucken et al., 2016; Payant et al., 2017). Also, the optimal operational conditions discussed above are outside the range of conditions considered during the experimental part of the presented in Section 7.3. (i.e. cross-flow velocity greater than 0.5 ms^{-1}). Hence, the estimated steady state flux for operation at a cross-flow velocity at 1.3 ms-1, using the relationships developed in Sections 7.1 and 7.3, must be validated during pilot trials.

The operational set point corresponding to the lowest overall cost for the spiral wound NF was operation at a permeate flux of approximately 12 $Lm^{-2}h^{-1}$. Sustained operation at this permeate flux requires a cross-flow velocity of approximately 0.1 m s^{-1}, and an inlet pressure of approximately 1.2 bar. Under these conditions, pressure drop along the length of the membrane module (i.e. 1 m) is approximately 0.6 bar. The overall cost associated with spiral wound NF operated at 12 $Lm^{-2}h^{-1}$ is approximately 11,800 $ per m^3h^{-1} produced for 20 years (i.e. approximately 0.07 $\$m^{-3}$). Note that the optimal operating flux determined in the present study is lower than that commonly applied in spiral wound NF systems (i.e. 15-30 $Lm^{-2}h^{-1}$) (Shetty and Chellam, 2003; Odegaard et al., 2010).

For the hollow fiber NF system the overall lowest cost was predicted at a relatively high operating permeate flux and corresponding high cross-flow velocity. This is because the assumed specific membrane costs are relatively high (i.e. 140 $\$m^{-2}$) and the increase in energy costs with an increase in cross-flow velocity are relatively modest. Hence, the overall cost is dominated by the membrane costs and the operating permeate flux corresponding to the lowest total cost is relatively high. In contrast, for the spiral wound NF system, the specific membrane costs are relatively low (35 $\$m^{-2}$) and the energy costs increase relatively rapidly with an increase in cross-flow velocity. Hence, for spiral wound NF systems, the overall cost is dominated by the energy costs and the operating permeate flux corresponding to the lowest total cost is relatively low.

8.2 Impact of Membrane Cost and Operational Life on Optimal Permeate Flux

Spiral wound NF is a well established technology and relatively accurate assumptions can be made with respect to the membrane costs. However, hollow fiber NF became commercially available relatively recently, making it more difficult to estimate the specific membrane cost. The sensitivity of the overall cost and optimal operating permeate flux, with respect to the specific membrane cost assumed for the hollow fiber NF system, was considered (see Figure 26).

To generate an overall cost for the hollow fiber NF system that is similar to that of the spiral wound NF system (i.e. 11,800 $), the specific membrane cost for the hollow fiber NF system would need to be approximately 60 $\$m^{-2}$ (i.e. about 1.7 times the price for spiral wound NF membranes). The corresponding optimal operating flux for this cost would be approximately 34

$Lm^{-2}h^{-1}$. Sustained operation at this permeate flux requires a cross-flow velocity of approximately 0.9 ms^{-1}.

Another assumption that was made for this cost estimation, with a relatively high uncertainty, is the expected membrane operating life. Relatively little data is available regarding the lifetime of NF membranes applied in drinking water treatment. However, it has to be noted that spiral wound NF membranes are commonly made with PA or CA as the selective barrier (Schäfer et al., 2005; Schäfer, 2007; Frank et al., 2001; Do et al., 2012). As previously discussed, the lifetime of these membranes is shorter than the lifetime of UF membranes that are typically made from PVDF or PES (see Section 2.4.3). However, the commercially available hollow fiber NF membrane is made from modified PES and, hence, a membrane lifetime similar to that of UF membranes can be expected. The sensitivity of the overall cost and optimal operating permeate flux with respect to the membrane operating life assumed for the hollow fiber NF system was considered (see Figure 27).

At a membrane lifetime of 10 years for the hollow fiber NF system, the overall cost would be approximately 12,300 $, which is relatively similar to the cost for the spiral wound system. However, the hollow fiber NF system requires less pre-treatment, which is not considered in the present cost analysis. At a membrane lifetime of 10 years, the operational set point corresponding to the lowest overall cost for the hollow fiber NF is operation at approximately 38 $Lm^{-2}h^{-1}$. Sustained operation at this permeate flux requires a cross-flow velocity of approximately 0.9 ms^{-1}, and an inlet pressure of approximately 4 bar. Under these conditions, pressure drop along the length of the membrane modules (i.e. 1.5 m) is approximately 0.4 bar.

The overall cost associated with a hollow fiber NF with a operating life of 10 years, operated at 38 $Lm^{-2}h^{-1}$, is approximately 12,300 $ (i.e. approximately 0.07 $\$m^{-3}$).

Overall, the cost comparison conducted in the present study demonstrates that hollow fiber NF systems can be competitive in terms of overall costs, when compared to spiral wound NF systems, despite their likely higher production costs. For a more accurate cost comparison and a more conclusive comparison, more accurate data is required, particularly with respect to the cost of hollow fiber NF membranes and their expected operational life. Hollow fiber NF systems are of interest because of their higher flexibility with respect to physical cleaning, such as applicability of backwash, forward flush and air assisted forward flush (Payant et al., 2017) and lower requirements for pre-treatment, compared to spiral wound NF.

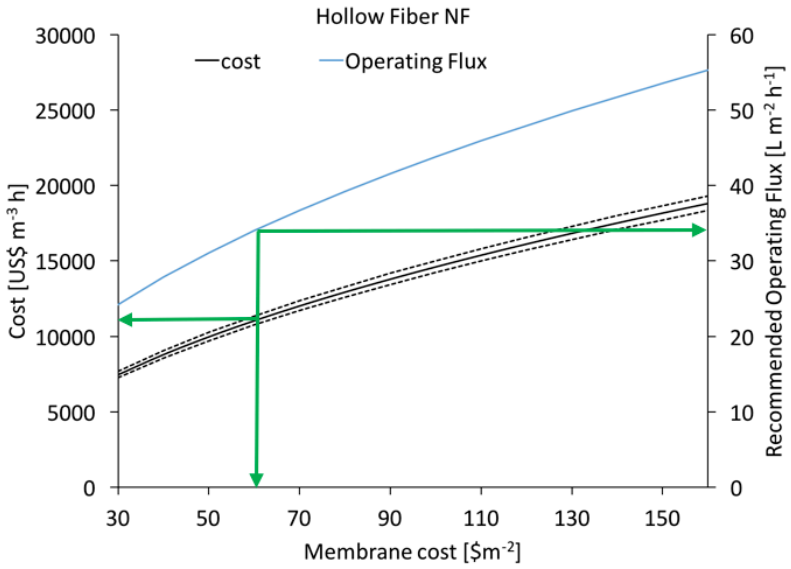

Figure 26: Hollow Fiber NF Cost and Operating Flux – Sensitivity to Specific Membrane Cost (dotted lines correspond to the confidence interval boundaries defined by the standard error of the fitted parameters; arrow presents optimal operating permeate flux corresponding to an overall cost of approximately 11,800 $)

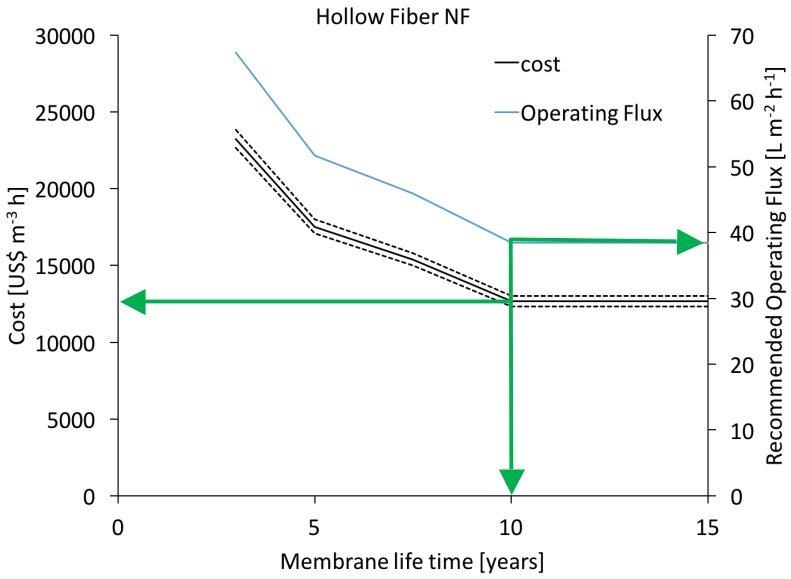

Figure 27: Hollow Fiber NF Cost and Operating Flux – Sensitivity to Membrane Lifetime (dotted lines correspond to the confidence interval boundaries defined by the standard error of the fitted parameters; arrow presents optimal operating permeate flux corresponding to the overall minimum cost for an assumed membrane operating life of 10 years)

Note that the sensitivity of the overall cost and optimal operating permeate flux with respect to the temperature and the energy cost was considered and is not further discussed in this section of the dissertation. This is because the uncertainty associated with these parameters is much less than the uncertainty associated with the membrane operating life and the membrane cost for hollow fiber NF. Plots of the sensitivity of the overall cost and optimal operating permeate flux with respect to the temperature and the energy cost considering the assumption stated in Table 8 are provided in Appendix F.

8.3 Conclusions

The following 4 main conclusions can be made based on the results of the present study.

- A relationship that relates cross-flow velocity to the permeate flux that can be sustained was used to estimate the optimal operating permeate flux, which corresponds to the lowest overall cost for hollow fiber NF and spiral wound NF membrane systems.

- The optimal operating conditions for hollow fiber NF and spiral wound NF systems differ substantially due to differing relationships between cross-flow velocity and pressure loss along the module length and the expected differences in manufacturing costs.

- The estimated optimal operating flux for hollow fiber NF is substantially higher than that commonly applied, while the estimated optimal operating flux for spiral wound NF is similar or lower to that of existing applications.

- Despite the expected higher manufacturing costs, hollow fiber NF could be cost competitive with spiral wound NF.

Chapter 9: Overall Discussions and Engineering Implications

When present in the source water, natural organic matter (NOM) removal is essential during drinking water treatment because of its contribution to color, odor and taste, as well as its role as a precursor for the formation of disinfection by-products. Along with the process of global warming, the content of NOM in many surface waters is expected to increase (Hejzlar et al., 2003; Domnisoru, 2007).

Biological filtration is cost effective and easy to operate. However, the extent of DOC removal is limited, making biological filtration only suitable for treatment of source waters with relatively low DOC concentrations (Odegaard et al., 2010). Despite the effect of pre-ozonation on the biodegradation kinetics of some raw waters, the increase in overall removal of NOM is limited (see Appendix A.1). A recent study, conducted in parallel to the research on NF and tight UF membranes presented in this dissertation, has demonstrated that the application of anionic ion exchange resins operated under conditions where biological activity is promoted (BIEx) is a promising alternative to conventional biological filtration, such as biological activated carbon (BAC) (see Appendix A.2). Over a 10-month test period, corresponding to over 15,000 empty bed volumes, the DOC removal efficiencies were stable in the BIEx system and in the BAC system. However, NOM removal efficiency was substantially higher for the BIEx system (56 ± 7 %) compared to the BAC system (15 ± 5 %). Hence, BIEx appears to be a promising treatment technology with advantages similar to those of conventional biological filtration, but with a substantially higher NOM removal efficiency. However, also with BIEx, NOM removal efficiencies are not sufficient for raw waters with very high NOM content. In addition, BIEx does not remove turbidity (as opposed to hollow fiber NF).

NF and tight UF can achieve high NOM rejection and the compliance with surface water requirements appear unproblematic, even if the raw water contains NOM at very high concentrations as demonstrated in the present study and reported by others (Schäfer, 2007; Lee et al., 2004; Lee et al., 2005a; Odegaard et al., 2010; Patterson et al., 2012; Lee et al., 2004). In the present study it was found that membranes with MWCOs below 2,000 Da have a high selectivity for NOM. These membranes are particularly well suited for source waters with high concentrations of NOM where other treatments are not able to achieve a sufficient NOM removal. The application of these NF and tight UF membranes is limited to date, mainly because of the challenges related to fouling, CP, system complexity and cost. The aim of the present study was to investigate these issues and to develop frameworks and recommendations for the design and operation of NF and tight UF membrane systems that enable a more widespread application of this technology.

The possibility of simplifying NF and tight UF systems applied for drinking water treatment by considering operation in dead end mode (i.e. no cross-flow applied at the membrane surface) was assessed. The question whether those systems can be operated in dead end mode is closely related to the role of concentration polarization (CP) in the application of NF and tight UF membranes for drinking water treatment. The studies conducted by Schäfer et al. (1998) and Yoon et al. (2005) indicated that CP contributes to the increase in resistance to permeate flow during filtration of raw waters containing NOM. However, comprehensive knowledge on the effect of (i) the type of NOM (e.g. polysaccharides and humic substances), (iii) the concentration of NOM, (iv) the presence of particulate matter and calcium, and (v) the membrane MWCO on

the contribution of CP to the total increase in resistance to permeate flow is had not been comprehensively studied. The present study revealed that the increase in resistance to permeate flow by CP is caused by humic substances. At high concentrations of humic substances (i.e. 10 mgL^{-1}) CP becomes extensive and a CP induced humic substances cake/gel layer likely forms. The formation of this cake/gel layer results in a rapid increase in resistance to permeate flow. The concentrations of humic substances considered are realistic in practice because humic substances are the typically present at high concentrations in natural surface waters (Zumstein and Buffle, 1989) and the retained material is concentrated during operation, particularly in dead-end systems. Hence, based on the results from the present study, continuous hydraulic control measures (i.e. cross-flow) operation should be considered for drinking water treatment, using NF and tight UF membranes to control CP, and dead-end operation cannot be recommended.

The application of low intensity continuous hydraulic control measures (i.e cross-flow) is efficient in mitigating CP and fouling. However, when calcium and particulate matter (i.e. kaolin) were present in the raw water containing humic substances and polysaccharides, and fouling dominates the increase in resistance to permeate flow (see Section 5.3), hydraulic control measures primarily affected the accumulation of polysaccharides and particulate matter. For the range of cross-flow velocities considered, the amount of polysaccharides and particulate matter accumulating at the membrane surface decreased as the cross-flow velocity increased. Therefore, a high intensity hydraulic control measure is recommended to minimize the increases in resistance to permeate flow during filtration using NF and tight UF membranes. As reported by Payant et al., (2017), periodic back-wash and air scouring could also enhance the effectiveness of

cross-flow. The filtration tests using permeate flux interruptions (i.e. relaxation) indicated that it was difficult to hydraulically remove the accumulated material once a foulant layer had been formed. Therefore, it is recommended to apply the high intensity hydraulic control measure continuously (i.e. apply high velocity cross-flow), to prevent the accumulation of polysaccharides and particulate matter at the membrane surface.

The last part of the present study (i.e. Chapters 7 and 8) focused on optimizing the conditions for cross-flow operation of NF and tight UF membranes applied to drinking water treatment. A framework was developed to compare the performance of NF membranes of different configurations (i.e. spiral wound and hollow fiber configurations) and geometries (i.e. size of flow channels) in terms of the permeate flux that can be sustained, and to optimize the operating set point of NF membranes with respect to system configuration, cross-flow velocity and sustainable operating flux. An approach for the cost optimization was developed that allows for a comprehensive optimization with respect to sustainable operating flux and cross-flow velocity (see Sections 8.1 and 8.2). Since the raw water characteristics are expected to affect the permeate flux that can be sustained, the cost estimation is case specific. Also, a better knowledge on the expected membrane lifetime, particularly for the hollow fiber NF, which became commercially available relatively recently, would improve the accuracy of the cost estimation. Nonetheless, the cost estimation and comparison conducted in the present study indicates that hollow fiber NF, despite the expected higher manufacturing costs, can be cost competitive with spiral wound NF. The cost optimization approach developed as part of the present research is expected to contribute to the lowering of costs for NF membrane systems applied to drinking water treatment.

Chapter 10: Conclusions and Recommendations

10.1 Conclusions

The study discussed in the present dissertation aimed to develop recommendations for the system design and operation of NF and tight UF membranes applied to drinking water treatment. The major conclusions of the study are listed below.

- Because NOM in most surface waters consists mainly of humic substances (i.e. lower molecular weight NOM) and because effective NOM removal is likely one of the main motivation to implement NF and tight UF membranes in drinking water treatment, membranes with lower MWCOs (i.e. < 2,000 Da) are recommended for this application.

- When filtering raw waters containing high concentrations of alginate (i.e. polysaccharides, high molecular weight NOM), the total increase in resistance to permeate flow is mainly dominated by fouling; when filtering raw waters containing predominantly humic substances (i.e. lower molecular weight NOM), the total increase in resistance to permeate flow is mainly dominated by CP. The impact of CP is greatest for membranes with low MWCOs (i.e. < 2,000 Da).

- When filtering raw waters containing high concentrations of humic substances (i.e. 10 mgL^{-1}) with the membrane with the lowest MWCO (i.e. 300 Da), the impact of CP became extensive and the increase in resistance was greater than observed for any other experimental condition considered, likely due to the formation of a CP induced cake/gel layer.

- Operation with control measures to continuously limit CP, such as cross-flow operation, should be considered in drinking water applications using NF and tight UF membranes. Dead end operation, which is typically used for drinking water production using UF, is not recommended because it cannot continuously limit CP.

- The results suggest that calcium and particulate matter decreased the diffusive back-transport of humic substances (i.e. SRNOM) away from the membrane into the bulk solution; hence, when filtering model raw water containing humic substances, calcium and particulate matter, the increase in resistance is dominated by fouling rather than CP, which differs from the results observed in the absence of calcium and particulate matter.

- When applying cross-flow when filtering a model raw water containing particulate matter, polysaccharides, humic substances and calcium, the extent of the increase in resistance to permeate flow resulting from fouling and CP decreases as the cross flow-velocity increased.

- When calcium and particulate matter (i.e. kaolin) were present in the raw water containing humic substances and polysaccharides (i.e. alginate), hydraulic control measures primarily affected the accumulation of polysaccharides and particulate matter.

- For the range of cross-flow velocities considered, the amount of polysaccharides and particulate matter accumulating at the membrane surface decreased as the cross-flow

velocity increased. For this reason, high intensity hydraulic control measures (i.e. high velocity cross-flow) are recommended to minimize the increase in resistance to permeate flow when filtering raw waters containing humic substances (i.e. SRNOM), polysaccharides (i.e. alginate), calcium and particulate matter (i.e. kaolin).

- Because it is difficult to hydraulically remove the accumulated material once a foulant layer has been formed, it is recommended to apply the high intensity hydraulic control measure (i.e. high velocity cross-flow) continuously.

- A semi-mechanistic relationship, based on the momentum equation, can be used to estimate the average shear stress induced by cross-flow at the membrane surface for different configurations and geometries.

- The extent of fouling and CP was dependent on the average shear stress at the membrane surface and independent of the spatial variability of the shear stress, and with that independent of the system configuration (i.e. spacer filled versus empty flow channels), as well as independent of the system geometry (i.e. hydrodynamic diameter).

- A relationship was developed that provides a framework to compare the performance of NF membranes of different configurations and geometries in terms of the permeate flux that can be sustained, and to optimize the operating set point of NF membranes with respect to system configuration, cross-flow velocity and operating flux.

- The optimal operating conditions for hollow fiber NF and spiral wound NF systems differ substantially due to differing relationships between cross-flow velocity and pressure loss along the module length and the expected differences in manufacturing costs.

- The estimated optimal operating flux for hollow fiber NF is substantially higher than that commonly applied, while the estimated optimal operating flux for spiral wound NF is similar or lower to that of existing applications.

- Despite the expected higher manufacturing costs, hollow fiber NF can be cost competitive to spiral wound NF.

10.2 Recommendations for Future Work

The research presented in the present dissertation provided insight into the application of NF and tight UF membranes for NOM removal and developed frameworks for the comparison and optimization of NF and tight UF membranes of different configurations. Some recommendations for future work are listed below.

- Results from the present work indicated that for raw water containing humic substances (i.e. SRNOM), polysaccharides (i.e. alginate) and particulate matter (i.e. kaolin), the accumulation of humic substances (i.e. SRNOM) at the membrane surface could not be effectively controlled using hydraulic control measures (i.e. cross-flow). It is recommended to study the time dependence of the accumulation of humic substances at

the membrane surface under these conditions to gain further insight into NF and tight UF CP and fouling.

- A relationship was developed that provides a framework to compare the performance of NF membranes of different configurations and geometries in terms of the permeate flux that can be sustained, and to optimize the operating set point of NF membranes with respect to system configuration, cross-flow velocity and operating flux. Additional research is needed to assess the input of raw water characteristics on the correlation relating the parameters obtained during the present study. Further, it is recommended to validate the framework developed, through testing at pilot scale.

- The cost estimation conducted in the present study demonstrated the sensitivity of the overall costs to the expected membrane lifetime. It is recommended to study the aging behavior of NF and tight UF membranes, to provide a better estimation of the membrane lifetime; this would enable more accurate cost estimations and decision making, as well as to enable the optimization of NF and tight UF membrane materials with respect to aging behavior (i.e. extending membrane lifetime).

- In the present study, the assessment and optimization of NF and tight UF membranes applied for drinking water treatment focused on the optimization of costs related to purchasing and replacing the membranes and energy costs, related to cross-flow operation and permeation. It is recommended to conduct a more comprehensive economic and environmental analysis using a life cycle approach.

References

Abdullah S.Z., 2014. Membrane Aging due to Chemical Cleaning Agent. Dissertation, The University of British Columbia, Vancouver, BC, Canada.

Ahn W.-Y., Kalinichev A. G., Clark M. M., 2008. Effects of background cations on the fouling of polyethersulfone membranes by natural organic matter: Experimental and molecular modeling study. Journal of Membrane Science 309, 128-140.

Aimar P., Causserand C., 2012. Impact of chemical cleaning of filtration membranes on their lifetime and properties. Procedia Engineering 44,19–20.

Al-Amoudi, A.S., 2010. Factors affecting natural organic matter (NOM) and scaling fouling in NF membranes: A review. Desalination 259 (1-3), 1–10.

Allgeier S. C., Summers R. S., 1995. Evaluating NF for DBP control with the RBSMT. Journal AWWA 87 (3), 87-99.

Amy G., Her N., 2004. Size exclusion chromatography (SEC) with multiple detectors: a powerful tool in treatment process selection and performance. Water Science & Technology 4 (4), 19-24.

Apell, J.N. and Boyer, T.H., 2010. Combined ion exchange treatment for removal of dissolved organic matter and hardness. Water Research 44, 2419–2430.

Arkhangelsky E., Kuzmenko D., Gitis V., 2007. Impact of chemical cleaning on properties and functioning of polyethersulfone membranes. Journal of Membrane Science 305 (1-2),176–184.

Atesok G., Somasundaran P., Morgan L.J., 1988. Adsorption Properties of Ca^{2+} on Na-Kaolinite and Its Effect on Flocculation Using Polyacrylamides. Colloids and Surfaces 32, 127-138.

AWWA, 2005. Standard Methods for the Examination of Water and Wastewater. 21st ed., American Water Works Association, Washington DC.

Bachin P., Aimar P., Field R.W., 2006. Critical and sustainable fluxes: Theory experiments and applications. Journal of membrane Science 281 (1-2), 42-69.

Bartels, C. et al., 2008. New generation of low fouling nanofiltration membranes. Desalination, 221(1-3), pp.158–167.

Belfort G., Davis R.H., Zydney A.L., 1994. The behavior of suspensions and macromolecular solutions in crossflow microfiltration. Jounral of Membrane Science 96, 1-58.

Bequet S., Remigy J.C., Rouch J.C., 2002. From ultrafiltration to nanofiltration hollow fiber membranes: a continuous UV-photografting process. Desalination 144 (1), 9-14.

Bhattacharjee S., Chen J. C., Elimelech M., 2001. Coupled model of concentration polarization and pore transport in cross-flow nanofiltration. AIChE Journal 47 (12), 2733-2745.

Biber M. V., Guelacar F.O., Buffle J., 1996. Seasonal Variations in Principal Groups of Organic Matter in a Eutrophic Lake using Pyrolysis/GC/MS. Environmental Science & Technology 30 (12), 3501-3507.

Black K. E., Bérubé P. R., 2014. Rate and extent NOM removal during oxidation and biofiltration. Water Research 52, 40-50.

Böhm L., Jankhah S., Tihon J., Bérubé P.R., Kraume M., 2014. Application of the electrodiffusion method to measure wall shear stress: Integrating theory and practice. Chemical Engineering & Technology 37, 938-950.

Bolto B., Dixon D., Eldridge R., King S., Linge K., 2002. Removal of Natural Organic Matter by Ion Exchange. Water Research 36, 5057-5065.

Bolton G., LaCasse D., Kuriyel R., 2006. Combined models of membrane fouling: Development and application to microfiltration and ultrafiltration of biological fluids. Journal of Membrane Science 277, 75-84.

Bonne P.A.C, Hiemstra P., van der Hoek J.P., Hofman J.H.M.A., 2002. Is direct nanofiltration with airflush an alternative for household water production in Amsterdam? Desalination 152, 263-269.

Boussu, K., Belpaire A., Volodin A., van Haesendonck C., van der Meeren P., Vandecasteele C., Van der Bruggen B., 2007. Influence of membrane and colloid characteristics on fouling of nanofiltration membranes. Journal of Membrane Science, 28, 220–230.

Bradley P.A., Heitz A., Joll C.A., Kagi R.I., Abbt Braun G., Frimmel F.H., Brinkmann T., Her N, Amy G., 2005. Size Exclusion Chromatography to Characterize DOC Removal in Drinking Water Treatment. Environmental Sciences Technology 39, 2334-2342.

Braghetta A., 1995. The influence of solution chemistry operating conditions on nanofiltration of charged and uncharged organic macromolecules. Ph.D. dissertation, Unversity of North Carolina, Chapel Hill.

Brian P. L. T., 1965. Concentration Polarization in Reverse Osmosis Desalination with Variable Flux and Incomplete Salt Rejection. Industrial & Engineering Chemistry Fundamentals 4 (4), 439-445.

Bucs S.S., Linares R.V., Marston J.O., Radu A.I., Vrouwenvelder J.S., Picioreanu C., 2015. Experimental and numerical characterization of the water flow in spacer-filled channels of spiral-wound membranes. Water Research 87, 299-310.

Burbano, B.Y.A.A., Adham, S.S., Pearce, W.R., 2007. The state of full-scale RO / NF desalination — results from a worldwide survey. American Water Works Association Journal, 116–127.

Byun S., Taurozzi J.S., Alpativa A.L., Wang F., Tarabara V.V., 2011. Performance of polymeric membranes treating ozonated surface water: Effect of ozone dosage. Separation and Purification Technology 81, 270-278.

Cabassud C., Laborie S., Durand-Bourlier L., Laine J.M., 2001. Air sparging in ultrafiltration hollow fibers: relationship between flux enhancement, cake characteristics and hydrodynamic parameters. Journal of Membrane Science 181, 57-69.

Chan C.C.V., Berube P.R., Hall E.R., 2011. Relationship between types of surface shear stress profiles and membrane fouling. Water Research 45, 6403-6416.

Chaiket T., Singer P.C., Moran M., Pallotta C., 2002. Effectiveness of coagulation, ozonation, and biofiltration in controlling DBPs. Journal AWWA 94, 81-95.

Carlson K., Amy G., 1997. The Formation of Filter-Removable Biodegradable Organic Matter During Ozonation. Ozone Science & Engineering 19, 179-199.

Chen B., Nam S.-N., Westerhoff P.K., Krasner S.W., Amy G., 2009. Fate of effluent organic matter and DBP precursors in an effluent-dominated river: A case study of wastewater impact on downstream water quality. Water Research 43, 1755-1765.

Chen F., 2016. Characterization Techniques for Organic and Colloidal Material of Relevance to Ultrafiltration Membranes in Drinking Water Treatment. Dissertation, The University of Waterloo, Waterloo, ON, Canada.

Chin Y.-P., Aiken G., O'Loughlin E., 1994. Molecular Weight, Polydispersity, and Spectroscopic Properties of Aquatic Humic Substances. Environmental Science Technology 28 (11), 1853-1858.

Chin A., Bérubé P., 2005. Removal of disinfection by-product precursors with ozone-UV advanced oxidation process. Water Research 39 (10), 2136-2144.

Cho, J., Amy, G. & Pellegrino, J., 1999. Membrane filtration of natural organic matter: initial comparison of rejection and flux decline characteristics with ultrafiltration and nanofiltration membranes. Water Research, 33 (11), 2517–2526.

Cho M., Haeshim K., Cho S., Yoon J., 2003. Investigation of Ozone Reaction in River Waters Causing Instantaneous Ozone Demand. Water Science & Technology 49, 57-62.

Chong T.H., Wong F.S., Fane A.G., 2008. Implications of critical flux and cake enhanced osmotic pressure (CEOP) on colloidal fouling in reverse osmosis: Experimental observations. Journal of Membrane Science 314, 101-111.

Chowdury F.L., Bérubé P. R., Mohseni M.,2008. Characteristics of Natural Organic Matter and Formation of Chlorinated Disinfection By-Products from Two Sources Waters that Respond Differently to Ozonation. Ozone Science & Engineering 30 (5), 321-331.

Clark M.M., Heneghan K.S., 1991. Ulftafiltration of lake water for potable production. Desalination 80, 243-249.

Contreras A. E., Kim A., Li Q., 2009. Combined fouling of nanofiltration membranes: mechanisms and effect of organic matter. Jornal of Membrane Science 327, 87-95.

Cornel P. K., Summers S. R., Roberts P. V., 1986. Diffusion of Humic Acid in Dilute Aqueous Solution. Journal of Colloid and Interface Science 110 (1), 149-164.

Cornelissen, E.R., Moreau, N., Siegers, W.G., Abrahamse, A.J., Rietveld, L.C., Grefte, A., Dignum, M., Amy, G., and Wessels, L.P., 2008. Selection of anionic exchange resins for removal of natural organic matter (NOM) fractions. Water Research 42, 413-423.

Costa A.R., Fane A.G., Wiley D.E., 1994. Spacer characteriztion and pressure drop modelling in spacer-filled channels for ultrafiltration. Jornal of Membrane Science 87, 79-98.

Costa A.R., de Pinho M.N., 2006. Performance and cost estimation of nanofiltration for surface water treatment in drinking water production. Desalination 196, 55-65.

Crittenden, J. C., Trussell, R. R., Hand, D. W., Howe, K. J. und Tchobanoglous, G., 2005. Water Treatment: Principles and Design. 2nd edition, MWH, John Wiley & Sons, Inc., Hoboken, NJ (USA)

Croue J.-P., Korshin G., Mark B. M., 1999. Characterization of natural organic matter in drinking water. AWWA Research Foundation (AWWARF). Denver, CO.

Di Martino P., Doumeche B., Galas L., Vaudry H., Heim V., Habarou H., 2007. Assessing chemical cleaning of nanofiltration membranes in a drinking water production plant: a combination of chemical composition analysis and fluorescence microscopy. Water Science & Technology 55 (8-9), 219-225.

Do V.T., Tang C.Y., Reinhard M.R., Leckie J.O., 2012. Effects of Chlorine Exposure Conditions on Physiochemical Properties and Performance of a Polyamide Membrane – Mechanisms and Implications. Environmental Sience & Technology 46, 13184-13192.

Domnisoru A., 2007. Long term effects of climate change on Europe's water resources. Techneau report D1.1.6c. URL: http://www.techneau.org/fileadmin/files/Publications/Publications/Deliverables/D1.1.6c.pdf (last access: 03/13/2017)

Dotson A., Westerhoff P., Krasner W., 2009. Nitrogen enriched dissolved organic matter (DOM) isolates and their affinity to form merging disinfection by-products. Water Science and Technology 60, 135-143.

Dreszer C., Flemming H.C., Zwijnenburg A., Kruithof J.C., Vrouwenvelder J.S., 2014. Impact of biofilm accumulation on transmembrane and feed channel pressure drop: effects of crossflow velocity, feed spacer and biodegradable nutrient. Water Research 50, 200-211.

Edzwald J.K., 1999. Water Quality and Treatment: A handbook on drinking water. American Water Works Association, Denver, CO, USA.

Eikebrokk, B., Juhna, T., and Østerhus, S. W., 2006. Water treatment by enhanced coagulation – Operational status and optimization issues. Techneau, D 5.3.1 – URL:https://www.techneau.org/fileadmin/files/Publications/Publications/Deliverables/D5.3.1A_Enhanced_coagulation_report.pdf (last access 05/30/2017)

Elimelech M, Bhattacharjee S., 1998. A novel approach for modeling concentration polarization in crossflow membrane filtration based on the equivalence of osmotic pressure model and filtration theory. Journal of Membrane Science 145, 223-241.

ElHadidy A.M., Peldszus S., van Dyke M.I., 2013. An evaluation of virus removal mechanisms by ultrafiltration membranes using MS2 and φX174 bacteriophage. Separation and Purification Technology 120 (13), 215-223.

Fabris, R., Lee, E.K., Chow, C.W.K., Chen, V. and Drikas, M., 2007. Pretreatments to reduce fouling of low pressure micro-filtration (MF) membranes. Journal of Membrane Science 289, 231-240.

Field R.W., Pearce G.K., 2011. Critical, sustainable and threshold fluxes for membrane filtration with water industry applications. Advances in Colloid and Interface Science 164 (2011), 38-44.

Field R.W., Wu D., Howell J.A., Gupta B.B., 1995. Critical flux concept for microfiltration fouling. Journal of Membrane Science 100 (3), 259-272.

Fonseca A. C., Summers R. S., Greenberg A. R., Hermandez M. T., 2007. Extra-cellular Polysaccharides, soluble microbial products, and natural organic matter impact on nanofiltration flux decline. Environmental Science Technology 41 (7), 2491-2497.

Frank M., Bargeman G., Zwijnenburg A., 2001. Capillary hollow fiber nanofiltration membranes. Separation and Purification Technology 22 (23), 499-506.

Fulton B.G., Redwood J., Tourais M., Bérubé P.R., 2011. Distribution of surface shear forces and bubble characteristics in full-scale gas sparged submerged hollow fiber membrane modules. Desalination 281, 128-141.

Futselaar H., Schonewille H., van der Meer W., 2003. Direct capillary nanofiltration for surface water. Desalination 157, 135-136.

Galapate R. P., Baes A. U., Okada M., 2001. Transformation of dissolved organic matter during ozonation: Effects on Trihalomethane formation potential. Water Research 35 (9), 2201-2206.

Gao W., Liang H. Ma J., Man M., Chen Z. L. Han Z. S., Li G. B., 2011. Membrane fouling control in ultrafiltration technology for drinking water water production: a review. Desalination 272 (1), 1-8.

Geraldes V., Semião V., de Pinho M. N., 2002. Flow management in nanofiltration spiral wound modules with ladder-type spacers. Journal of Membrane Science 203, 87-102.

Gorenflo, A. & Frimmel, F.H., 2002. Nanofiltration of a German groundwater of high hardness and NOM content: performance and costs. Desalination, 151, 253–265.

Gorenflo A., 2003. Rückhalt und Fouling von natürlichen organischen Substanzen bei Nano-und Ultrafiltration. Schriftenreihe des Lehrstuhls für Wasserchemie und der DVWG-Forschungsstelle am Engler-Bunte-institut der Universität Karlsruhe (TH) Band 38.

Goslan E. H., Gurses F., Banks J., Parsons S. A., 2006. An investigation into reservoir NOM reduction by UV photolysis and advanced oxidation processes. Chemosphere 65, 1113–1119.

Gottschalk C., Libra J. A., Saupe A., 2000. Ozonation of Water and Waste Water – A practical Guide to Understanding Ozone and its Application. Wiley-VCH Verlag, Weinheim, Germany.

Green N., McInnis D., Hertkorn N., Maurice P.A., Perdue E.M., 2015.Suwannee River Natural Organic Matter: Isolation of the 2R101N Reference Sample by Reverse Osmosis. Environmental Engineering Science 32 (1), 38-44.

Grefte A., 2013. Removal of Natural Organic Matter Fractions by Anion Exchange – Impact on drinking water treatment processes and biological stability. Dissertation, TU Delft, Delft, Netherlands.

Gu B., Xia Y. X., Adjiman C.S., 2017. A predictive model for spiral wound reverse osmosis membrane modules: The effect of winding geometry and accurate geometric details. Computers and Chemical Engineering 96, 248-265.

Haas C. N.; Meyer M. A.; Paller M. S., 1983. Microbial Alterations in Water Distribution Systems and their Relationship to Physical-Chemical characteristics. Jornal AWWA 75, 475-481.

Haberkamp J., Ruhl A. S., Ernst M., Jekel M., 2007. Impact of coagulation and adsorption on DOC fractions of secondary effluent and resulting fouling behaviour in ultrafiltration. Water Research 41, 3794-3802.

Halle C., Huck P.M., Peldszus S., Haberkamp J., Jekel M., 2009. Assessing the Performance of Biological Filtration As Pretreatment to Low Pressure Membranes for Drinking Water, Environmental Sciences Technology 43, 3878-3884.

Hammes F., Salhi E., Koester O., Kaiser H.-P., Egli T., von Gunten U., 2006. Mechanistic and kinetic evaluation of organic disinfection by-products and assimilable organic carbon (AOC) formation during the ozonation of drinking water. Water Research 40, 2275-2286.

Health Canada, 2006. Guidelines for Drinking Water Quality: Guidelines Technical Document – Trihalomethanes. Federal-Provincial-Territorial Committee on Drinking Water of the Federal-Provincial-Territorial Committee on Health and the Environment – URL: http://www.hc-sc.gc.ca/ewh-semt/alt_formats/hecs-sesc/pdf/pubs/water-eau/trihalomethanes/trihalomethanes-eng.pdf (last access: 03/13/2017).

Hejzlar J., Dubrovsky M., Buchtele J., Rucicka M., 2003. The apparent and potential effects of climate change on the inferred concentration of dissolved organic matter in a temperate stream (the Malse River, South Bohemia). The Science of the Total Environment 310, 143-152.

Her N., Amy G., Jarusutthirak, 2000. Seasonal variations in nanofiltration (NF) foulants: indentification and control. Desalination 132, 143-160.

Her N., Amy G., Foss D., Cho J., Yoon Y., Kosenka P., 2002. Optimization of Method for Detecting and Characterizing NOM by HPLC-Size Exclusion Chromatography with UV and On-Line DOC detection. Environmental Sciences Technology 36 (5), 1069-1076.

Her N., Amy G., Park H.-R., Song M., 2004. Characterizing algogenic organic matter (AOM) and evaluating associated NF membrane fouling. Water Research 38, 1427-1438.

Her N., Amy G., Plottu-Pecheux A., Yoon Y., 2007. Identification of nanofiltration foulants. Water Research 41 (17), 3936-3947.

Her N., Amy G., Sohn J., von Gunten U., 2008. UV absorbance ratio index with size exclusion chromatography (URI-SEC) as an NOM property indicator. Journal of Water Supply: Research and Technology-Aqua 57, 35-44.

Hermia J., 1982. Constant Pressure Blocking Filtration Laws – Application to Power-Law Non-Newtonian Fluids. Chemical Engineering Research and Design 60 (3), 183-187.

Hesse S., Kleiser G., Frimmel F., 1999. Characterisation of refractory organic substances (ROS) in water treatment. Water Science and Technology 40 (9), 1-7.

Hincks S.S., Mackie G.L., 1997. Effect of pH, calcium, alkalinity, hardness, and chlorophyll and the survival, growth, and reproductive success of zebra mussel (Dreissena polymarpha) in Ontario lakes. Canadian Journal of Fisheries and Aquatic Sciences 54 (9), 2049-2057.

Hoek E. M. V., Elimelech M., 2003. Cake-Enhanced Concentration Polarization - A New Fouling Mechanism for Salt-Rejecting Membranes. Environmental Science Technology 37 (24), 5581-5588.

Hollender J., Zimmermann S.G., Koepke S., Krauss M., McArdell C.S., Ort C., Singer H., von Gunten U., Siegrist H., 2009. Elimination of Organic Micropollutants in a Minicipal Wastewater Treatment Plant Upgraded with a Full-Scale Post-Ozonation Followed by Sand Filtration. Environmental Science Technology 43, 7862-7869.

Hong S., Faibish R.S., Elimelech M., 1997. Kinetics of Permeate Flux Decline in Crossflow Membrane Filtration of Colloidal Suspensions. Journal of Colloid Interface Science 196, 267-277.

Hozalski, R.M., Bouwer, E.J. & Goel, S., 1999. Removal of natural organic matter from drinking water supplies by ozone-biofiltration. Water Science and Technology, 40 (9), 157-163.

Huang W.-J., Chen L.-Y., Peng H.-S., 2004. Effect of NOM characteristics on brominated organics formation by ozonation. Environmental International 29, 1049-1055.

Huang H., Lee N., Young T., Amy G., Lozier J.C., Jacangelo J.G., 2007. Natural organic matter fouling of low-pressure, hollow-fiber membranes: effects of NOM source and hydrodynamic conditions. Water Research 41 (17), 3823–3832.

Huang, H., Cho, H.H., Schwab, K.J. and Jacangelo, J.G., 2012. Effects of magnetic ion exchange pretreatment on low pressure membrane filtration of natural surface water. Water Research 46, 5483-5490.

Huber S.A., Balz A., Abert M. Pronk W., 2011. Characterisation of aquatic humic and non-humic matter with size-exclusion chromatograpgy – organic carbon detection – organic nitrogen detection (LC-OCD-OND). Water Research 45 (2), 879-885.

Itoh M., Kunikane S., Magara Y., 2001. Evaluation of nanofiltration for disinfection by-products control in drinking water treatment. Water Science & Technology: Water Supply 1 (5-6), 233-243.

Jankhah S., 2013. Effect of bubble size and sparging frequency on the power transferred onto membranes for fouling control. Dissertation, The University of British Columbia, Vancouver, BC, Canada.

Jarusutthirak C., Amy G., Croue J.-P., 2002. Fouling characteristics of wastewater effluent organic matter (EfOM) isolates on NF and UF membranes. Desalination 145 (1-3), 247-255.

Jermann D., Pronk W., Meylan S., Boller M., 2007. Interplay of different NOM fouling mechanisms during ultrafiltration of drinking water production. Water Research 41 (8), 1713-1722.

Jermann D. Pronk W., Kägi R. Halbeisen M., Boller M., 2008. Influence of interactions between NOM and particles on UF fouling mechanism. Water Research 42 (14), 3870-3878.

Joss A., Keller E., Alder A.C., Goebel A., McArdell C.S., Ternes T., Siegsrist H., 2005. Removal of pharmaceuticals and fragrances in biological wastewater treatment. Water Research 39, 3139-3152.

Joss A., Siegrist H., Ternes T.A., 2008. Are we about upgrading wastewater treatment for removing organic micropollutants? Water Science and Technology 57, 251-255.

Juhna T., Melin E., 2006. Ozonation and Biofiltration in Water Treatment – Operational Status and Optimization Issues. Techneau, D.5.3.1 B – URL: http://www.techneau.org/fileadmin/files/Publications/Publications/Deliverables/D5.3.1B-OBF.pdf (last access: 04/26/2017).

Kaeocha A., 2008. Ion exchange for NOM removal in drinking water. Dissertation, TU Delft, Delft, Netherlands.

Karnik B., Davies S., Chen K., Jaglowski D., Baumann M., Masten S., 2005. Effects of ozonation on the permeate flux of nanocrystaline ceramic membranes. Water Research 39, 728-734.

Keucken A., Wang Y., Tng K.H., Leslie G., Spanjer T., Koehler S.J., 2016. Optimizing Hollow Fiber Nanofiltration for Organic Matter Rich Lake Water. Water 8, 430.

Kim J., Davies S., Baumann M., Tarabara V., Masten S., 2008. Effect of ozone dosage and hydrodynamic conditions on the permeate flux in a hybrid ozonation-ceramic ultrafiltration system treating natural waters. Journal of Membrane Sciences 311 (1-2), 165-172.

Kleiser G., Frimmel F. H., 2000. Removal of precursors for disinfection by-products (DBPs) - differences between ozone and OH radical induced oxidation. Science of the Total Environment 256 (1), 1-9.

Ko Y.-W., Abbt-Braun G, Frimmel F. H., 2000. Effect of Preozonation on the Formation of Chlorinated Disinfection By-products for River Ruhr. Acta hydrochimica et hydrobiologica 28 (5), 256-261.

Koutsou C.P., Yiantsios S.G., Karabelas A.J., 2007. Direct numerical simulation of flow in spacer-filled channels: Effect of spacer geometrical characteristics. Journal of Membrane Science 291, 53-69.

Koutsou C.P., Yiantsios S.G., Karabelas A.J., 2009. A numerical and experimental study of mass transfer in spacer-filled channels: Effects of spacer geometrical characteristics and Schmidt number. Journal of Membrane Science 326, 234-251.

Kwon Y.-N., Leckie J. O., 2006. Hypochlorite degradation of cross linked polyamide membranesII. Changes in hydrogen bonding behavior and performance.

Journal of Membrane Science 282 (1-2), 456–464.

Laabs C., Amy G., Jekel M., 2006. Understanding the Size and character of Fouling-Causing Substances from Effluent Organic Matter (EfOM) in Low Pressure Membrane filtration. Environmental Science Technology 40 (14), 4495-4499.

Laborie S., Cabassud C., Durrand-Bourlier L., Laine J.M., 1999. Characterisation of gas-liquid two-phase flow inside capillaries. Chemical Engineering Science 54, 5723-5735.

Laine J.-M., Clark M.M., Mallevialle J., 1990. Ultrafiltration of lake water: effect of pretreatment on the partitioning of organics, THMF, and flux. Journal AWWA 82, 82-87.

Lankes, U., Müller, M., Weber, M., & Frimmel, F. H., 2009. Reconsidering the quantities analysis of organic carbon concentration in size exclusion chromatography. Water Research 43, 915-924.

Lee N., Amy G., Croué J.-P., Buisson H., 2004. Identification and understanding of fouling in low-pressure membrane (MF/UF) filtration by natural organic matter (NOM). Water Research 38 (20), 4511–4523.

Lee S., Cho J., 2004. Comparison of ceramic and polymeric membranes for natural organic matter (NOM) removal. Desalination 160 (3), 223-232.

Lee S., Lee K., Wan W. M., Choi Y., 2005a. Comparison of membrane permeability and a fouling mechanism by pre-ozonation followed by membrane filtration and residual ozone in membrane cells. Desalination 178 (1-3), pp. 287-294.

Lee S., Cho J., Elimelech M., 2005b. Combined influence of natural organic matter (NOM) and colloidal particles on nanofiltration membrane fouling. Journal of Membrane Science 262, 27-41.

Lee W., Westerhoff P., Croue J.-P., 2007. Dissolved Organic Nitrogen as a Precursor for Chloroform, Dichloroacetonitrile, N-Notrosodimenthylamine, and Trichloronitromethane. Environmental Science Technology 41, 5485-5490.

Leenheer J.A., Croue J.-P., 2003. Characterizing Dissolved Aquatic Organic Matter. Environmental Science and Technology 37, 19A-26A.

Levitsky I., Duek A., Arkhangelsky E., Pinchev D., Kadoshian T., Shetrit H., Naim R., Gitis V., 2011. Understanding the oxidative cleaning of UF membranes. Journal of Membrane Science 377 (1-2), 206–213.

Li Q., Elimelech M., 2004. Organic Fouling and Chemical Cleaning of Nanofiltration Membranes: Measurements and Mechanisms. Environmental Science & Technology, 38 (17), 4683–4693.

Li Q., Elimelech M., 2006. Synergistic effects in combined fouling of a loose nanofiltration membrane by colloidal materials and natural organic matter. Journal of Membrane Science 278, 72-82.

Liden A., Persson K.M., 2016. Feasibility Study of Advanced NOM-Reduction by Hollow Fiber Ultrafiltration and Nanofiltration at a Swedish Surface Water Treatment Plant. Water 8, 150.

Liikanen R., Yli-Kuivila J., Laukkanen R., 2002. Efficiency of various chemical cleanings for nanofiltration membrane fouled by conventionally-treated surface water. Journal of Membrane Science, 195 (2), .265–276.

Lin C.F., Lin Y.-C.A., Chandana S.P., Tsai C.-Y., 2009. Effects of mass retention of dissolved organic matter and membrane pore size on membrane fouling and flux decline. Water Research 43 (2), 389-394.

Listiarini K., Chun W., Sun D. D., Leckie J., 2009. Fouling mechanism and resistance analyses of systems containing sodium alginate, calcium, alum and their combination in dead-end fouling of nanofiltration membranes. Journal of Membrane Science 344, 244-251.

Maeng S.K., Sharma S.K., Magic-Knezev A., Amy G., 2008. Fate of effluent organic matter (EfOM) and natural organic matter (NOM) through riverbank filtration. Water Science and Technology 57, 1999-2007.

Mahlangu T.O., Thwala J.M., Mamba B.B., D'Haese A., Verliefde A.R.D., 2015. Factors governing combined fouling by organic and colloidal foulants in cross-flow nanofiltration. Journal of Membrane Science 49, 53-62.

Malek, A., Hawlader, M.N.A., Ho, J. C., 1996. Design and economics of RO seawater desalination. Desalination 105, 245-261.

Matilainen A., Iivari P., Sallanko J., Heiska E., Tuhkanen T., 2006. The role of ozonation and activated carbon filtration in the natural organic matter removal from drinking water. Environmental Technology 27, 1171-1180.

Matilainen A., Vepsäläinen M., Sillanpää M., 2010. Natural organic matter removal by coagulation during drinking water treatment: A review. Advances in Colloid and Interface Science 159, 189-197.

McAdam E.J., Judd S.J., 2008. Biological treatment of ion-exchange brine regenerant for re-use: A review. Separation Purification Technology 62, 264-272.

Melin T., Rautenbach R., 2004. Membranverfahren – Grundlagen der Modul- und Anlagenauslegung. 2. Auflage, Springer Verlag, Heidelberg, Germany.

Mellevialle J., Odendaal P.E., Wiesner M.R., 1996. Water Treatment Membrane Processes. American Water Works Association Research Foundation, McGraw-Hill, New York, United States of America.

Meng F., Chae S.-R., Drews A., Kraume M., Shin H.-S., Yang F., 2009. Recent advances in membrane bioreactors (MBRs): Membrane fouling and membrane material. Water Research, 43 (6), 1489–1512.

Meng F., Chae S.-R., Shin H.-S., Yang F., Zhou Z., 2012. Recent advances in membrane bioreactors: configuration development, pollutant elimination, and sludge reduction. Environmental Engineering Science, 29 (3), 139–160.

Moore B.Y.K.W., Huck P.M., Siverns S., 2008. Arsenic removal using oxidative media and nanofiltration. AWWA Journal 100 (12), 74-83..

Mosqueda-Jimenez D.B., Huck P.M., 2009. Effect of biofiltration as pretreatment on the fouling of nanofiltration membranes. Desalination 245, 60-72.

Mulder M., 1996. Basic Principles of Membrane Technology, 2nd ed., Kluwer Academic, Dordrecht, Netherlands.

Nguyen S.T., Roddick F.A., 2010. Effects of ozonation and biological filtration on membrane fouling in ultrafiltration of an activated sludge effluent. Journal of Membrane Science 363, 271-277.

Nyström M., Kaipia L., Luque S., 1995. Fouling and retention of nanofiltration membranes. Journal of Membrane Science 98, 249-262.

Oh J., Urase T., Yamamoto K., 1998. Effect of pH on rejection of different species of arsenic by nanofiltration. Desalination 117, 11–18.

Odegaard H., Osterhus S., Melin E., Eikebrokk B., 2010. NOM removal technologies – Norwegian experiences. Drinking Water Engineering and Science 3, 1-9.

Patterson C., Anderson A., Sinha R., Muhammad N., Pearson D., 2012. Nanofiltration Membranes for Removal of Color and pathogens in Small Drinking Water Sources. Journal of Environmental Engineering 138 (1), 48-57.

Payant A., Bérubé P.R., Barbeau B., 2017. Physical cleaning efficacy of hollow fiber nanofiltration membranes in drinking water applications. Desalination and Water Treatment 63, 15-23.

Pelekani C., Newcombe G., Snoeyink V., Hepplewhite C., Assemi S., Beckett R., 1999. Characterization of Natural Organic Matter Using High Performance Size Exclusion Chromatography. Environmental Science Technology 33, 2807-2813.

Peng, W., Escobar, I.C., 2005. Evaluation of factors influencing membrane performance. Environmental Progress 24 (4), 392–399.

Perminova I. V., Frimmel F. H., Kudryavtsev A. V., Kultikova N. A., Abbt-Braun G., Hesse S., Petrosyan V. S., 2003. Molecular Weight Characteristics of Humic Substances from Different Environments as Determined by Size Exclusion Chromatography and their Statistical Evaluation. Environmental Science Technology 37, 2477-2485.

Porcelli N., Judd S., 2010. Chemical cleaning of potable water membranes: A review. Separation and Purification Technologyc71c(2), 137–143.

Quentel F., Filella M., 2008. Quantification of refractory organic substances in freshwater: further inside into the voltammetric method. Analytical and Bioanalytical Chemistry 396 (6), 1225-1230.

Radu A.I., van Steen M.S.H., Vrouwenfelder J.S., van Loosdrecht M.C.M., Picioreanu C., 2014. Spacer geometry and particle deposition in spiral wound membrane feed channels. Water Research 64, 160-176.

Ratkovich N., Berube P.R., Nopens I., 2011. Assessment of mass transfer coefficients in coalescing slug flow in vertical pipes and applications to tubular airlift membrane bioreactors. Chemical Engineering Science 66, 1254-1268.

Rautenbach R., Albrecht R.: Membrane Processes, 1989. John Wiley & Sons, New York.

Rechnungswesen-verstehen.de – URL: http://www.rechnungswesen-verstehen.de/investition-finanzierung/Kapitalwertmethode.php (last access: 05/11/2017)

Reiss C.R., Taylor J.S., Robert C., 1999. Surface water treatment using nanofiltration - pilot testing results and design considerations. Desalination and the Environment 125, 97–112.

Rittmann B.E. and Stilwell D., 2002. Modelling biological processes in water treatment: The integrated biofiltration model. Journal of Water Supply: Research and Technology - AQUA, 51 (1), 1-14.

Sadmani, A. H. M. Anwar; Andrews, Robert C.; Bagley, David M., 2014. Impact of natural water colloids and cations on the rejection of pharmaceutically active and endocrine disrupting compounds by nanofiltration. Journal of Membrane Science 450, 271-281.

Samhaber W.M., Nguyen M.T., 2014. Applicability and costs of nanofiltration in combination with photocatalysis for the treatment of dye house effluents. Beilstein Journal of Nanotechnology 5, 476-484.

Sarathy S., 2009. Effects of UV/H_2O_2 advanced oxidation on physical and chemical characteristics of natural organic matter. PhD thesis, University of British Columbia, Vancouver, BC, Canada.

Sarathy S., Mohseni M., 2009. The fate of natural organic matter during UV/H_2O_2 advanced oxidation of drinking water. Canadian Journal of Civil Engineering 36 (1), 160-169.

Sari M.A., Chellam S., 2013. Surface water nanofiltration incorporating (electro) coagulation-microfiltration pretreatment: Fouling control and membrane characterization. Journal of Membrane Science 437, 249-256.

Sato Y., Kang M., Kamei T., Magara Y., 2002. Performance of nanofiltration for arsenic removal. Water Research 36 (13), 3371-3377.

Schäfer A. I., Fane A. G., Waite T. D., 1998. Nanofiltration of natural organic matter: Removal, fouling and influence of multivalent ions. Desalination 118 (1-3), 109-122.

Schäfer A. I., Fane A. G., Waite T. D., 2005. Nanofiltration: Principles and Applications: Elsevier, Oxford, U.K., New York, N.Y.

Schäfer A. I., 2007. Natural Organics Removal using Membranes – Principles, Performance and Cost: Technomic Publishing, Lancaster.

Schock G., Miquel A., 1987. Mass transfer and pressure loss in spiral wound modules. Desalination 64, 339-352.

Schultz M., Winter J., Wray H., Barbeau B., Bérubé P., 2017. Biologically-active ion exchange (BIEX) for NOM-removal and membrane fouling prevention. Water Science and Technology: Water Supply, in press.

Seidel A., Elimelech M., 2002. Coupling between chemical and physical interactions in natural organic matter (NOM) fouling of nanofiltration membranes: implications for fouling control. Journal of Membrane Science 203, 245-255.

Sethi S., Wiesner M.R., 1997. Modeling of transient permeate flux in cross-flow membrane filtration incorporating multiple particle transport mechanisms. Journal of Membrane Science 136, 191-205.

Sethi S., Wiesner M.R., 2000. Simulated Cost Comparison of Hollow-Fiber and Integrated Nanofiltration Configurations. Water Research 34, 2589-2597.

Sharp E. L., Parsons S. A., Jefferson B., 2006. Seasonal variations in natural organic matter and its impact on coagulation in water treatment. Science of the Total Environment 363, 183– 194.

Shetty G.R., Chellam S., 2003. Predicting membrane fouling during municipal drinking water nanofiltration using artificial neural networks. Journal of Membrane Science 217, 69-86.

Shon, H.K. et al., 2013. Nanofiltration for water and wastewater treatment – a mini review. Drinking Water Engineering and Science, 6 (1), 47–53.

Shon H.-K., Kim S.-H., Erdei L., Vigneswaran S., 2006. Analytical methods of size distribution for organic matter in water and wastewater. Korean Journal Chemical Engineering 23, 581-591.

Singer P. C., 1994. Control of Disinfection By-Products in Drinking Water. Journal of Environmental Engineering – Am. Soc. Civ. Eng. (4), 727-744.

Singer P.C., 2004. Disinfection by-products in US drinking water: past, present and future. Water Science and Technology: Water Supply 4, 151-157.

Song L., Elimelech M., 1995. Particle deposition onto a permeable surface in laminar flow, Journal of Colloid and Interface Science 173 (1), 165–180.

Song L., 1998. Flux decline in crossflow microfiltration and ultrafiltration: mechanisms and modeling membrane fouling. Journal of Membrane Science 139 (2), 183-200.

Song H., Shao J., He Y., Hou J., Chao W., 2011. Natural organic matter removal and flux decline with charged ultrafiltration and nanofiltration membranes. Journal of Membrane Science, 376, 179-187.

Specht, C. H., & Frimmel, F., 2000. Specific interactions in size-exclusion chromatography. Environmental Science & Technology 34, 2361-2366.

Spruck M., Hoefer G., Fili G., Gleinser D., Ruech A., Schmidt-Baldassari M., Rupprich M., 2013. Preparation and characterization of composite multichannel capillary membranes on the way to nanofiltration. Desalination 314, 28-33.

Swietlik J., Dabrowska A., Raczyk-Stanisławiak U., Nawrocki J., 2004. Reactivity of natural organic matter fractions with chlorine dioxide and ozone. Water Research 38, 547-558.

Tarabara V.V., Wiesner M.R., 2003. Computational fluid dynamics modeling of the flow in a laboratory membrane filtration cell operated at low recoveries. Chemical Engineering Science 58, 239-246.

Tatzel A., Panglisch S, Kraus G., Lickes J.-P., 2009. Pilotstudie über verschiedene Aufbereitungskonzepte der SEBES Trinkwasserproduktion in Luxenburg. In proceedings: Aachener Tagung Wasser und Membranen 2009, Aachen,Germany.

Thorsen T., Flogstat H., 2006. Nanofiltration in drinking water treatment – literature review. Techneau report D5.3.4B – URL: https://www.techneau.org/fileadmin/files/Publications/Publications/Deliverables/D5.3.4b.pdf (last access: 05/30/2017)

Tian J.-Y., Xu Y.-P., Chen Z.-L., Li G.-B., 2010. Air bubbling for alleviating membrane fouling in immersed hollow-fiber membrane for ultrafiltration of river water. Desalination 260, 225-230.

Tian J.-Y., Ernst M., Cui F., Jekel M., 2013. Effect of particle size and concentration on the synergistic UF membrane fouling by particles and NOM fractions. Journal of Membrane Science 446, 1-9.

Tinghir, A., Bonnelye, V. & Masereel, P., 2009. Degrémont's largest nanofiltration plant: NOM removal at the Vegi 2000. Desalination and Water Treatment 5(1-3), 178–182.

Tipping E., Backes C.A., Hurley M.A., 1988. The complexation of protons, aluminum and calcium by aquatic humic substances: a model inroporating binding site heterogeneity and macroionic effects. Water Research 22 (5), 597-611.

USEPA, 2002: 40 CFR Parts 9, 141, and 142 National Primary Drinking Water Regulations – URL: https://www.epa.gov/sites/production/files/2015-11/documents/howepargulates_cfr-2003-title40-vol20-part141_0.pdf (last access: 03/13/2017).

USIEA 2017: Table 5.6.A. Average Price of Electricity to Ultimate Customers by End-Use Sector, by State, May 2017 and 2016 – URL:

https://www.eia.gov/electricity/monthly/epm_table_grapher.php?t=epmt_5_6_a *(last access: 07/26/2017).*

Van den Berg G. B., Smolders C. A., 1990. Flux Decline in Ultrafiltration Processes. Desalination 77, 101-133.

Van der Bruggen B, Vandecasteele C., van Gestel T., Doyen W., Leysen R., 2003. A Review of Pressur-Driven Membrane Processes in Wastewater Treatment and Drinking Water Production. Environmental Progress 22 (1), 46-56.

Van der Bruggen B., Vandecasteele C., 2003. Removal of pollutants from surface water and groundwater by nanofiltration : overview of possible applications in the drinking water industry. Environmental Pollution 122, 435–445.

Van der Bruggen, B., Schaep J., Maes W., Wilms D, Vandecasteele C., 1998. Nanofiltration as a treatment method for the removal of pesticides from ground waters. Desalination 117(1-3), 139–147.

Van der Kooij D., 1992. Assimilable Organic Carbon as an Indicator of Bacterial Regrowth. Journal AWWA 84, 57-65.

Velten S., 2008. Adsorption capacity and biological activity of biological activated carbon filters in drinking water treatment. Doctoral Dissertation, Swiss Federal Institute of Technology Zurich).

Verberk J. Q. J. C., van Dijk J. C., 2006. Air Sparging in Capillary Nanofiltration. Journal of Membrane Science 284 (1-2), 339-351.

Verissimo S., Peinemann K.V., Bordado J., 2005. New composite hollow fiber membrane for nanofiltration. Desalination 184 (1-3), 1-11.

Von Gunten U., 2003a. Ozonation of drinking water: Part I. Oxidation kinetics and product formation. Water Research 37, 1443-1467.

Von Gunten U., 2003b. Ozonation of drinking water: Part II. Disinfection and by-product formation in presence of bromide, iodide or chlorine. Water Research 37, 1469-1487.

Wang G.-S., Hsieh S.-T., 2001. Monitoring natural organic matter in water with scanning spectrophotometer. Environmental International 26 (4), 205-212.

Wend C.F., Stewart P.S., Jones W., Camper A.K., 2003. Pretreatment of membrane water treatment systems: a laboratory study. Water Research 37, 3367-3378.

Westerhoff P., Aiken G., Amy G., Bebroux J., 1999. Relationships between the structures of natural organic matter and its reactivity towards molecular ozone and hydroxyl radicals. Water Research 33 (10), 2265-2276.

Westerhoff P., Mash H., 2002. Dissolved organic nitrogen in drinking water supplies: a review. Journal of Water Supply: Research and Technology – Aqua 5, 415-448.

White F.M., 2003. Fluid Mechanics, 5th edition. McGraw-Hill, New York, NY.

WHO, 2008: Guidelines for drinking-water quality: incorporating 1st and 2nd addenda, Vol.1, Recommendations. – 3rd ed – URL: www.who.int/water_sanitation_health/dwq/fulltext.pdf (last access: 03/13/2017).

Winter J., Bérubé P.R., Uhl W. and Barbeau B. (2013) Biodegradation of Organic Matter and Effect of Pre-Ozonation, Proceedings of the AWWA Water Quality Technology Conference, Long Beach, CA.

Winter J., Uhl W., Bérubé P. R., 2016. Integrated Oxidation Membrane Filtration Process – NOM Rejection and Membrane Fouling. Water Research 104, 418-424.

Wray H.E., Andrews R.C., Bérubé P.R., 2013. Surface shear stress and membrane fouling when considering natural water matrices. Desalination 330, 22-27.

Wu J., Le-Clech P., Stuetz R.M., Fane A.G., Chen V., 2008. Effects of relexation and backwashing conditions on fouling in membrane bioreactor. Journal of Membrane Science 324, 26-32.

Xia L., Law A.W.-K., Fane A.G., 2013. Hydrodynamic effects of air sparging on hollow fiber membranes in a bubble column reactor. Water Research 47, 3762-3772.

Yadav K., Morison K., Staiger M. P., 2009. Effects of hypochlorite treatment on the surface morphology and mechanical properties of polyethersulfone ultrafiltration membranes. Polymer Degradation and Stability 94 (11), 1955–1961.

Ye, Y., Le-Clech P., Chen V., Fane A.G., Jefferson B., 2005. Fouling mechanisms of alginate solutions as model extracellular polymeric substances. Desalination 175, 7-20.

Yoon Y., Amy G., Cho J., Her N., 2005. Effects of retained natural organic matter (NOM) on NOM rejection and membrane flux decline with nanofiltration and ultrafiltration. Desalination 173 (3), 209-221.

Yu W., Graham N. J. D; Fowler G. D., 2016. Coagulation and oxidation for controlling ultrafiltration membrane fouling in drinking water treatment: Application of ozone at low dose in submerged membrane tank. Water Research 95, 1-10.

Zheng X., Ernst M., Jekel M., 2009. Identification and quantification of major organic foulants in treated domestic wastewater affecting filterability in dead-end ultrafiltration. Water Research 43 (1), 238–244.

Zheng X., Ernst M., Jekel M., 2010. Pilot-scale investigation on the removal of organic foulants in secondary effluent by slow sand filtration prior to ultrafiltration. Water Research 44, 3203-3213.

Zhu I.X., Getting T., Bruce D., 2010. Review of biologically active filters in drinking water applications. Journal AWWA 102, 67-77.

Zondervan E., Zwijnenburg A., Roffel B., 2007. Statistical analysis of data from accelerated ageing tests of PES UF membranes. Journal of Membrane Science 300 (1-2), 111–116.

Zularisam A. W., Ismail A. F., Salim M. R., Sakinah M, Ozaki H, 2007. The effects of natural organic matter (NOM) fractions on fouling characteristics and flux recovery of ultrafiltration membranes. Desalination 212 (1-3), 191-208.

Zumstein J., Buffle J., 1989. Circulation of Pedogenic and Aquagenic Organic Matter in an Eutrophic Lake. Water Research 23 (2), 229-239.

Appendices

Appendix A Biological Filtration for NOM Removal

A.1 Insight into Biodegradation of Organic Matter from Different Waters and the Effect of Pre-Ozonation

This work is included in in the Appendices of this thesis, because it was conducted during the PhD program and is relates to the thesis work by investigating a NOM removal technology. However, it does not directly address any of the research questions of the thesis work.

This work has been presented at the AWWA Water Quality Technology Conference 2013 in Long Beach, CA.

Abstract

The present study investigated the biodegradation of different NOM sources with and without pre-ozonation. DOC was characterized in terms of non-biodegradable (NBDOC) and biodegradable (BDOC) fractions, and the rate constant for the biodegradation was quantified for three different source waters. LC-OCD-OND analyses were carried out and the biodegradation characteristics of each fraction of organic matter were determined.

Ozone was only able to slightly increase the BDOC (statistically not significant). The effect of ozone on biodegradation kinetics depended on the NOM source. An increase in the biodegradation rate constant was related to an increase in smaller molecular weight fractions and to structural changes within different fractions of organic matter.

Introduction

Biofiltration has been reported to be suitable for DOC removal, reduction in disinfection by-product formation potential and chlorine demand (Carlson and Amy, 1997; Chaiket et al., 2002; Zhu et al., 2010; Black, 2011). Efficient removal of biodegradable organic matter can further control microbial regrowth and biofilm formation in distribution systems. In water treatment, ozone is commonly used prior to biofiltration to increase the fraction of organic matter that can be removed within biofilters. Although a number of studies have focused on characterizing the biodegradable fractions of the DOC, the kinetics that govern the removal of the biodegradable fraction of DOC remain poorly understood. To gain insight into the biodegradation, the DOC was characterized in terms of non-biodegradable (NBDOC) and biodegradable (BDOC) fractions, and the rate constant for biodegradation was quantified for three different source waters. LC-OCD-OND (Liquid chromatography, organic carbon detection/organic nitrogen detection) analyses were carried out and the biodegradation characteristics of each fraction of organic matter as classified by Huber et al. (2011) were determined.

Materials and Methods

For the present study, three different source water were used: (i) effluent from the WWTP Kaditz (Dresden, Germany), (ii) effluent from the pilot plant at the University of British Columbia (Vancouver, Canada) and (iii) a surface water collected at Jericho Pond (Vancouver, Canada) that is characterized by a high DOC content (likely derived from microbial activity (algal blooms) and run off containing terrestrial organic matter). All waters were diluted with tap water to a DOC concentration of approximately 4.5 mg C/L.

Oxidation with ozone was performed using a solution ozone test approach similar to that described by Rakness (2005). With this approach, an aliquot of ozone saturated Milli-Q water was added to a concentrated solution of the model raw water to achieve a dose of 1 mg_{ozone}/mg_{DOC}, as well as the concentrations presented in Table 1. The mixture was then sealed and allowed to react until all of the ozone was consumed.

Batch biodegradation tests were conducted to quantify the biodegradation kinetics and NDBOC and BDOC. The filter material (i.e. granular activated carbon) was harvested from acclimatized bench scale biological filters (EBCT = 20 min). Batch reactors containing harvested filter material and sample were placed in incubated shaker and temperature was controlled at 21°C. A decay curve was obtained that allowed to determining the kinetic rate constant, NBDOC and BDOC.

The DOC concentrations were determined using a Dohrmann Phoenix 8000 UV-Persulfate Analyzer. Size exclusion chromatography was conducted using a LC-OCD-OND (Liquid chromatography, organic carbon detection/organic nitrogen detection) analyzer model 8 (DOC Labor Dr. Huber, Germany).

Results and Discussion

A preliminary study assessed the effect of different raw water matrices on the biodegradation characteristics. Experiments were carried out as batch tests (see above). The biomass for batch tests was harvested from GAC biofilters acclimatized (7 months) to ozonated and non ozonated waters from two different sources (i.e. in total 4 different waters). The results indicate that the biodegradation rates were not dependent on the type of water used for biomass acclimatization.

Results for BDOC obtained from batch biodegradation tests with effluent from the WWTP Kaditz (EfOM DD), effluent from the pilot plant at the University of British Columbia (EfOM UBC) and a surface water collected at Jericho Pond (JPW) are presented in Figure 1. A consistent but not statistically significant increase in BDOC was observed following ozonation, resulting in a lower DOC concentration following biodegradation.

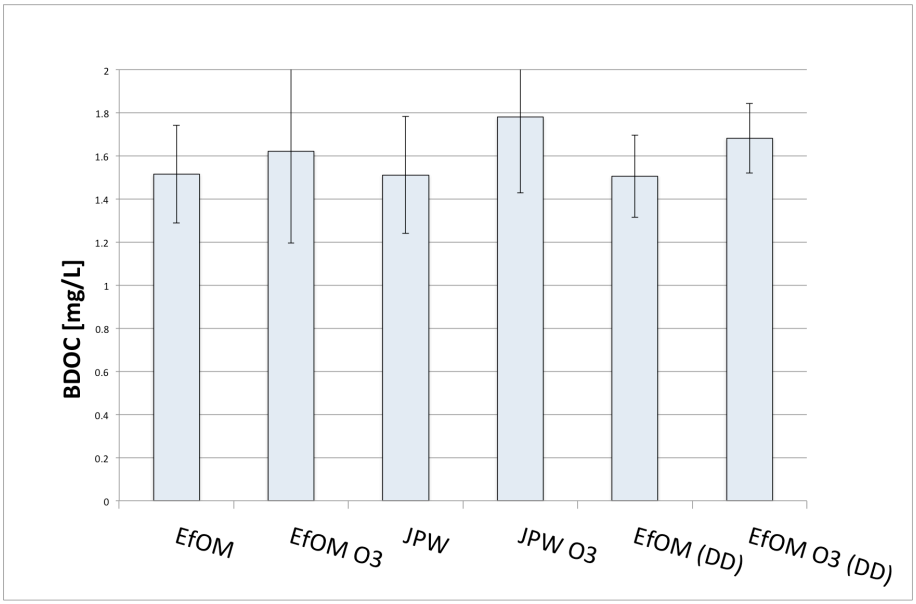

Figure 1: BDOC obtained from batch biodegradation tests for the waters investigated; error bars correspond to a 90 % confidence interval

Results for the effect of ozonation on the overall biodegradation rate constant, as illustrated in Figure 2, were dependent on the raw water characteristics. Ozonation increased the rate constant for the raw water with an initially low rate constant, and decreased the rate constant for the raw water with an initially high rate constant (although the decrease was not statistically different).

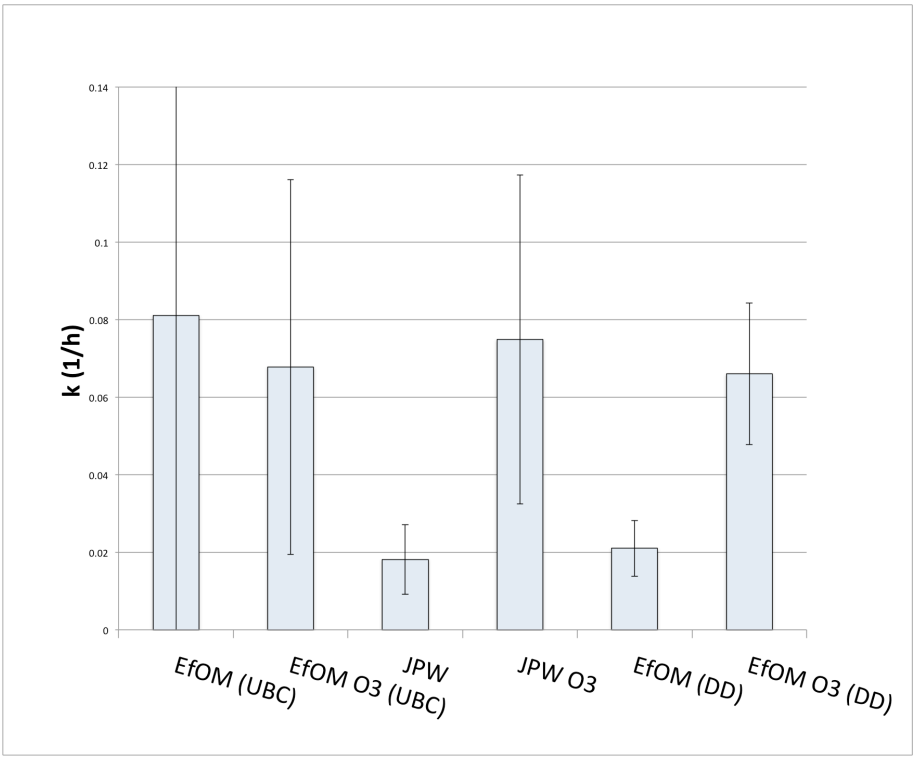

Figure 2: kinetic rate constant (k) obtained from batch biodegradation tests for the waters investigated; error bars correspond to a 90 % confidence interval

When an overall increase in the biodegradation rate constant was observed, it resulted from an increase in the biodegradation rate constant for most molecular weight fractions, except biopolymers. Figure 3 illustrates the kinetic rate constants for the fractions of EfOM and ozonated EfOM from WWTP Dresden Kaditz (i.e. a water for which ozone increased the biodegradation rate constant). For these conditions, ozonation also seemed to increase the concentration of the lower molecular weight compounds - i.e. building blocks and low molecular weight acids.

a) b)

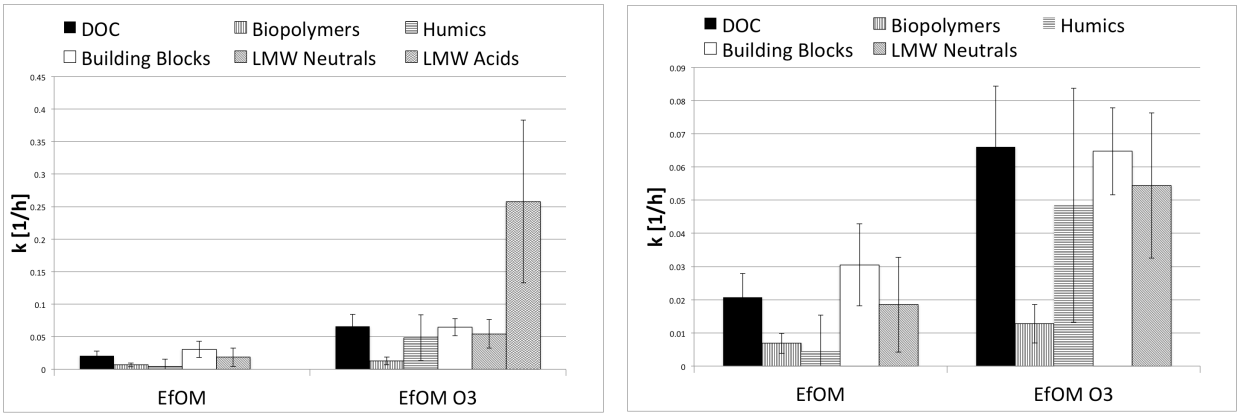

Figure 3: Kinetic rate constant (k) of EfOM DD for different fractions of NOM as classified by Huber et al. (2011), (a) with LMW acids included and (b) without LMW acids (i.e. to adjust scale); error bars correspond to a 90 % confidence interval

Conclusions

A consistent but not statistically significant increase in BDOC was observed following ozonation. Ozonation did not have a consistent effect on the biodegradation kinetic rate constant. Ozonation appeared to increase the rate constants for waters with poorly biodegradable NOM. The increase in biodegradation rate constant was likely due to an increase in smaller molecular weight fractions and due to structural changes within fractions of organic matter as classified by Huber et al. (2011).

Acknowledgements

I want to acknowledge the co-authors, Pierre R. Bérubé, Benoit Barbeau and Wolfgang Uhl, for their valuable input und fruitful discussions. I also want to thank Res'Eau WaterNet for funding this research.

A.2 Biological Filtration for NOM-Removal – Biological Ion Exchange and Biological Activated Carbon

This work is included in in the Appendices of this thesis, because it was conducted during the PhD program and is relates to the thesis work by developing and investigating a novel NOM removal technology. However, it does not directly address any of the research questions of the thesis work.

This work has been presented at the AWWA Water Quality Technology Conference 2016 in Indianapolis, IN.

Abstract

The present study investigated the performance of an ion exchange resin system in which biological activity was promoted (i.e. Biological Ion Exchange or BIEx) and a biological activated carbon system (BAC) over a period of ten months, corresponding to approximately 15,000 bed volumes. NOM removal efficiencies were relatively stable in both systems over the whole test period. However, NOM removal efficiency was substantially higher for the BIEx system (56 ± 7 %) compared to the BAC system (15 ± 5 %). In contrast to the BAC system, the BIEx system predominantly removed UV_{254} absorbing NOM constituents (i.e. carbon double bonds and aromatic compounds). The reduction in UV absorbance at 254 nm was 75 ± 1.6 % and 10 ± 1.6 % for the BIEx and the BAC system, respectively. Overall, the present study demonstrates that BIEx systems exhibit superior NOM removal compared to conventional biological filtration approaches, such as BAC. On the other hand, the observed stable DOC removal over the 10 months test period, corresponding to approximately 15,000 bed volumes, without regeneration demonstrates that the costs of BIEx systems are substantially less than those of traditional ion exchange systems.

Introduction

Biological filtration is cost effective, easy to operate and has been reported to be suitable for DOC removal, reduction in disinfection by-product formation potential and chlorine demand (Carlson and Amy, 1997; Chaiket et al., 2002; Zhu et al., 2010; Black and Bérubé, 2014). However, the extent of DOC removal is limited, making conventional biological filtration not suitable for treatment of source waters with higher DOC concentrations (Odegaard et al., 2010). Technologies that can provide more extensive DOC removal are increasingly of interest. Along with global warming DOC concentrations in source waters will likely increase (Hejzlar et al., 2003). One technology that can provide higher DOC removal efficiencies is ion exchange. However, a main drawback of ion exchange is the required frequent regeneration of the resin. Results of a previous study suggested that operating an ion exchange resin system in which biological activity is promoted (BIEx) extends the time until breakthrough compared to conventional ion exchange, without compromising the efficiency of resin regeneration (Schulz et al., 2016). However, a BIEx system has not been operated for longer than three months. The present study investigated the performance of BIEx in terms of DOC removal over approximately 10 months and 15,000 bed volumes and in terms of the reduction of the Disinfection by-product (DBP) formation potential. Furthermore, the performance of the BIEx system was compared to that of a biological activated carbon system as a reference for a conventional biological filter.

Materials and Methods

A strongly basic anion exchange resin (Purolite A860 – Dow Chemicals) designed for NOM removal applications was used. The filtration velocity was set to 0.2 m/h (≈ 2 BV/h), resulting in an empty bed contact time (EBCT) of approximately 30 minutes and 48 bed volumes (BV) per day. The temperature was 22 (± 1) °C. The BAC used (Picabiol® granular activated carbon - PICA Carbon) was harvested from a BAC column that has been in operation for over 6 years and for which all adsorption capacity is exhausted. Operational conditions, such as filtration velocity and bed volume and temperature, were kept consistent with those of the anion exchange resin filters. The raw water was a natural surface water (Jericho Pond, Vancouver Canada), pre-filtered through 1 μm glass fiber filters (Cat # 1827-125, Whatman, UK) and adjusted to a dissolved organic concentration (DOC) concentration of approximately 5 mgL^{-1} with tap water.

The organic composition of raw water and IEX-filtrate samples was characterized using total organic carbon analysis (Phoenix 8000 TOC analyser, Dohrmann, US) as well as specific light absorption at 254 nm (UVA254) (UV300 UV-vis spectrometer, Spectronic Unicam, US). DBP formation potential was assessed according to the Uniform Formation Conditions (UFC) technique (Summers et al. 1996) where THM and HAA5 concentrations are measured after a contact time of 24h with a free chlorine residual of 1 mg Cl2/L at pH 8.0 and T 22oC. Prior to all analyses, samples were pre-filtered using 0.45 μm cellulose nitrate membrane filters (Cat. # 09-719-555, Fisher Scientific, CA). Any samples that could not be analysed immediately were stored at 4 °C. All analyses were carried out at least in duplicate.

Results and Discussion

The BIEx and BAC filters were operated for approximately 10 months, which corresponded to just over 15,000 bed volumes. For the duration of those tests, the DOC removal was relatively constant in both systems (see Figure 1). However, a substantially higher DOC removal efficiency was observed for the BIEx system than for the BAC system with 56 (± 7) % and 15 (± 5) % for the BIEx and BAC, respectively. Figure 2 illustrates the change in $SUVA_{254}$ normalized to the $SUVA_{254}$ in the source water. In the BAC system, $SUVA_{254}$ slightly increased. This was expected, because biological filters predominantly remove fractions of organic matter that do not absorb UV light at 254 nm (i.e. that do not contain carbon double bonds and aromatic compounds) (Zheng et al., 2010, Winter et al., 2013). In contrast, the $SUVA_{254}$ decreased during BIEx, suggesting that the degradation of organic matter in the BIEx system followed a different pathway than in the conventional biological filters. Further research is required to gain insight into the removal mechanism in the BIEx filters. However, the results discussed above suggest that BIEx and BAC predominantly remove different fractions of organic matter and, hence, operated in series may act complementary in terms of DOC removal. During the last 5.5 weeks of the test period presented, corresponding to 13,200 to 15,200 bed volumes, one of the BIEx filter was operated in series with one of the BAC filter. The DOC of the effluent following BIEx and BAC in series was consistently lower than the DOC of the effluent of the BAC or the BIEx (see Figure 3). However, the increase in DOC removal efficiency of the combined BAC + BIEx system was in average only 4 % compared to the BIEx system alone, suggesting that for overall DOC removal the improvement of the combined system was only marginally. A combination of both systems might still be beneficial, if the removal of specific fractions of organic matter is of interest. Size exclusion chromatography analysis of samples from those tests will provide further

insight into the removal of organic matter of BIEx, BAC and the combined system with respect to specific fractions, such as biopolymers, humic substances, building blocks, low molecular weight acids and low molecular weight neutrals.

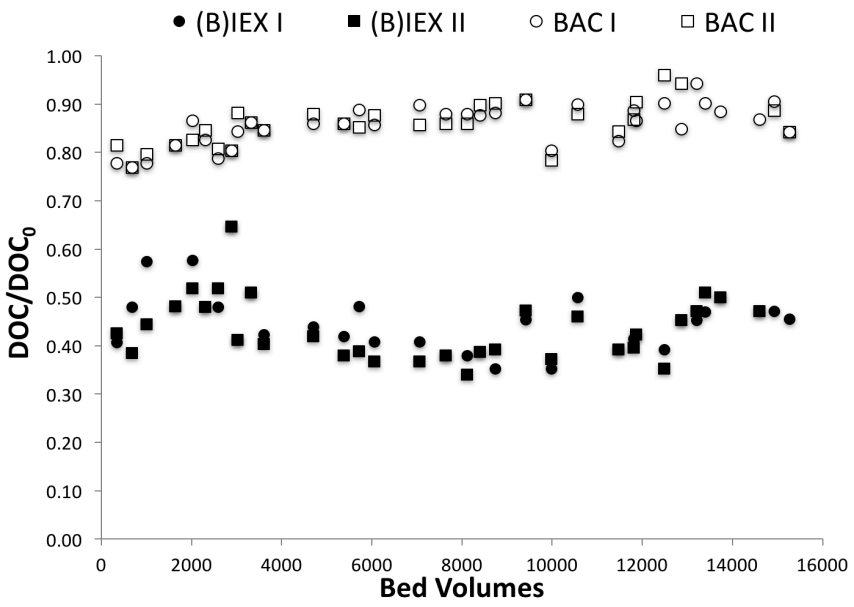

Figure 1: Relative change in DOC concentration during BIEx and BAC filtration

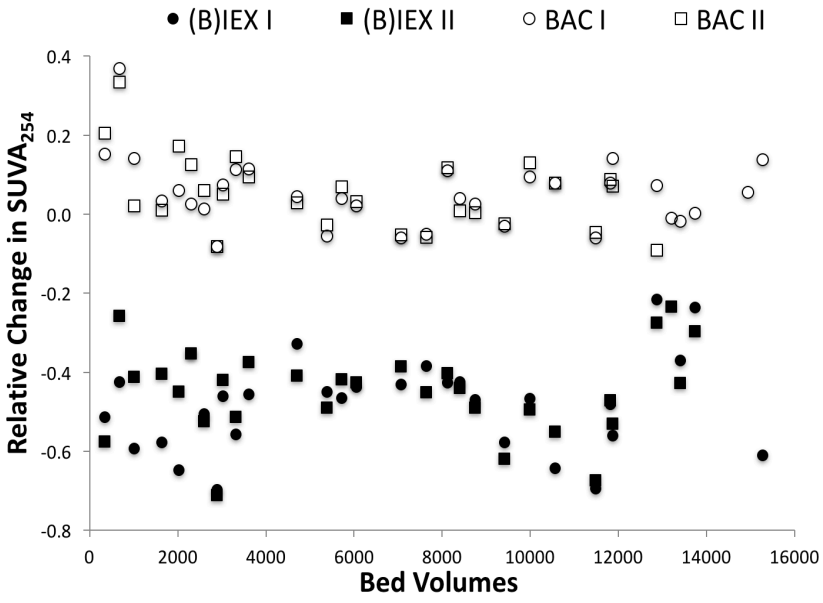

Figure 2: Relative change in SUVA during BIEx and BAC filtration

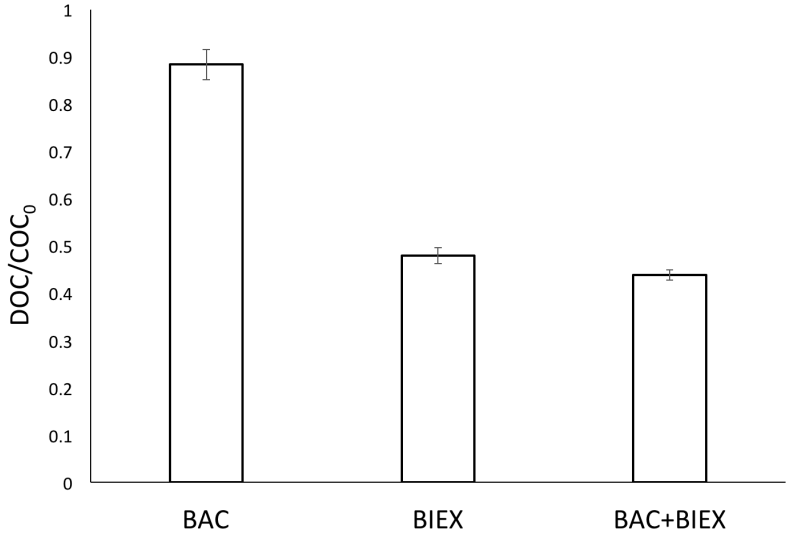

Figure 3: Normalized DOC for tests with BAC+BIEx in series; error bars correspond to the standard error

Because the decrease in DBP formation potential is a main motivation for the removal of DOC from source waters, the THM and HAA formation potential of the source water, the BAC treated and the BIEx treated water was analysed for three different sampling dates. While both BAC and BIEx were able to substantially decrease the DBP formation potential, BIEx was superior regarding the decrease in THM and HAA formation potential. The effluent of the BIEx system would have reliably met the Canadian Drinking Water Guidelines for disinfection by-products.

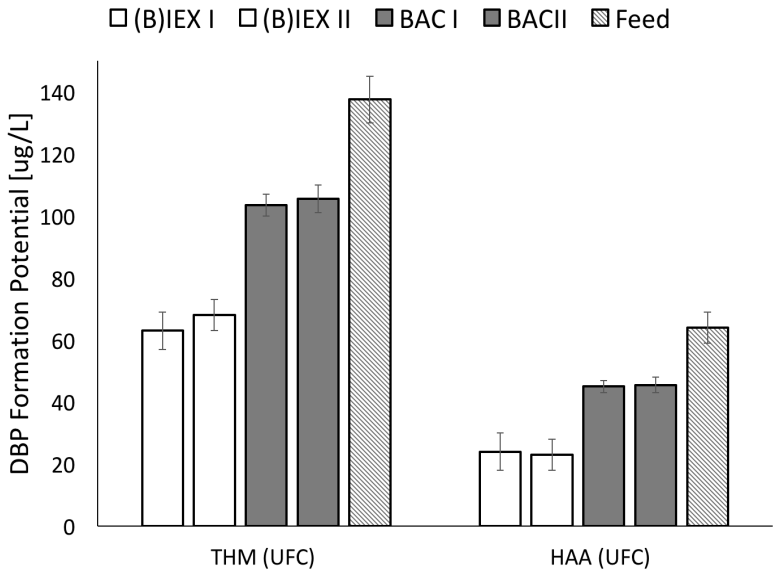

Figure 4: DBP formation potential; error bars correspond to the standard error

Conclusions

Biological ion exchange (BIEx) provided high DOC removal efficiencies of 56 (± 7) % compared to BAC with 15 (± 5) %. The DBP formation potential was substantially lower after BIEx than after BAC than in the source water. In regards to operation, the results presented

suggest that BIEx can be operated similar to a conventional biological filter and without generation. Hence, BIEx combines the advantages of process simplicity and low costs of conventional biological filtration with the high DOC removal efficiency of conventional ion exchange. In addition, the option of regeneration, which is not affected by the biological activity, adds resiliency to the system.

Acknowledgements

I want to acknowledge the co-authors, Pierre R. Bérubé, Benoit Barbeau, Heather Wray and Martin Schulz, for their valuable input und fruitful discussions and Heather Wray and Martin Schulz also for conducting some of the early work for this project. The present research was funded by the Natural Science and Engineering Research Council of Canada RES'EAU-Waternet Strategic Network, which is aimed at developing drinking water treatment processes and technologies for small and remote communities, and Opus International Consultants Ltd.

Appendix B Supplemental Material to Chapter 4

B.1 Characterization of Jericho Pond Water

The figure below shows a typical LC-OCD chromatogram of SRNOM. To obtain this chromatogram, Jericho Pond water was characterized using LC-OCD as described by Huber et al. (2011) and the figure LC-OCD analysis demonstrated the presence of a broad spectrum of NOM fractions present in Jericho Pond.

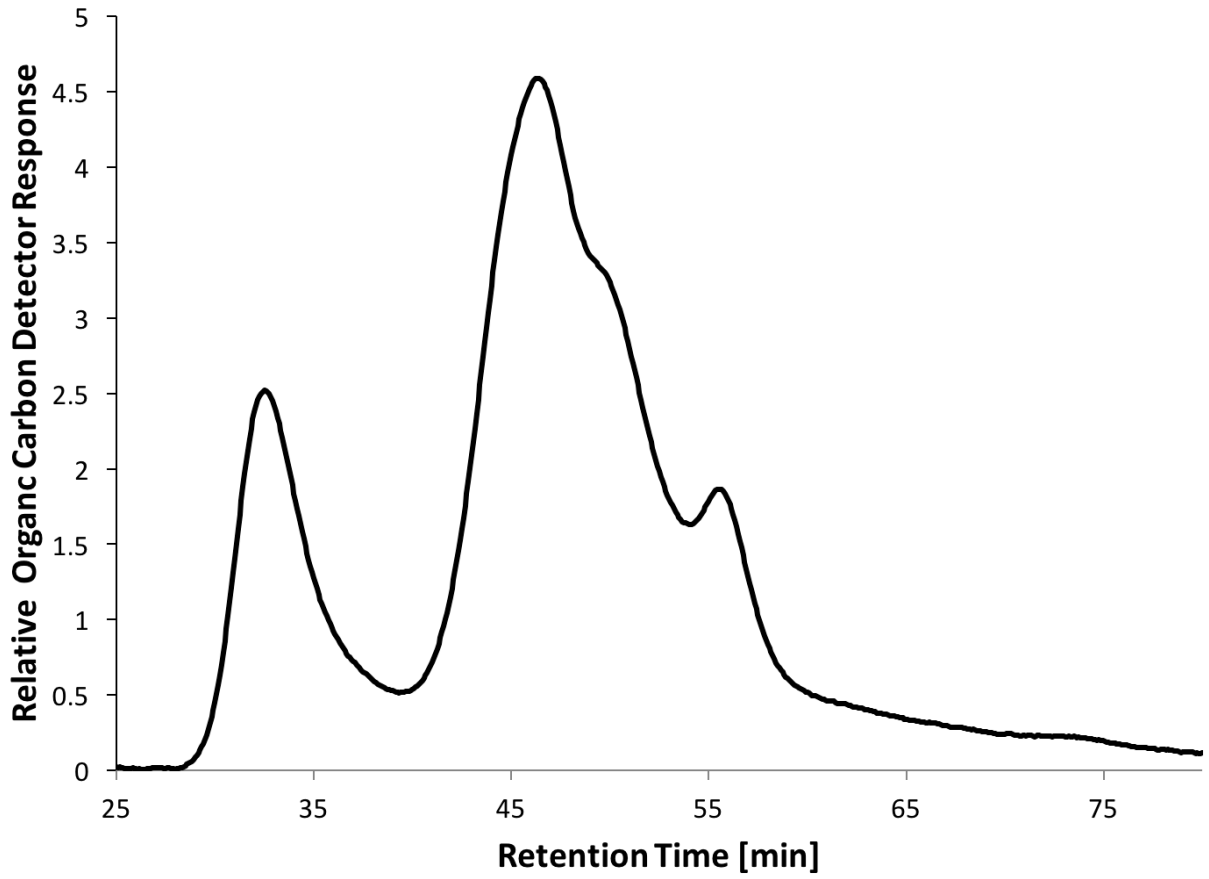

B.2 Increase in Resistance Related to Alkalinity

The osmotic pressure resulting from the alkalinity in the model raw water was estimated according to Schäfer (2007). The calculated osmotic pressure corresponded to an increase in

resistance to permeate flow as presented in the Figure below for the membrane with a MWCO if 300 Da, which was the membrane that retained the alkalinity present in the model raw water most efficiently (i.e. approximately 40 % of the sodium bi-carbonate was retained). The figure illustrates the extent of the increase resistance to permeate flow associated with the alkalinity present in the model raw water to the overall increase in resistance during the filtration tests.

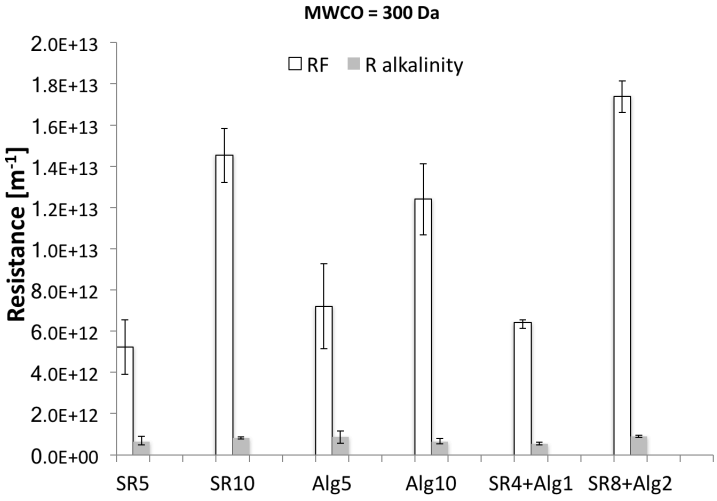

Appendix C Supplemental Material to Chapter 5

C.1 Correlation between Absolute Recovery and Initial Rapid Increase in Resistance for Model Raw Waters containing Alginate

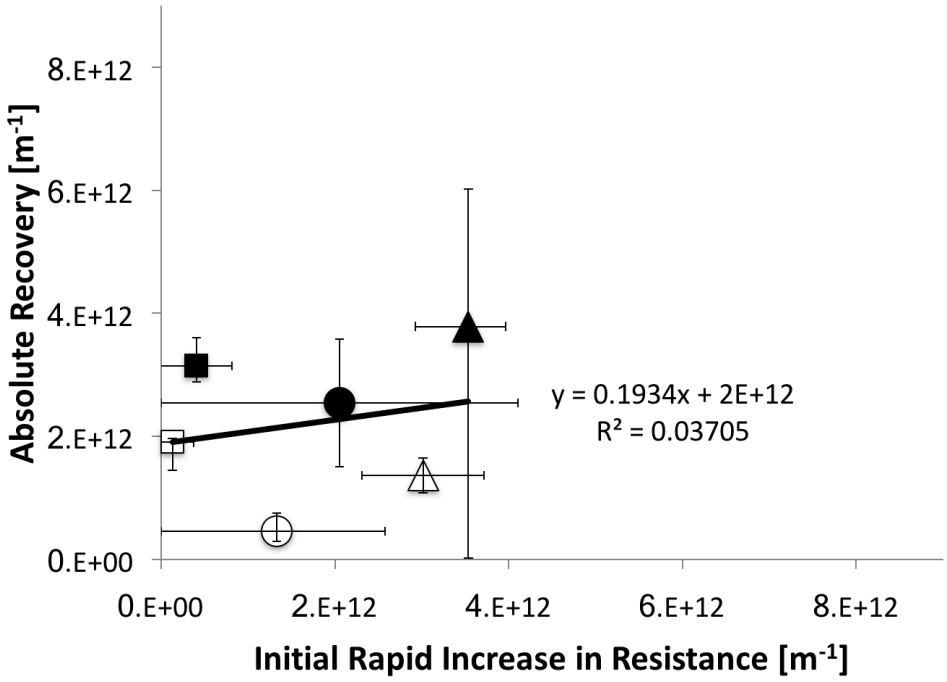

(model raw waters containing alginate; solid line: linear regression, R^2=0.04; error bars correspond to minimum/maximum values)

Appendix D Supplemental Material to Chapter 6

D.1 Mass Balance – Expected Amount of Material in the Foulant Layer

As discussed in Sections 4.6.3 and 6.2, an additional test was conducted to evaluate the amount of material that was expected to deposit on the membrane surface by conducting a mass balance. The experimental setup described in Section 4.5.1 was used, but it was operated with only one CF042 test cell. For this mass balance, the retentate was collected and the volume of the retentate as well as the concentration of material (i.e. particulate material, polysaccharides, and humic substances) in the retentate was determined. Because the membrane with a MWCO of 300 Da essentially removed all of the particulate material, polysaccharides, and humic substances, the concentration of material in the feed stream multiplied by the permeate volume corresponds to the expected to the mass in the foulant layer, if convective transport dominates (see Section 6.2).

- Expected mass towards membrane: Concentration in the feed times the permeate volume.
- Actual mass towards the membrane: Concentration in the feed times the sum of the permeate and the retentate volume, minus the concentration in the retentate times the volume of the retentate.
- Expected normalized mass (i.e. without loss of material during sampling and analysis): The ratio of actual mass towards the membrane and expected mass towards the membrane.

Table: Mass Balance – Expected Amount of Material in the Foulant Layer

	Concentration in the Feed [mgL^{-1}]	Concentration in the Retentate [mgL^{-1}]	Permeate Volume [mL]	Retentate Volume [mL]	Expected mass towards membrane [mg]	Actual mass towards membrane [mg]	Expected normalized mass
Particulate Matter	15	15.9	743	754	11.15	10.47	0.94
Poly-saccharides	1	1	743	754	0.74	0.75	1.01
Humic Substances	4	6.4	743	754	2.97	1.16	0.39

Appendix E Supplemental Material to Chapter 7

E.1 Filtration Model Fitted to Experimental Data from First Set of Experiments (Typical Results)

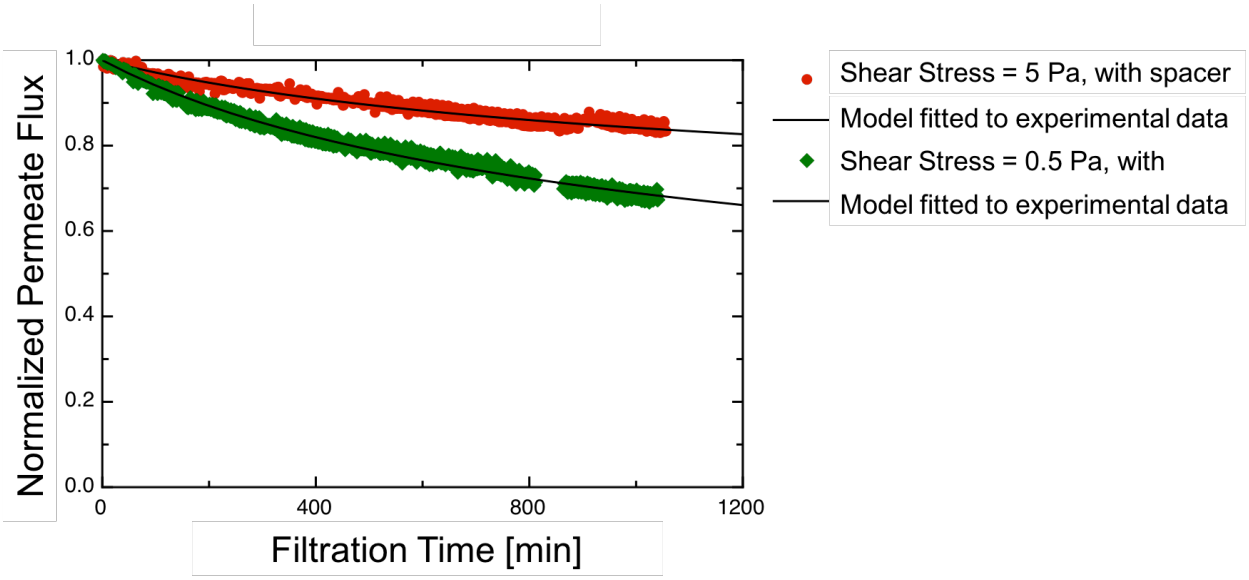

Appendix F Supplemental Material to Chapter 8

For the data related to the cost estimation please see assumptions stated in Table 8 (see Section 8.1).

F.1 Spiral Wound NF Cost and Operating Flux – Sensitivity to Membrane lifetime

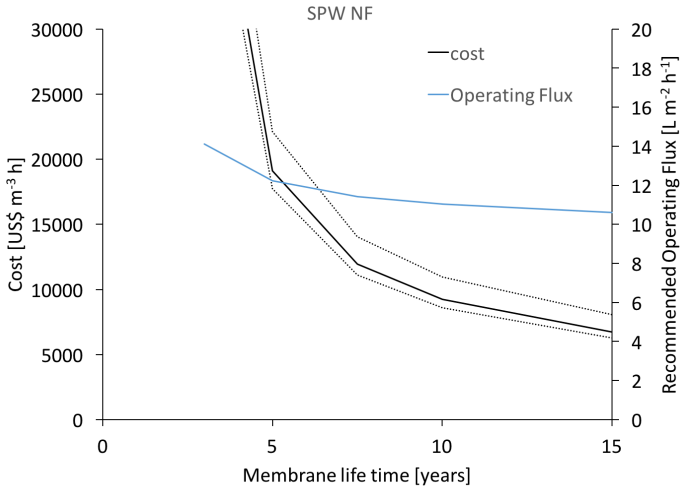

F.2 Hollow Fiber NF Cost and Operating Flux – Sensitivity to Temperature

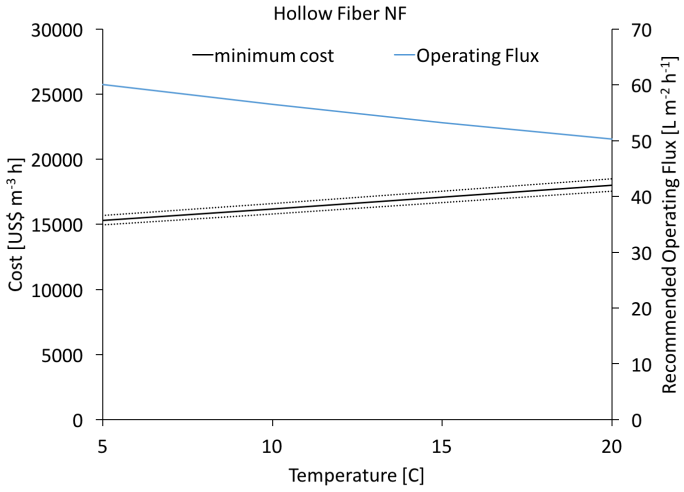

F.3 Spiral Wound NF Cost and Operating Flux – Sensitivity to Temperature

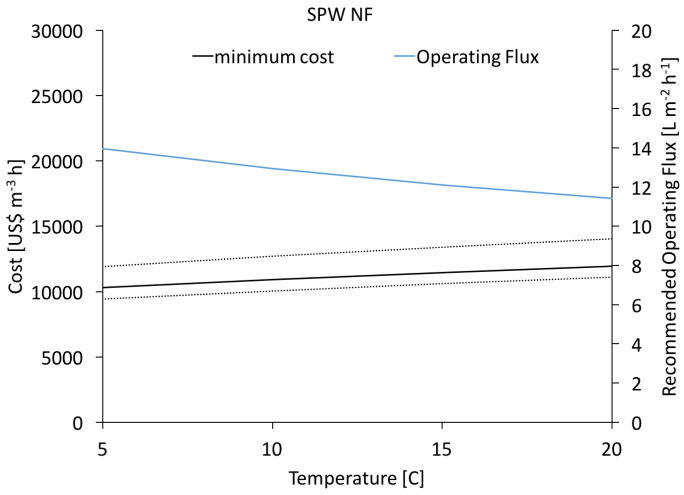

F.4 Hollow Fiber NF Cost and Operating Flux – Sensitivity to Energy Cost

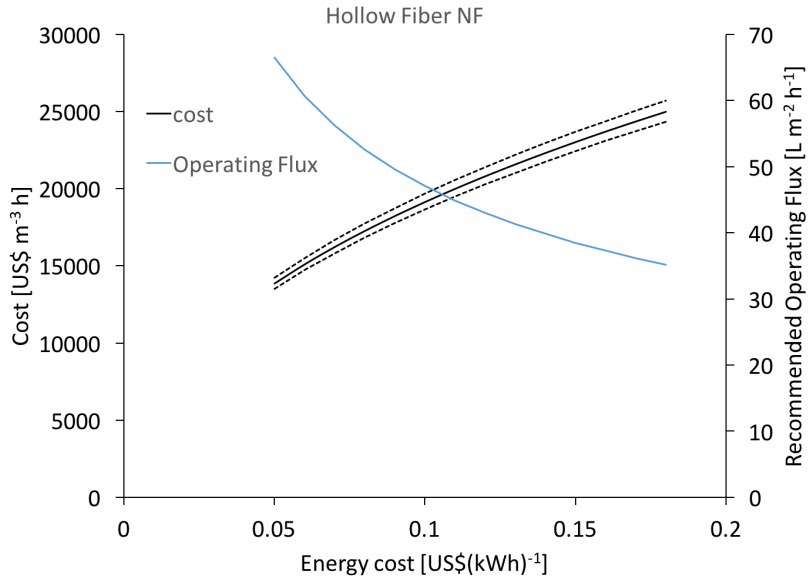

F.5 Spiral Wound NF – Sensitivity to Energy Cost